



Norwegian University of Life Sciences
Faculty of Environmental Sciences
and Natural Resource Management

Philosophiae Doctor (PhD)
Thesis 2019:105

Sensitivity analyses of the Weather Research and Forecasting model for wind resource assessment in coastal Ghana

Følsomhetsanalyser med modell for vær
og vindressursprognoser for kystområder
i Ghana

Denis Edem Kwame Dzebre

Sensitivity analyses of the Weather Research and Forecasting model for wind resource assessment in coastal Ghana

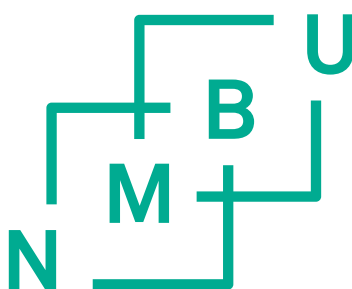
Følsomhetsanalyser med modell for vær og vindressursprognoser for kystområder i Ghana

Philosophiae Doctor (PhD) Thesis

Denis Edem Kwame Dzebre

Norwegian University of Life Sciences
Faculty of Environmental Sciences and Natural Resource Management

Ås (2019)



Supervisors

Professor Muyiwa Samuel Adaramola (Main Supervisor)
Renewable Energy Group
Faculty of Environmental Sciences and Natural Resource Management (MINA)
Norwegian University of Life Sciences (NMBU)
P. O. Box 5003, NMBU, 1432 Ås, Norway.

Dr. Joshua Ampofo (Co-supervisor)
Department of Mechanical Engineering
Kwame Nkrumah University of Science and Technology (KNUST)
Private Mail Bag, Kumasi, Ghana.

Dr. Akwasi Afrifa Acheampong (Co-supervisor)
Department of Geomatic Engineering
Kwame Nkrumah University of Science and Technology (KNUST)
Private Mail Bag, Kumasi, Ghana.

Evaluation Committee

Senior Scientist Xiaoli Guo Larsen (First Opponent)
DTU Wind Energy, Department of Wind Energy
The Technical University of Denmark (DTU).

Post-Doc Researcher Theodore M. Giannaros (Second Opponent)
Institute of Environmental Research and Sustainable Development
National Observatory of Athens, Greece.

Assoc. Professor Nils-Otto Kitterød (Committee coordinator)
Faculty of Environmental Sciences and Natural Resource Management (MINA)
Norwegian University of Life Sciences (NMBU)
P. O. Box 5003, NMBU, 1432 Ås, Norway.

To my Parents
For Atta (of Blessed Memory) and
Uncle Kosi (of Blessed Memory)

Acknowledgements

I am most grateful to my main supervisor, Prof. Samuel Muiyiwa Adaramola, for his guidance, tolerance, patience and encouragement throughout this journey. I also thank my co supervisors; Dr. J Ampofo for being a source of inspiration since my days as an undergraduate, and Dr. Afrifa for his encouragement throughout this programme.

I am also grateful to Dr. Michel Mesquita and his m2lab.org team for allowing me to enroll in the Regional Climate Modeling with WRF online course. Valuable lessons on the workflow of the WRF model were acquired from this course. I also acknowledge my colleague, Pablo Duran for his suggestions and tips with the model.

I gratefully acknowledge the scholarship support from the Energy and Petroleum (EnPe) Project of the Norwegian Agency for Development Cooperation (Norad), and the UPERCRET-KNUST Program and its coordinator, Dr. Lena Dzifa Mensah. I will also like to acknowledge my employer, the Kwame Nkrumah University of Science and Technology (KNUST), Ghana, for granting me study leave to undertake my studies. Administrative support from the Faculty of Environmental Sciences and Natural Resource Management (MINA), NMBU as well as The Brew-Hammond Energy Centre (TBHEC) at KNUST is also gratefully appreciated.

I am indebted to Dr. Francis Kemausuor of KNUST for his assistance in acquiring the data for the study. I am also grateful to Mr. Julius Nkansah-Nyarko of the Energy Commission of Ghana and Mr. Michael Wuddah-Martey of Upwind Ayitepa Ltd., Ghana for their prompt response to my enquiries during my fieldwork in Ghana.

To my parents, and my siblings (Nutifafa, Lizzy and Vanessa), your words of encouragement and support are forever appreciated. Same goes for other family members, especially Mr. Benjamin Meteku, (who always made time to listen to my rants of frustration at all ungodly hours of the night), as well as all my friends (Majeed, Augustine, Kuukua, Peter, Jamjam, and others). Finally, to Ebo, Kow, Olympia, Dorcas, Fiona, Gakii, my Ubuntu family of Maryama, Micah, Chavez, Afari-Djan, and others, as well as (current and former) colleagues at MINA (David, Saeed, Mekdes, Thomas, Yennie, Pablo, Miguel, Greyson and EVERYONE!!!), I want to say thanks for the warm friendship and company throughout this journey.

“Akpe na mikatãã”

Denis Edem Kwame Dzebre

Ås, Norway

(October 2019)

Summary

With the rise of modern wind turbines, wind energy has grown to become a major source of generated electricity, alongside other renewable and conventional energy sources. The geographical and time dependent nature of wind warrants detailed assessments to judge the feasibility of power projects. Pre-feasibility studies play crucial roles in this assessment process and include the performing of large area screening of feasible wind power project sites, designing of effective measurement campaigns and feasibility assessments of projects. A source of data for such assessments that has increasingly become popular over the years, is downscaled meteorological datasets which are sometimes produced with Numerical Weather Prediction (NWP) models. Due to uncertainties (from several sources) associated with the outputs of NWP models, their validation is an important step towards their optimization and application for desired purposes. Wind varies geographically. Therefore, the validation of NWP models is an important step towards their application for wind data downscaling for a geographic location.

Though studies have suggested that wind projects are feasible in Ghana, development of the resource still suffers from several challenges, including inadequate resource assessments. This thesis focuses on the application-oriented use of the Mesoscale Weather Research and Forecasting (WRF) model for wind prediction applications in the coast of Ghana and neighboring countries in the West African sub-region.

A local sensitivity assessment of selected numerical options (simulation length or run time and methods of applying the WRF model's Four-Dimensional Data Assimilation (FDDA) nudging technique), as well as selected terrestrial and meteorological datasets on downscaled wind data for coastal Ghana were conducted. Validation of the simulations was done with statistical error metrics from prediction-observation comparisons. The error metrics were compared with performance benchmarks for wind prediction by NWP models that have been reported in scientific literature. In addition, Weibull distribution parameters, as well as probability and cumulative density functions of measured and predicted data were also compared.

Results of this thesis were communicated in four Papers. Paper I sought to deepen the understanding of the impacts of combining varying simulation run time and selected options in the method of applying the WRF model's FDDA nudging technique for wind simulations. It was found that the method of applying nudging above levels automatically determined by the WRF model has a more consistent impact on model predictions. Paper II and Paper III assessed the impacts of Planetary Boundary Layer (PBL) and Surface Layer (SL) parameterization schemes on predictions from the model. It was concluded that the Turbulent Kinetic Energy (TKE) Mellor–Yamada Nakanishi Niino Level 3 (MYNN3) PBL scheme often had relatively better impact on downscaled data, when paired with the Eta SL scheme for simulations. On the terrestrial datasets, it was found that the two global Land Use and Land Cover (LULC) datasets available in the WRF

Geographical Data did not differ significantly in their impact on downscaled data. In addition, among the Gridded Binary (GRIB) meteorological datasets available in the National Center for Atmospheric Research Data Archives, it was realized that the data assimilation systems used in producing these datasets is probably a good criterion for their selection for downscaling for the study area. The findings of this study were reported in Paper IV.

Results of a simulation covering a year with a model configuration based on the findings of the four papers showed that the model is capable of downscaling wind data with error metrics that can meet most of the performance benchmarks that have been reported in literature. The results from this final evaluation also suggest that the configuration established from the studies is probably suitable for offshore assessments in the area but will require further verification.

Table of Contents

Summary.....	vii
List of Figures.....	xi
List of Papers.....	xiii
Abbreviations.....	xv
INTRODUCTION.....	1
1.1 Background.....	1
1.2 Nature of Wind.....	2
1.3 The Role of Numerical Weather Prediction in Wind Resource Assessments.....	3
1.4 Motivation.....	4
1.5 Aim and Objectives.....	5
1.6 Thesis outline.....	6
DATA AND METHODOLOGY.....	7
2.1 A Brief Overview of the Weather Research and Forecasting Model (WRF).....	7
2.1.1 The WRF Software Infrastructure.....	7
2.1.1.1 The ARW Dynamics and Numerics.....	7
2.1.1.2 The ARW Physics Parameterization Options.....	10
2.1.1.3 WRF Nudging.....	10
2.1.2 Input Data and the WRF Preprocessing System (WPS).....	11
2.2 Methodology.....	12
2.2.1 Study Framework.....	12
2.2.2 Evaluation Criteria and Observational Data.....	12
2.2.3 Postprocessing of Model Outputs.....	13
SUMMARY OF MAIN FINDINGS.....	15
3.1 Overview.....	15
3.2 Impact of Simulation Run times and vertical levels for nudging.....	15
3.3 Impact of PBL and SL parameterization schemes on predictions.....	16
3.4 Possible impact of different Input Datasets.....	17
3.5 Performance assessment of based on the sensitivity tests.....	18
CONCLUSION AND RECOMMENDATIONS FOR FUTURE WORK.....	19
4.1 Conclusions.....	19

4.2 Recommendations for Future Work	20
APPENDIX.....	21
Configuration and results of evaluation run	21
Selected Formulas that were applied in the evaluation of options.....	23
REFERENCES.....	25
PAPERS	28
ERRATA	

List of Figures

Figure 1: Typical time and spatial scales of meteorological phenomena.	2
Figure 2: Typical wind speed profiles in the Surface Layer	3
Figure 3: A Schematic of the main components of the WRF model.....	7
Figure 4: Horizontal and vertical grids of the ARW solver.	9
Figure 5: Interaction of parameterization schemes in WRF.....	10
Figure 6: Schematic of the program components and data flow in and out of the WPS.....	11
Figure 7: Study Framework.....	12
Figure 8: Flowchart for postprocessing of model outputs.....	14
Figure 9: Comparative performance (at 60 m) of two methods of applying nudging	16
Figure 10: Flowchart of test approach used in Paper II.....	17

List of Papers

- Paper I** **Dzebre, D.E.K.** Acheampong A.A., Ampofo J, Adaramola M.S., A sensitivity study of Surface Wind simulations over Coastal Ghana to selected Time Control and Nudging options in the Weather Research and Forecasting Model. *Heliyon*, 2019. 5, e01385 DOI: 10.1016/j.heliyon.2019.e01385.
- Paper II** **Dzebre, D.E.K.** and M.S. Adaramola, A preliminary sensitivity study of Planetary Boundary Layer Parameterisation schemes in the weather research and forecasting model to surface winds in coastal Ghana. *Renewable Energy*, 2020. 146: p. 66-86.
- Paper III** **Dzebre, D.E.K.** and M.S. Adaramola, Impact of Selected Options in the Weather Research and Forecasting Model on Surface Wind Hindcasts in Coastal Ghana. *Energies*, 2019. 12(19): p. 3670.
- Paper IV** **Dzebre, D.E.K.** and M.S. Adaramola, Impacts of selected Meteorological and Land Cover Datasets on dynamically Downscaled wind speeds for a coastal area using the Weather Research and Forecasting Model, Manuscript.

Other Paper

Dzebre D.E.K., Acheampong A.A., Ampofo J, Adaramola M.S. An Overview of utility-scale wind power development in Ghana. Submitted to *International Journal of Ambient Energy*, June 2018.

Abbreviations

ARW	Advanced Research WRF
CC	Correlation Coefficient
FDDA	Four-Dimensional Data Assimilation
GRIB	Gridded Binary
GW	Gigawatt
LSM	Land Surface Model
LULC	Land Use Land Cover
MASS	Mesoscale Atmospheric Simulation System
ME	Mean Error
MODIS	Moderate Resolution Imaging Spectroradiometer
MYJ	Mellor-Yamada-Janjic
MYNN3	Mellor-Yamada Nakanishi Niino Level 3
NCAR	National Center for Atmospheric Research
NCEP	National Centers for Environment Prediction
NWP	Numerical Weather Prediction
PBL	Planetary Boundary Layer
PV	Photovoltaic
STDE	Standard Deviation of Error
SL	Surface Layer
TKE	Turbulent Kinetic Energy
RDA	Research Data Archive
RMSE	Root Mean Squared Error
USGS	United States Geographical Survey
UW-TKE	University of Washington-Turbulent Kinetic Energy
WPS	WRF Preprocessing System
WRA	Wind Resource Assessment
WRF	Weather Research and Forecasting
WSI	WRF Software Infrastructure
YSU	Yonsei University

SYNOPSIS

INTRODUCTION

This chapter introduces wind and how wind characteristics affect power production from the resource. The need for wind resource assessment and the role that Numerical Weather Prediction models play in this process is briefly explained. This is followed by the motivation, aim and objectives of the thesis. Thereafter the structure of the rest of the thesis is presented.

1.1 Background

Global energy consumption has been on the rise over the years. This has been in response to factors such as increasing population and industrialization, and better living standards. The increase in energy consumption, coupled with concerns about the greenhouse gases emissions from the utilization of fossil fuels for energy generation, in addition to other reasons, has also increased the global demand for renewable energy over the years. Wind, or the kinetic energy of air flow, has been used in transport, industry and agriculture for thousands of years, and has become one of the three major renewable energy resources that is exploited on a large scale for global power generation [1]. The other two are hydro power, which uses potential energy of flowing river or stored water to generate electricity and solar Photovoltaic (PV) that converts solar radiation directly to electricity. The rise of modern wind turbines, which harness this energy and turn it into electricity has placed the resource as a major power source alongside other renewables and conventional energy sources. As of 2018, global installations of wind power stood at 591 GW, having quadrupled in the past decade [2].

Extractable wind energy depends on wind characteristics such as its speed, density, and prevailing directions. These characteristics play important roles in several aspects of wind energy exploitation (such as the prediction of the economic viability of projects). Wind speed, in particular, is of key interest, as wind power depends on the cube of this characteristic. However, like most renewable energy resources, wind characteristics that can support economical wind energy exploitation exhibit spatial and temporal dependencies. Therefore, understanding the characteristics of the resource in an area is an important step towards the exploitation of the resource. This requires good quality data on wind characteristics, which are best acquired through actual ground-based measurement campaigns. However, owing to the costly nature of these measurement campaigns, data from other sources have increasingly been used in resource assessments activities such as site selection, prefeasibility studies of projects and designing of measurement campaigns.

This thesis focuses on the application-oriented use of the meteorological Mesoscale Numerical Weather Prediction (NWP) Weather Research and Forecasting (WRF) model, as a tool for generating such alternative data by the dynamical downscaling of meteorological datasets.

1.2 Nature of Wind

Wind is the movement of large volumes of air masses. It is generated by pressure differences arising from unequal heating of the earth's surface and are driven by several forces (such as pressure gradient, Coriolis, and turbulent drag among others) which are also sources of variabilities in the wind [3]. As a result of these variations, like other atmospheric phenomena, wind occurs on a wide range of atmospheric scales, as illustrated in Figure 1. Global winds are primarily due to pressure gradients from unequal heating of the earth's surface and the influence of the Coriolis force and exhibit relatively less variation. However, within lowest 1 to 2 km of the earth's atmosphere, referred to as the atmospheric or planetary boundary layer (PBL), factors such as friction at the ground, the orography and the vertical distribution of temperature and pressure give rise to local winds and other wind phenomena (such as turbulence), which vary more significantly, on smaller scales (see Figure 1). Pressure and temperature differences interact with variations in local topography and surface conditions to create circulation systems such as land-sea, cross-valley and along-valley circulations. These result in local winds, common examples of which are land, sea and mountain valley breezes [4, 5]. In addition, synoptically windy conditions can result in winds being modified by mountains producing gap winds, mountain waves, among others [4]. These phenomena are well explained in several textbooks [3-6].

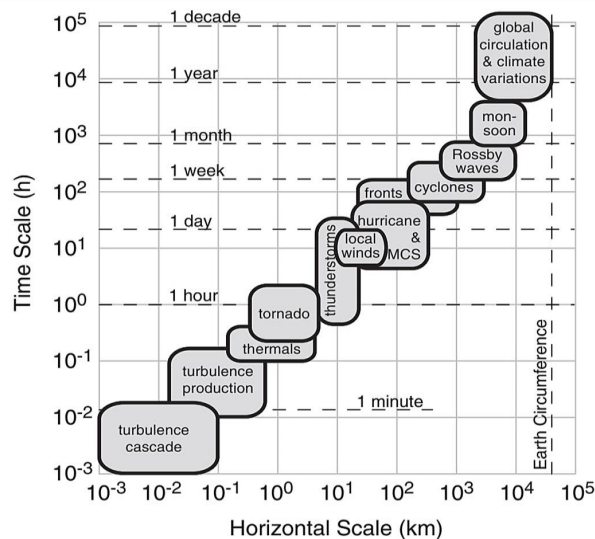


Figure 1: Typical time and spatial scales of meteorological phenomena [3]. The phenomena can be classified according to horizontal scale as; Macroscale (700 – 40000 km), Mesoscale (3 – 700 km), microscale (3 mm- 3 km) [3].

Vertically, wind also varies in the PBL. Wind turbines operate at heights within the PBL, which makes the understanding of vertical variation of wind characteristics within the layer important. A key determinant of the vertical wind speed profile (in addition to terrain, surface

roughness, and topography) is the stability of the atmospheric boundary layer. Atmospheric stability can be defined as the tendency to remain in hydrostatic equilibrium with respect to vertical displacements [7]. It is usually explained by the air parcel concept [7] and expressed in terms of the rates at which the temperature of the environment and a parcel of air decrease with increasing height (the environmental and adiabatic lapse rates respectively). In terms of the environmental lapse rate, the atmosphere can be unstable, stable, or neutral. These are well explained in textbooks such as [3, 4, 6, 8, 9]. The vertical wind profile under the three stability conditions is shown in Figure 2.

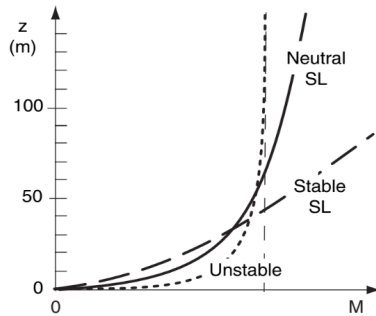


Figure 2: Typical wind speed profiles in the Surface Layer (bottom 5% of the ABL) [3]

1.3 The Role of Numerical Weather Prediction in Wind Resource Assessments

The speed characteristic of wind is of key interest in Wind Resource Assessments (WRA) as the amount of wind energy that can be generated depends on the cube of this characteristic. Due to this relationship, variabilities, uncertainties and errors in wind speeds tend to be amplified, with implications for wind power generation. Therefore, the optimal design of wind projects depends on an accurate and detailed understanding of the distribution of the wind speeds and other characteristics in the project area. This helps in a robust estimation of the energy production over the lifetime of a wind project. WRA involves the use of both existing measurements and modeling approaches to identify potential wind farm sites and determine the optimum siting of wind turbines (micro-siting) in wind farms to estimate the long-term energy production of a project. Though this can be done with relatively easy to acquire data from sources such as nearby meteorological stations, the best source of data for these purposes is measurements of the wind characteristics. However, owing to the expensive and time-consuming nature of wind mast measurement campaigns, it has increasingly become popular over the years to perform preliminary resource assessments with wind data that is downscaled from meteorological datasets.

Mesoscale Numerical Weather Prediction (NWP) models are popular dynamical downscaling tools in this regard. They belong to a category of meteorological models that are used for process studies and weather predictions [10]. They have increasingly been adapted for wind flow prediction over limited areas over the years. They make predictions of the wind speed for

locations (that correspond to the model grid) in an area by numerically downscaling meteorological datasets and can be coupled to microscale models for these purposes. They have traditionally been applied in the generation of wind maps for large area screening of feasible wind power project sites. However, in recent times, downscaled data are also being used in the design of mast measurement campaigns and to conduct pre-feasibility assessments of wind power projects.

Model validation (or reliability assessments) assesses uncertainties in the predictions of NWP models. The process plays a key role in the optimization of these models for desired purposes. Uncertainties (, as explained by [10]) are primarily due to;

- (a) an imperfect understanding of atmospheric processes, especially at the sub-grid scale,
- (b) insufficient simulation of these processes because of the models' grid resolutions, and
- (c) errors associated with the numerical assumptions.

The validation process of NWP models involves several techniques (as described by [10]), which may be applied separately to address specific needs. Sensitivity analyses are one such validation techniques. The Sensitivity analyses of NWP models involves verifications of model predictions made with different model options or inputs to establish the extent to which an option performs better than another, and the possible explanations for the difference in performance [10]. Wind sensitivity studies that have been reported in scientific literature have been found to adopt the local approach, which, as explained by [10], examines the impact of a limited range of inputs and options on the estimation of specific events or output parameters by NWP models. A challenge with sensitivity analyses for wind prediction applications is that, due to the influence of local factors (such as terrain features and atmospheric conditions which vary geographically) on the performance of some of the options (such as parameterization schemes) in NWP models [1, 2], it is often difficult to generalize the results of such studies for different geographic areas.

1.4 Motivation

With an Energy use per capita that is equivalent to one-third that of the world, the problem of low and unreliable access to electricity is one of Sub-Saharan Africa's greatest obstacles to social and economic development [11]. Power crises stemming from low and unreliable access to electricity is an issue all over the region.

Ghana has experienced not less than four of such crises since the turn of the century, costing the nation about US\$680 million in 2014 alone [12]. Electricity supply challenges in Ghana have stemmed from several factors over the years. These include over-dependence on electricity from thermal and hydro sources (which together constitute over 99% of the country's electricity mix). Demand for electricity in Ghana increased by over 50 percent between 2006 and 2016 [12] and currently, electricity from thermal plants that run on fossil fuels alone constitutes over 60% of the total generation capacity of the country. Solving the country's electricity challenges requires

measures that include diversifying the electricity generation mix through the development of other energy sources, including renewable sources such as wind and solar energy [12]. Several studies have reported the feasibility of the large-scale generation of electricity from wind in Ghana [13-19]. And though some efforts (such as a wind mapping activity in 2004, and ground-based mast measurements in selected areas along the coast) have been made towards the exploitation of the resource, development of the sector is still facing several challenges. These include limited or non-availability of reliable data for pre-feasibility or feasibility studies of projects [20].

Numerical Weather Prediction (NWP) models have increasingly been adapted for limited area mesoscale (and even microscale) downscaling of wind data from meteorological datasets for the purpose of mapping wind resources and providing data for pre-feasibility studies. Indeed, the wind mapping (at 50 m) for Ghana was conducted with one such Mesoscale-Microscale coupled models; the MESOMAP system from AWS Truepower (which comprises the Mesoscale Atmospheric Simulation System (MASS) and WindMap Microscale models). However, in addition to being a propriety model, limited verifications and adjustments were done during that exercise, due to a lack of adequate mast measurements at the time [21]. In addition, with the increasing hub heights of modern wind turbines, assessments at higher heights (other than the 50 m of the 2004 mapping), and the availability of time-series to enable the effective designing of mast measurements and pre-feasibility studies on power projects, are increasingly warranted. Furthermore, due to climate change and change in land use in Ghana over the past years, there is the need to update wind maps for Ghana using reliable and easily accessible tools.

The NWP Weather Research and Forecasting (WRF) model [22] is a widely used operational and research mesoscale model. Owing to diverse physics and dynamics options, several model-validation studies towards the application of the model for different purposes have been reported in the literature. However, no known studies have been reported on the validation of the model towards wind resource assessments in Ghana and the West African sub-region. Furthermore, sensitivity tests (of the WRF model for wind energy applications) in the international literature, have often been limited to high wind speed periods. In addition, they have often not considered all PBL schemes (which have been found to significantly affect model wind outputs) with all compatible surface layer physics options, and have often used decision making criteria that in our opinion, leaves room for potentially misleading conclusions to be drawn from these studies.

1.5 Aim and Objectives

Against this background, this thesis sought to verify the capability of the WRF model to dynamically downscale wind data from large-scale global meteorological datasets for resource assessments in Coastal Ghana. The aim was to identify and suggest possible ways of optimization of the WRF model (in terms of selected options) for applications such as wind mapping and

generation of time series data for pre-feasibility wind assessments primarily along the coast of Ghana.

The thesis involved a local sensitivity study (as explained earlier) of selected numerical and input data options of the model, to wind predictions at three heights. The options, (which are explained in Chapter two of this thesis) are;

- i. Simulation length and options in the WRF's Analysis Nudging technique (Paper I),
- ii. Planetary Boundary and surface layer Parameterization options (Paper II and Paper III), and
- iii. Input Land Use and Land Cover (LULC) and meteorological Gridded Binary (GRIB) datasets (Paper IV).

In achieving the aim of this thesis, insights, other than what had been reported in the literature, were offered into optimum combinations of the simulation run time and nudging options for wind simulations (Paper I). An alternative experimental approach in sensitivity studies of PBL schemes that deviates from a common practice in past studies in that, it considers high and low wind periods (as against the common practice of considering only high wind periods), is explored in Paper II. In addition, another limitation in the scope of several sensitivity studies in the tropics (in not exploring all SL schemes that can be used with a PBL scheme) is explored in Paper III. Factors that should be considered in selecting meteorological datasets from the NCAR's RDA archive for dynamical downloading to generate time series data for coastal Ghana were explored (Paper IV). The consistency in performance of the options, irrespective of evaluation criteria is used as a decision-making criterion to reduce the potential of drawing incidental test conclusions.

1.6 Thesis outline

Following this chapter, Chapter 2 of this thesis presents the verification data and criteria. The chapter begins with a brief description of the key features and options of the WRF model, with emphasis on the model options that were tested in this thesis. Details of the data that are used for the validation of model outputs are also presented in this chapter. The evaluation criteria on which the tested model options were inter-compared are also introduced.

The main findings from the tests are summarized and briefly discussed in Chapter 3. The main conclusions of each test and their possible implications for model performance in predicting wind speeds for resource assessment purposes are also discussed. The overall conclusion drawn from the thesis is presented in chapter 4, with recommendations for future researches.

An Appendix of Supplementary test results, as well as the 4 papers that were produced from the thesis follow the four chapters of this thesis.

DATA AND METHODOLOGY

This chapter presents brief overview of the WRF model. The overview covers descriptions of key model components, and the options that were the focus of this study. This is followed by the general framework of the thesis, and brief descriptions of verification criteria and the verification (or reference) data. The postprocessing method for model output is also presented

2.1 A Brief Overview of the Weather Research and Forecasting Model (WRF)

The WRF model is the product of a multi-organizational effort to build a mesoscale forecast and assimilation system that would be accurate, efficient, scalable to small atmospheric scales – primarily 1 to 10 km – and capable of operating on workstation-computer platforms [10]. As was the case in this thesis, all the simulations for this thesis were run on a workstation laptop with a quad-core (Xeon E3-1505M v6) processor. The model comprises the following principal programs, illustrated in Figure 3;

- a. The WRF Preprocessing System (WPS) which creates inputs for the ARW pre-processor (real) program for real-data simulations by using meteorological and terrestrial data
- b. the WRF software infrastructure (WSI) which accommodates key program components that includes the WRF the dynamics solvers; the Non-hydrostatic Mesoscale Model (NMM) core, and Advanced Research WRF (ARW) core, physics schemes and interface to interact with the dynamics, among other key programs.
- c. Postprocessors for analysis and verification of predictions.

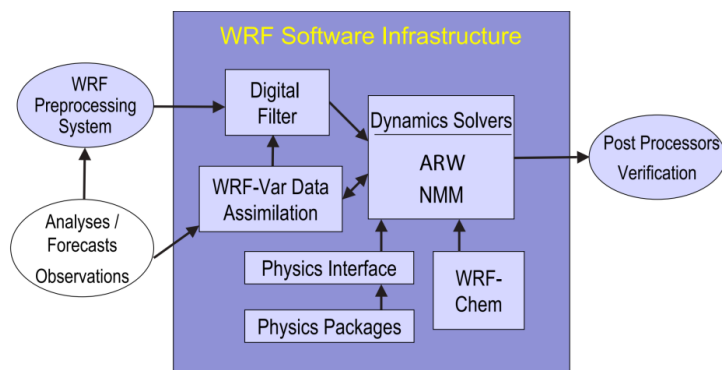


Figure 3: A Schematic of the main components of the WRF model [22]

2.1.1 The WRF Software Infrastructure

2.1.1.1 The ARW Dynamics and Numerics

The Governing Equations

The ARW core of the WRF model was used in this thesis. It incorporates fully compressible, non-hydrostatic Euler equations (with a run-time hydrostatic option available).

Descriptions of how the Euler equations are derived and other details are provided by [22]. Simplified versions of these governing equations (neglecting the Coriolis effect) as presented by [10] in cartesian coordinates comprise;

The equation of steady state given as;

$$p = \rho R_d T \quad (1)$$

The conservation law of mass;

$$\frac{\partial \rho}{\partial t} + \frac{\partial U}{\partial x} + \frac{\partial V}{\partial y} + \frac{\partial W}{\partial z} = 0 \quad (2)$$

Conservation law of momentum;

$$\frac{\partial U}{\partial t} + c_p \Theta \frac{\partial \pi}{\partial x} = -\frac{\partial Uu}{\partial x} - \frac{\partial Vu}{\partial y} - \frac{\partial Wu}{\partial z} + F_x \quad (3.1)$$

$$\frac{\partial V}{\partial t} + c_p \Theta \frac{\partial \pi}{\partial y} = -\frac{\partial Uv}{\partial x} - \frac{\partial Vv}{\partial y} - \frac{\partial Wv}{\partial z} + F_y \quad (3.2)$$

$$\frac{\partial W}{\partial t} + c_p \Theta \frac{\partial \pi}{\partial z} + g\rho = -\frac{\partial Uw}{\partial x} - \frac{\partial Vw}{\partial y} - \frac{\partial Ww}{\partial z} + F_z \quad (3.3)$$

Conservation law of energy;

$$\frac{\partial \theta}{\partial t} = -\frac{\partial U\theta}{\partial x} - \frac{\partial V\theta}{\partial y} - \frac{\partial W\theta}{\partial z} = 0 \quad (4)$$

In the above equations, $U = \rho u$, $V = \rho v$, $W = \rho w$, $\Theta = \rho\theta$. T is the absolute temperature, $c_p = 1004.5 JK^{-1}kg^{-1}$ and $R_d = (2/7)c_p$ is the heat capacity and the gas constant for dry air respectively, F_y , F_x and F_z are friction terms. π denotes the Exner function which is given as $(p/p_o)^{\wedge}(R_d/c_p)$, where p_o is the reference pressure.

In formulating these equations, the Earth's atmosphere over a geographic region is represented in the model by a three-dimensional (x, y, z) grid. The x and y dimensions are in equally spaced Cartesian coordinates, while the z dimension is over vertical levels in a terrain-following sigma or mass vertical coordinate system. For the flat (x, y) projection of the earth's spherical surface, map projections are used. Several map projection schemes are supported by the solver. However, specific projections are recommended to keep the map-scale factor (a measure of distance distortions from the transformation) close to 1 for numerical stability [23]. The map scale factor is defined as the ratio of the distance in computational space (Δx , Δy) to the corresponding distance on the earth's surface [22].

Denoted by η , the vertical coordinate varies in spacing and ranges in value from one at the surface of the earth to a value of zero at the top of the atmosphere in the model (defined as constant pressure surface). The η coordinate at each level is calculated as;

$$\eta = (p - p_t) / (p_s - p_t) \quad (5)$$

where p is the pressure at a particular level in the atmosphere, p_s is the surface pressure, and p_t is the pressure at the top of the atmosphere.

Model discretization and other issues for Numerical stability

Numerical solutions to the governing equations are solved using finite-difference approximations which requires the simulation domains to be discretized and the equations reduced to their finite difference equivalents [3]. For temporal discretization, the ARW solver uses the third order Runge-Kutta (RK3) time-split integration scheme [24]. An explanation of the scheme and how the ARW solver uses the scheme to advance a solution for prognostic equations at model time steps is provided by [10]. The model time step is limited by the advective Courant number, with implications for numerical stability, as explained by [10]. To ensure numerical stability in the WRF model, it is recommended that its value (in seconds) is maximum six times the horizontal grid distance in kilometers [22, 25].

The spatial discretization is performed on the staggered Arakawa C-grid, which allows for resolving gravity waves more accurately [7]. On the staggered C-grid the westerly (U) wind component is evaluated at the centres of the left and right grid faces and the southerly (V) and vertically (W) wind components at the centres of the upper and lower grid faces as illustrated in Figure 4. Further details of the grid system are provided by [7, 10].

Other numerical issues as well representation of sub-grid scale processes such as turbulence mixing, that cannot be solved on the simulation grid are addressed by filter and damping options as well as other formulations in the ARW solver [7]. Detailed descriptions of these are provided by [10, 22]. Vertical mixing filtering is disabled when a PBL parameterization is applied in simulations, as it is parametrized within the PBL physics [10]. Selection of filter and damping options in this thesis followed recommendations from [25].

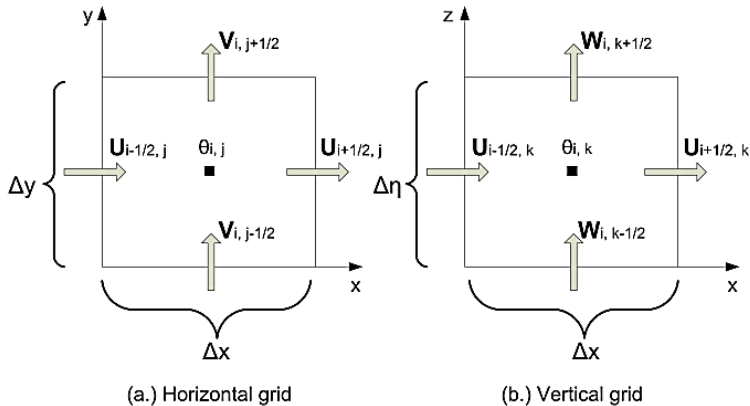


Figure 4: (a) Horizontal and (b) vertical grids of the ARW solver [7].

2.1.1.2 The ARW Physics Parameterization Options

Unresolved physical processes are approximated by physics parameterization schemes in the ARW solver. The physics parameterization schemes in WRF are divided into the following categories; Long-wave and Short-wave Radiation, Microphysics, Cumulus, Planetary Boundary Layer (PBL), and Surface (which comprises the Surface Layer (SL) as well as Land Surface Model (LSM) schemes) categories. A schematic of the interactions of the parameterization scheme categories is illustrated in Figure 5. Atmospheric temperature tendencies and surface radiative (downward longwave and shortwave) fluxes for the surface heat budget are provided by the radiation schemes [7]. Cumulus schemes parameterize vertical convective motions at sub-grid scales and provide atmospheric heat and moisture vertical profiles and sometimes cloud and rainfall tendency profiles in the atmospheric column [7]. The PBL and Surface (LSM and SL) schemes interact directly to parameterize the vertical sub-grid scale transport processes in the atmosphere.

Turbulence (which produces vertical mixing) plays a key role in these processes and acts as a feedback mechanism in wind circulation [5, 29, 30]. In addition, several studies have reported significant impacts of the choice of PBL schemes in wind energy applications of the WRF model. Therefore Papers 1 and 2 examined the impacts of these options on the wind prediction capability of the WRF model. The choice of all the other parameterization options were based on practices from past studies (mostly in the tropics) [26-30] and recommendations from [25]. A more detailed overview of PBL and SL parameterization in WRF is provided in Paper III. Details and descriptions of the PBL, SL and LSM schemes available in the WRF model are available in several papers and textbooks [7, 8, 10, 31-33].

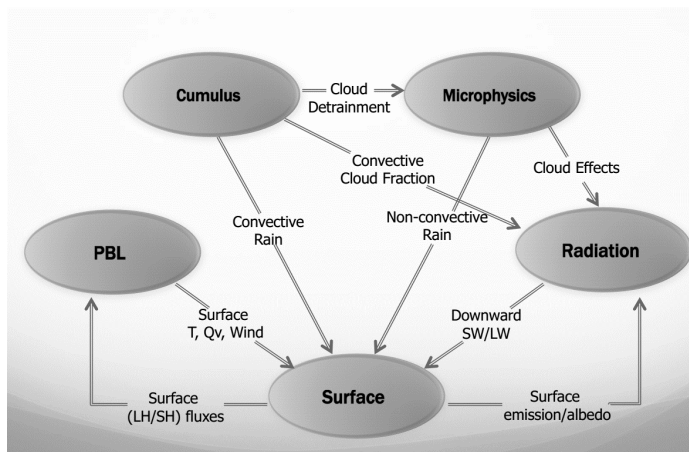


Figure 5: Interaction of parameterization schemes in WRF [34]

2.1.1.3 WRF Nudging

Nudging is a technique in the Four-Dimensional Assimilation (FDDA) [35-39] system of the WRF model, that helps keep the simulations close to the analyses or/and observations over a

simulation period (Skamarock et al., 2008). The available nudging techniques in the WRF model can be used for dynamical initialization, to create four-dimensional meteorological datasets and to improve the boundary conditions for the solver. However, the analysis or grid nudging technique attempts to bridge the gap between predictions of physical variables and time-interpolated large-scale meteorological conditions from the input data [7] by adding an additional tendency term to the nudged variable's equation, as explained by [40]. The technique has been used in several studies [20, 51, 52] on wind downscaling. Options in using the technique include; a choice of variables to nudge, the nudging strength or co-efficient, and the choice of whether to nudge variables in the PBL or not. Disabling nudging in the PBL is a common practice in simulations, followed with the aim of allowing mesoscale processes to freely develop (within the PBL) [29, 41, 42]. To achieve this in WRF, one can choose to apply nudging to variables above a fixed vertical level, or apply it to levels above a model-determined level (that corresponds to PBL height predictions) during the simulations [43, 44]. It has been reported that the two methods have different impacts on wind simulations [44]. Paper I investigated the impacts of combining these methods (in addition to a third method) of applying nudging with varying simulation lengths (run times) on model predictions of wind.

2.1.2 Input Data and the WRF Preprocessing System (WPS)

Input data for WRF model comprises terrestrial or static data (land-use, terrain, soil types) and time-varying meteorological fields (from forecast, analysis/re-analysis and climate model data) of different origins and different horizontal resolutions and projections. The program real in the ARW prepares the initial and lateral boundary conditions for the WRF solver with these datasets after they have been interpolated onto the projected simulation domains by the WRF Preprocessing System (WPS). The program components and data flow in and out of the WPS is shown in Figure 6. The model comes with several LULC datasets and two terrain datasets the USGS GTOPO30 [45], and the GMTED2010 [46]. It is possible to run the model with datasets apart from these.

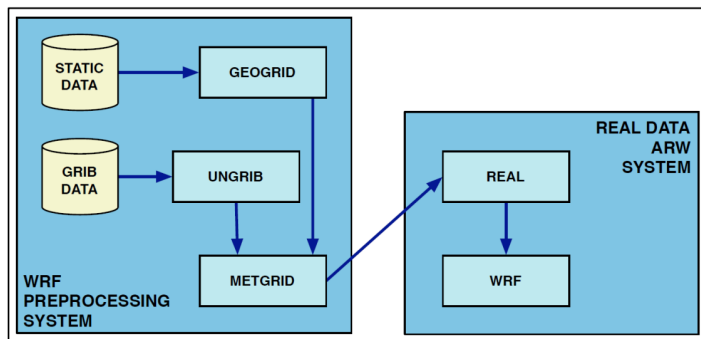


Figure 6: Schematic of the program components and data flow in and out of the WPS [22]

The impacts of selected input datasets on data downscaled with the WRF model were examined in Paper IV. The input datasets comprised the two global LULC datasets that are available on the WRF version 3 Geographical Static Data Downloads Page [47], as well as selected Gridded Binary (GRIB) datasets from the National Centre of Atmospheric Research (NCAR) Research Data Archive (RDA) [48]. Descriptions and characteristics of the datasets are summarized in Paper IV. Terrain datasets were not tested as we found little difference between the two global datasets that cover coastal Ghana in the results of a comparison presented by [49].

2.2 Methodology

2.2.1 Study Framework

The general framework for the thesis (illustrated in Figure 7) is based on a proposed framework by [50] for exploring optimal model configurations of NWP models for different purposes. The reference data, evaluation criteria, and model options that were selected for testing are elaborated on in the sections that follow.

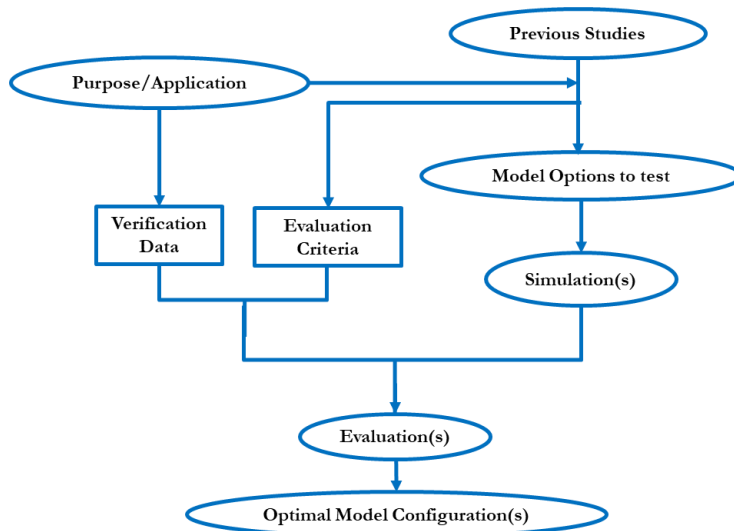


Figure 7: Study Framework.

2.2.2 Evaluation Criteria and Observational Data

Several verification criteria can be used in sensitivity studies [10]. In this thesis, statistical verifications of the model predictions were done by prediction-observation comparisons, in which the following statistical error metrics (which were selected based on their use in similar wind sensitivity studies [30, 41, 51-53]) were calculated;

- i. Mean Error or Mean Bias (ME) which was used as a measure of the tendency of the options to underpredict or overpredict wind speeds,
- ii. Root Mean Squared Error, which was used as a measure of accuracy,

- iii. Standard Deviation of the Error (STDE) which was used as a measure of error dispersion and consistency [41, 52], and
- iv. Correlation Coefficient (CC).

The error metrics were calculated according to formulations (which are provided in the appendix) taken from past WRF wind sensitivity studies such as [30, 41, 51-53]. They were combined into a Skill Score which was calculated with the formulation from [54]. The skill score was used to rank the options. In addition, error metric benchmarks (RMSE < 2 m/s, ME < ± 0.5 m/s, CC ≥ 0.7) as used by [28, 55]) were also used to evaluate the impacts of the options on model performance.

The Weibull distribution is widely used in many fields of the wind energy industry for modelling wind speed data [56]. Therefore, the model predictions were also verified in comparisons of the Weibull probability and cumulative density plots generated from predicted and observational data. Quantitative comparisons of the Weibull cumulative densities errors as well as mean wind power densities estimated from predictions and observations were also compared. Formulations of the Weibull parameter estimations and the functions of the distributions were as has been used in several past studies [14, 40].

The observational data for evaluations were derived from mast measurements of wind data that were conducted by the Energy Commission of Ghana, in the year 2013. Selected details of the data and instrumentation are summarized in Table 1. In addition to these data, monthly average wind speeds of measurements at 60 m from [57] were also used for verification.

Table 1: Selected Details of Observational data and instrumentation.

Period	12 months (January - December 2013)
Data time step	10 minutes
Mast location	5.7861 °N and 0.9188 °E
Mast type	NRG 60m XHD
Measurement heights	40 m, 50 m, 60 m
Anemometer type	NRG #40C

2.2.3 Postprocessing of Model Outputs

As the WRF model predicts wind speed components on vertical levels, (not heights in meters at which observational data were measured), and given the staggered nature of the wind components, postprocessing of model outputs were necessary to determine actual wind speeds at the heights (in m) at which observational data were measured and at the mast location for direct comparison. In this thesis, all such postprocessing calculations were done with a script written in the R programming software. The script generally followed the steps outlined in the flowchart shown in Figure 8.

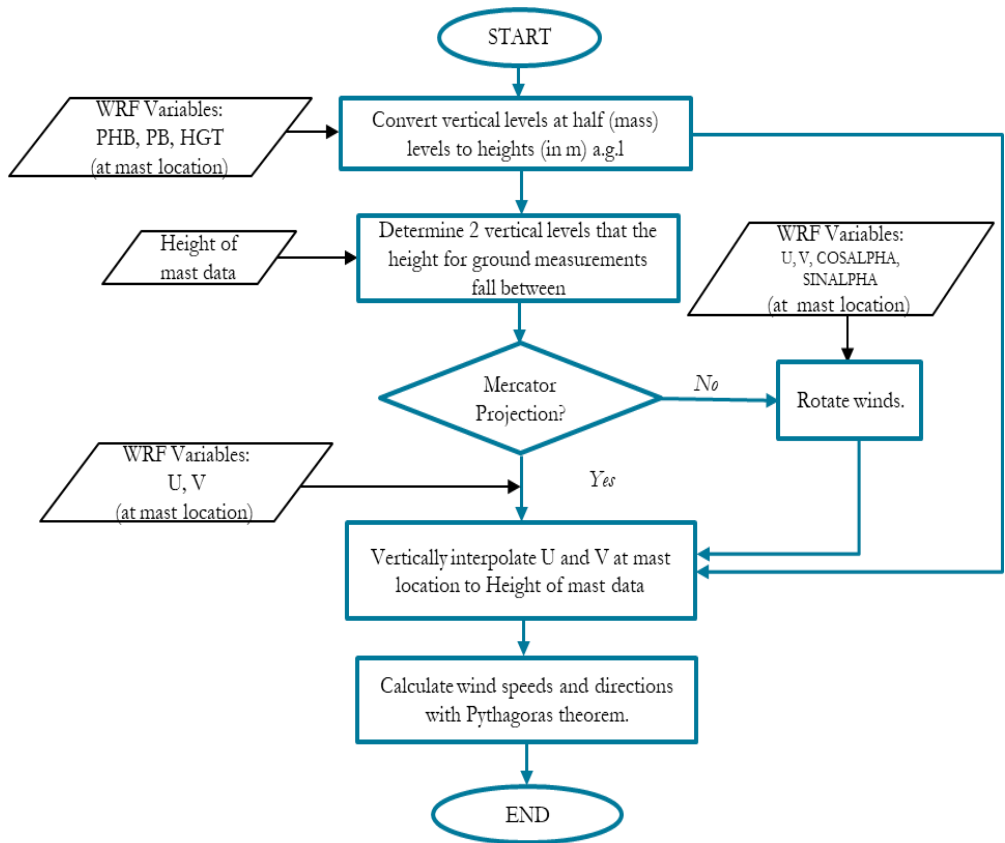


Figure 8: Flowchart for postprocessing of model outputs. Conversion of the vertical levels to heights in meters used formulations from [58, 59], and rotation of winds was according to [60].

SUMMARY OF MAIN FINDINGS

Results and findings were communicated in four papers, which are summarized and discussed here. In addition, supplementary results from an evaluation run of the model with a configuration based on the finding of the four papers is also discussed.

3.1 Overview

In achieving the aim of this thesis, the relative impacts on wind predictions of the choices of model simulation run times, vertical levels above which predictions should be nudged, planetary boundary and surface layer parameterization schemes, as well as input (terrestrial and GRIB meteorological) datasets were investigated.

NWP models diverge and accumulate approximation errors with increasing simulation run times [30, 52]. Carvalho et al. [52] reported that, relatively short run times of 2 days, combined with grid nudging reduces this error. Ohsawa et al. [1] reported that, applying nudging above PBL heights predicted by the Mellor-Yamada-Janjic (MYJ) PBL scheme produces better results as compared to disabling it below a fixed height. Paper I was aimed at deepening the understanding of the impact of several combinations of these two options on wind simulations. It combined five run times that had commonly been used in other studies [29, 30, 32, 33, 41, 52, 61-63], with three methods of applying nudging. On the choice of PBL schemes to use in simulations, it was also realized from studies in the literature that most sensitivity studies on wind predictions do not test PBL schemes with all their compatible SL schemes. These issues (comparative performance of different PBL schemes, and they affected when paired with different SL schemes) were investigated in Paper II and Paper III. A potentially more effective (and more novice friendly) approach to sensitivity studies of PBL options (and possibly other options) was used in Paper II. Paper IV explored impacts of selected terrestrial datasets from [47], and available Gridded Binary (GriB) datasets available from [48] on model performance. The main findings from the four papers are summarized in the sections that follow.

3.2 Impact of Simulation Run times and vertical levels for nudging.

Graphical comparisons of the error metrics of the options tested in Paper I are presented in Figure 9. As can be seen, a combination of simulations of shorter runs with the grid nudging technique did improve most of the speed prediction error metrics from the WRF model as reported by [52]. However, it was found that the margin varied with choice of method of applying (disabling) nudging. In short simulations (lasting 1 or 2 days at a time), nudging above the default 10 vertical levels (N-10-L) resulted in predictions with relatively better bias (lower ME) and accuracy (lower RMSE), but relatively worse consistency (higher STDE) and prediction-observation correlation (CC). However, with increasing run times, all error metrics deteriorated at a relatively faster rate,

as compared to an alternative approach of nudging (above a model determined level (N-PBLH)). In addition, the latter approach exhibited relatively better consistency (lower STDE) and acceptable prediction-observation correlation ($CC \geq 0.7$), irrespective of the run times it was tested with. Results of the third method and the first (N-10-L) were very similar, so they are not presented here.

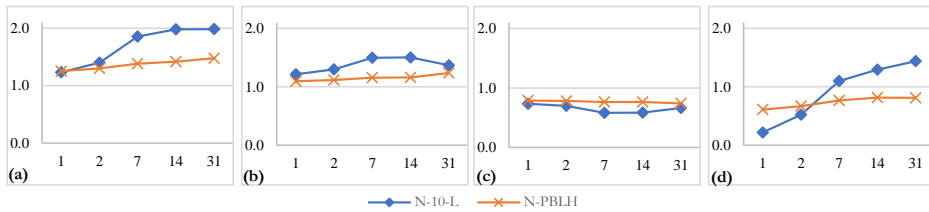


Figure 9: Comparative performance (at 60 m) of two methods of applying nudging in terms of; (a) RMSE (b) STDE (c) CC (d) Absolute ME

Based on results on speed prediction from Paper I, it was concluded that, consistent with the findings of [52], running simulations of relatively shorter run times does reduce prediction error metrics in wind data that is downscaled with the WRF model. The analysis nudging option of disabling nudging variables above a model determined vertical level offers more consistent and better observation-correlated predictions. Furthermore, consistent with the reports of [44], with relatively longer run times it was also more accurate, as compared to its alternative option (of nudging above the default 10 levels). Based on these, it was concluded that it is probably the more reliable method for applying nudging during downscaling of wind data with the WRF model.

3.3 Impact of PBL and SL parameterization schemes on predictions.

Given the importance of PBL-SL pairs in modelling wind flow in the PBL, their impact was also examined in Paper II and Paper III. A limitation that was realized in several of the past studies in the tropics [26-30] that were consulted during this study was that, they often did not test PBL schemes with multiple compatible SL schemes. In addition, it was realized it is common practice in studies for studies to be conducted in periods with high wind speed conditions only. Furthermore, few studies have examined the relative performance of all the available PBL schemes in WRF over a period comprising a wide range of wind conditions. In Paper II, a preliminary assessment of almost all the PBL schemes with their most commonly paired SL schemes (in the literature) was conducted. This preliminary assessment aimed at reducing the number of PBL schemes to be examined with all their compatible SL schemes. A second aim was to see how the results of a novel approach for conducting these sensitivity tests (illustrated in Figure 10) would compare with findings that have been reported in the literature. The approach differs from what has been used in previous published studies in that, it relies on the criterion of consistency in

performance (in terms of several error metrics) of assessing the relative performance of the PBL schemes being tested. In addition, it considers a wider range of wind conditions (high and low wind speed conditions as against the common practice of only high wind conditions for tests as observed in the literature) and uses fewer simulations to draw a conclusion on the relative performance of the schemes. Based on the results of this preliminary assessment (which was found to be largely consistent with what had been reported in other studies in the tropics), five PBL schemes were selected for further testing with all their compatible SL schemes. Findings of this second test are reported in Paper III.

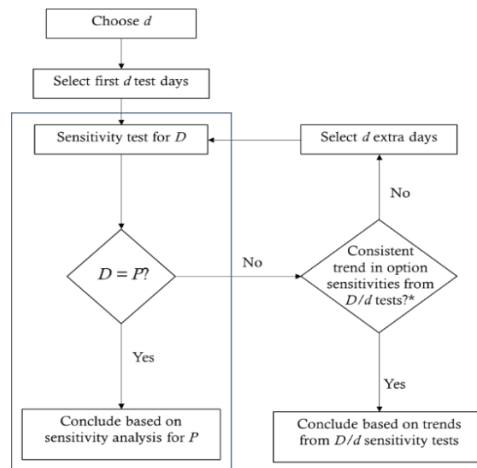


Figure 10: Flowchart of test approach used in Paper II.

(d = number of test days for each sensitivity test (2 was used in Paper II); D = Total number of test days; P = total number of days in entire test period; *Larger D/d means more points to assess trend.)

Based on results of the two tests, it was concluded that the second order Mellor–Yamada Nakanishi Niino Level 3 (MYNN3) Turbulent Kinetic Energy (TKE) PBL scheme is probably best for wind predictions at this site and perhaps coastal Ghana. The MYNN3 often predicted wind speeds with the best, (or one of the best) combination of error metrics when it was paired with the Eta SL scheme. In addition, Wind Power Densities (WPD) and cumulative probability estimates of the scheme often compared relatively better to estimates from the mast data. Furthermore, predictions of the MYNN3-Eta PBL-SL pair for 4 other locations in the regions were mostly found to be within the benchmarks for error metrics. Based on these, it was concluded that the MYNN3-Eta PBL-SL pair is probably good for wind speed downscaling with the WRF model for coastal Ghana and perhaps other coastal areas in the West-African sub-region.

3.4 Possible impact of different Input Datasets.

The possible impact of five Gridded Binary (GriB) datasets available from [48] and the two LULC datasets available for version of the WRF model from [47] were investigated in Paper IV. Available static terrain datasets (, also from [47]) were not included in this study as, based on

results of a comparison from [49], it was concluded that concluded there is little difference between them for coastal Ghana. Results suggested that the Moderate Resolution Imaging Spectroradiometer (MODIS) LULC generally produced downscaled data with better error metrics and more accurate Mean Wind Power Densities (WPD), probably because it is relatively newer than the United States Geological Survey (USGS) LULC. However, the difference between the error metrics and Mean WPD of the two were not so large. On the Gridded Binary (GRIB) meteorological datasets that were tested, it was realized that data assimilation techniques that were used during the analysis/reanalysis process of preparing these datasets often correlated well with how well they performed in terms of verification. It was therefore concluded that this characteristic of the datasets could probably be a good criterion for selection of datasets for downscaling wind data. The Japan Meteorological Agency Reanalysis (JRA-55) and the National Centre for Environmental Prediction Final Operational Global Analysis (NCEP GFS-FNL) performed relatively better than the 3 other datasets that were tested in this study.

3.5 Performance assessment of based on the sensitivity tests.

Following the findings reported above, a configuration based on the findings of the four papers was tested in an evaluation run spanning the entire year of 2013. This configuration is presented in Table A1 in the Appendix. Results for the site at which we had full data, (presented in Table A2 in the Appendix) indicate that the proposed configuration could predict annual wind speeds for coastal Ghana, with most error metrics within the benchmarks. However, the predictions for the two locations further inland (i.e., SEG, and DEN) exhibited larger bias compared to the two locations nearer to the coast (See Table A3 in the Appendix). This suggests that predictions of the configuration tend deteriorate further inland, when the annual mean prevailing wind direction in the area (shown in Figure A1 in the appendix) is considered in addition to this trend. They also suggest that the configuration is probably good for downscaling data for offshore areas near Ghana.

CONCLUSION AND RECOMMENDATIONS FOR FUTURE WORK

4.1 Conclusions

The focus of this thesis was on the sensitivity analyses of the Weather Research and Forecasting (WRF) model towards its application for the dynamical downscaling of wind data for wind resource assessment in Coastal Ghana. Wind data that were downscaled with selected numerical options and input data options were compared with observations to assess the relative capabilities and limitations of the options, so that informed decisions can be made on how to apply them for wind resource assessment purposes in coastal Ghana. It is concluded from the results of the study that;

- The method of disabling analysis nudging below a model-determined level is probably more reliable for wind predictions, especially in simulations with relatively longer run times (more than 2 days in our tests). And the choosing of simulation run times should for wind data downscaling should probably be done taking nudging options into consideration.
- A test approach that considers the consistency in performance of candidate model options when assessed with several criteria, is worth considering as a decision-making criterion in sensitivity tests, especially by novices and people without the requisite background in Meteorology who want to apply the WRF model. In addition, future sensitivity tests (for wind energy applications) should be over a wider range of wind conditions and should consider PBL schemes with all their compatible SL schemes.
- The Higher order TKE closure Mellor–Yamada Nakanishi Niino Level 3 (MYNN3) Planetary Boundary Layer (PBL) scheme is probably better for wind simulations at this site (and probably Coastal Ghana and perhaps west Africa, given the similarity in climate), when combined with the Eta Surface Layer scheme. The prevailing annual mean wind directions and the mast locations suggest that, these schemes are probably also good for predicting offshore wind in Ghana. However, verification is needed on this. Other PBL schemes that show promise include the University of Washington-TKE (UW-TKE), and the Yonsei University (YSU) schemes.
- The two global Land Use Land Cover datasets from WRF Geographical Static Data probably do not differ significantly, in their impacts on wind data that is downscaled for Coastal Ghana with the WRF model. The impacts of different Gridded Binary (GRIB) meteorological datasets vary more significantly. And the data assimilations techniques that are used in the reanalysis/analysis process of preparing these datasets is worth considering as a criterion for their selection for downscaling with the WRF model.
- When correctly configured, the WRF model is capable of downscaling time series wind data that can meet the benchmarks used in this study for this site (and probably other areas in coastal Ghana, and the West African sub-region).

4.2 Recommendations for Future Work

The following are recommended for consideration in future works;

- Given the limited amount of mast measurement data that was used in this study, future studies should focus on the verification of the promising configurations with data from other locations and preferably at greater heights and over longer study periods. Verifications of the offshore wind prediction capability of the model along the Ghanaian and West-African Coast should also be investigated.
- Future tests of the input meteorological datasets at better temporal resolutions. In addition, given the nature of the local wind, the test of different Sea Surface Temperature (SST) data is also recommended.
- Ensemble prediction systems incorporating multiple relatively good options to reduce uncertainty should also be investigated.

APPENDIX

Configuration and results of evaluation run.

Table A1: Configuration for one-year evaluation test

Initial and boundary conditions	NCEP Final Analysis (GFS-FNL): 1° x 1° and 6 hrs resolution.		
Land Use data	MODIS (with lakes) + WRF defaults (Paper IV)		
Topographical data	30-arc-second USGS GMTED2010		
Map Projection	Mercator		
Vertical Resolution	45 terrain following eta levels (automatically set)		
Horizontal resolution (km)	25	5	1
Domain size (grid points)	121 x 120	141 x 186	181 x 121
Model timestep (seconds)	120		
Simulation length and Nudging options	Monthly runs with Nudging above model determined levels (Paper I)		
Parameterization Schemes:			
Cloud Microphysics (MP)	Eta microphysics (ETA) [64]		
Long-wave Radiation (LW-Rad)	Rapid Radiative Transfer Model (RRTMG) [65]		
Short-wave Radiation (SW-Rad)	Dudhia [66]		
Surface Layer (SL)	Eta Similarity (Eta) [67-69] (Paper III)		
Land Surface Model (LSM)	Unified Noah [70]		
Planetary Boundary Layer (PBL)	MYNN3 (Paper II and Paper III)		
Cumulus	Kain-Fritsch [71] (for domain 3 only [22, 52])		

Table A2: Wind speed comparisons at 60 m for mast and WRF downscaled data at site ANL

	Jan	Feb	Mar	Apr	May	Jun	Jul	Aug	Sep	Oct	Nov	Dec	Annual
Mast Mean	5.14	6.33	6.57	5.42	4.68	6.79	6.95	7.10	7.43	6.35	5.98	5.92	6.21
WRF Mean	5.28	6.67	7.41	6.11	5.51	7.87	7.18	7.26	7.04	6.23	6.06	5.54	6.51
Mean Error	0.14	0.33	0.84	0.70	0.84	1.08	0.24	0.17	-0.39	-0.12	0.08	-0.37	0.29
RMSE	1.67	1.42	1.71	1.96	2.25	2.78	1.55	1.53	1.20	1.22	1.21	1.38	1.72
STDE	1.66	1.38	1.48	1.83	2.08	2.57	1.53	1.52	1.14	1.21	1.21	1.33	1.69
CC	0.63	0.76	0.55	0.56	0.42	0.27	0.50	0.42	0.73	0.73	0.69	0.74	0.61

Table A3: Comparisons of error metrics (from monthly averages of data) for three other sites.

	ME	RMSE	STDE	CC
SEG (5.872° N, 0.345° E)	-0.80	1.00	0.60	0.73
DEN (6.112° N, 1.141° E)	-1.19	1.31	0.56	0.66
DZI (5.774° N, 0.714° E)	-0.20	0.53	0.50	0.84

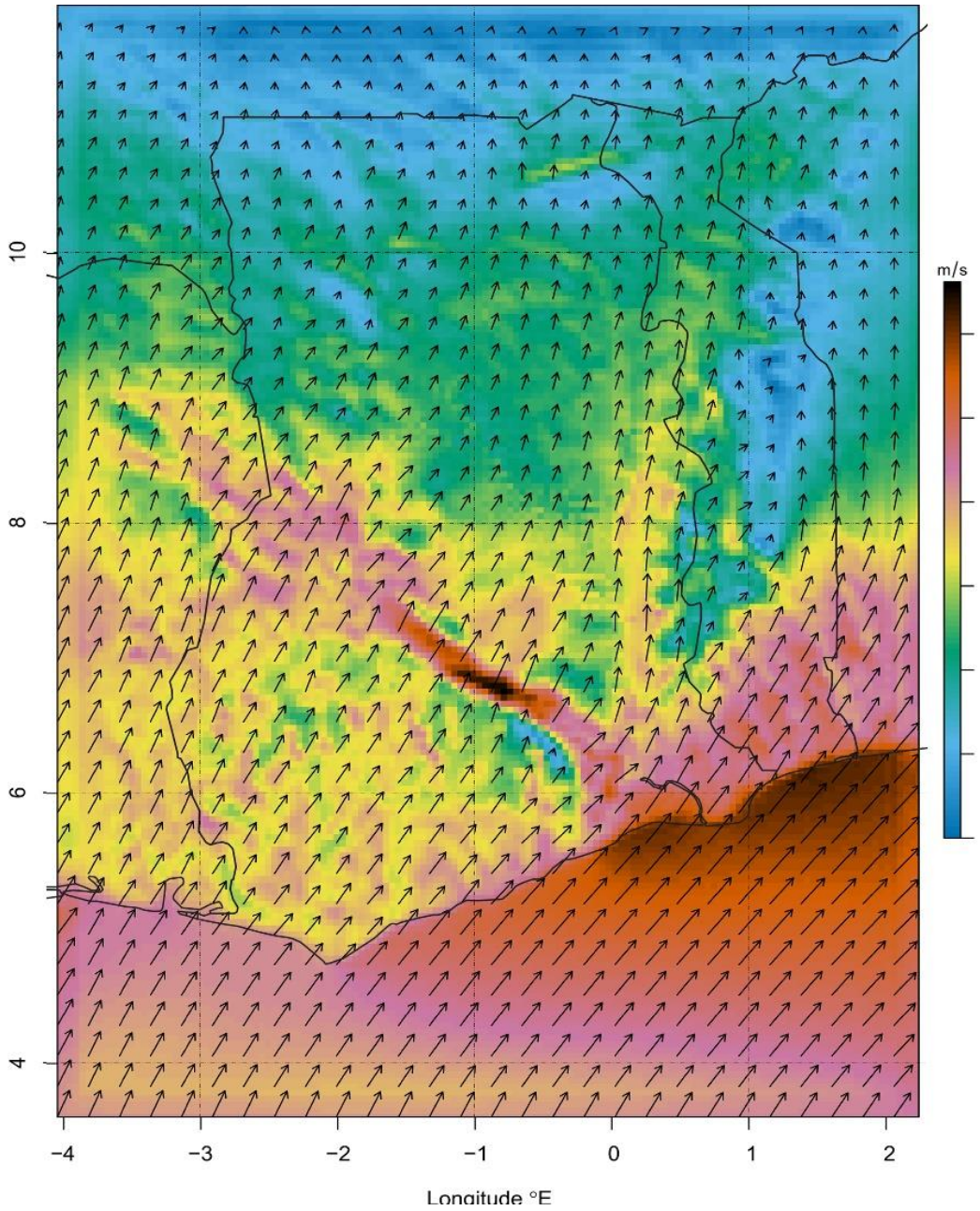


Figure A1: Annual mean wind fields for Ghana and neighboring countries
(at 60 m a.s.l on 5 km x 5 km grid)

Selected Formulas that were applied in the evaluation of options

- Root Mean Squared Error

$$RMSE = \left(\frac{1}{N} \sum_i^N (v_{sim} - v_{obs})^2 \right)^{0.5}$$

N – number of data points, v_{sim} – downscaled wind speed, v_{obs} – observed wind speed

- Mean Error (Mean Bias)

$$ME = \frac{1}{N} \sum_i^N (v_{sim} - v_{obs})$$

- Standard Deviation of the Error

$$STDE = (RMSE^2 - ME^2)^{0.5}$$

- Correlation Coefficient

$$CC = \frac{\sum (X - \bar{X})(Y - \bar{Y})}{\sqrt{\sum (X - \bar{X})^2 \sum (Y - \bar{Y})^2}}$$

where X and Y are the simulated and observed wind speeds respectively

- Combined Error Metrics (Skill Score)

$$\text{Skill Score} = (1 - RMSE_{NORMALIZED}) + (1 - |ME|_{NORMALIZED}) + (1 - STDE_{NORMALIZED}) + CC_{NORMALIZED}$$

- Empirical method of calculating dimensionless Weibull parameters

$$k = \left(\frac{\sigma}{\bar{v}} \right)^{-1.086}$$

$$c = \frac{\bar{v}}{\Gamma\left(1 + \frac{1}{k}\right)}$$

k – shape parameter, c – scale parameter, \bar{v} – average wind speed, Γ – gamma function

- Weibull Cumulative Distribution Function

$$F(v) = 1 - \exp\left[-\left(\frac{v}{c}\right)^k\right]$$

- Maximum absolute Cumulative Density Function Error

$$\text{Max CDF Error} = \max |F(v_i)_{obs} - F(v_i)_{sim}|$$

- Mean Wind Power Density

$$\text{Mean WPD} = \left[\frac{1}{2} \rho c^3 \Gamma \left(1 + \frac{3}{k} \right) \right]$$

ρ - density.

REFERENCES

1. Breeze, P., *Chapter 11 - Wind Power*, in *Power Generation Technologies (Third Edition)*, P. Breeze, Editor. 2019, Newnes. p. 251-273.
2. Global Wind Energy Council, *GWEC Global Wind Report - 2018*. 2018.
3. Stull, R., *Practical meteorology: An Algebra-based Survey of Atmospheric Science*. BC Campus. 2016
4. Stull, R., *Meteorology for scientists and engineers*. Brooks/Cole. 2000
5. Tarbuck, E.J. and F.K. Lutgens, *The Atmosphere: An Introduction to Meteorology*. Prentice Hall. 1979
6. Wallace, J.M. and P.V. Hobbs, *Atmospheric Science: An introductory Survey*. Vol. 92. Elsevier. 2006
7. Giannakopoulou, E.M., *Land–Boundary Layer–Sea Interactions in the Middle East*. 2012.
8. Salby, M.L., *Fundamentals of Atmospheric Physics*. Elsevier Science. London NW1 7BY, UK 1996
9. Stull, R.B., *An introduction to boundary layer meteorology*. Vol. 13. Kluwer Academic Publishers. Dordrecht, The Netherlands. 1988
10. Giannaros, C., *Sensitivity analysis and optimization of a mesoscale atmospheric model*. Vol. Doctor of Philosophy. Aristotle University of Thessaloniki, Faculty of Physics. Thessaloniki, Greece, . 2018
11. Hafner, M., S. Tagliapietra, and L. De Strasser, *Energy in Africa: Challenges and Opportunities*. Springer. 2018
12. Kumi, E.N., *The electricity situation in Ghana: Challenges and opportunities*. 2017
13. Asumadu-Sarkodie, S. and P.A. Owusu, *The potential and economic viability of wind farms in Ghana*. Energy Sources, Part A: Recovery, Utilization, and Environmental Effects, 2016. **38**(5): p. 695-701.
14. Adaramola, M.S., M. Agelin-Chaab, and S.S. Paul *Assessment of wind power generation along the coast of Ghana*. Energy Conversion and Management, 2014. **77**, 61-69 DOI: <http://dx.doi.org/10.1016/j.enconman.2013.09.005>.
15. Mallet, V. *Renewable Energy – what is Ghana’s wind power potential?* Available from: <http://www.arrakis-group.com/energy/renewable-energy-what-is-ghanas-wind-power-potential/> [Accessed on 25/09 2016]
16. Zusammenarbeit, D.G.f.I. and G. GmbH, *Wind Energy in Ghana Potential, Opportunities and Challenges*, F.M.f.E.A.a. Energy, Editor. 2015, Federal Ministry for Economic Affairs and Energy: Germany.
17. Energy Commission of Ghana, *The SWERA Ghana Project*. n.d., Energy Commission of Ghana, .
18. Safo, P., *Wind power plant potentials in Ghana*. 2013, Vaasan ammattikorkeakoulu.
19. Osei Yeboah, E., *Technical and Financial Assessment of a 50 MW Wind Power Plant in Ghana*, in *Department of Mechanical Engineering*. 2010, Kwame Nkrumah University of Science and Technology. p. 90.
20. Essandoh, E.O., E.Y. Osei, and F.W. Adam, *Prospects of wind power generation in Ghana*. Int. J. for Mech. Eng. and Technology, 2014. **5**(10): p. 156-179.
21. National Renewable Energy Laboratory (NREL), *Ghana Wind Energy Resource Mapping Activity*. NREL. Golden, CO, USA. 2004
22. Skamarock, W.C., J. B. Klemp, J. Dudhia, D. O. Gill, D. M. Barker, M. G Duda, X.-Y. Huang, W. Wang, and J. G. Powers *A Description of the Advanced Research WRF Version 3*. NCAR Tech. Note NCAR/TN-475+STR, 2008. DOI: doi:10.5065/D68S4MVH
23. Warner, T.T., *Numerical weather and climate prediction*. Cambridge University Press. Cambridge CB2 8RU, UK. 2011
24. Wicker, L.J. and W.C. Skamarock, *Time-Splitting Methods for Elastic Models Using Forward Time Schemes*. Monthly Weather Review, 2002. **130**(8): p. 2088-2097.
25. UCAR. *WRF Model Users' Page: namelist.input: Best Practices*. Available from: http://www2.mmm.ucar.edu/wrf/users/namelist_best_prac_wrf.html [Accessed on 10 Sep 2019]
26. Madala, S., et al. *Mesoscale atmospheric flow-field simulations for air quality modeling over complex terrain region of Ranchi in eastern India using WRF*. Atmospheric Environment, 2015. **107**, 315-328 DOI: 10.1016/j.atmosenv.2015.02.059.
27. Mughal, M.O., et al. *Wind modelling, validation and sensitivity study using Weather Research and Forecasting model in complex terrain*. Environmental Modelling & Software, 2017. **90**, 107-125 DOI: 10.1016/j.envsoft.2017.01.009.
28. Gunwani, P. and M. Mohan *Sensitivity of WRF model estimates to various PBL parameterizations in different climatic zones over India*. Atmospheric Research, 2017. **194**, 43-65 DOI: 10.1016/j.atmosres.2017.04.026.
29. Surussavadee, C. *Evaluation of WRF near-surface wind simulations in tropics employing different planetary boundary layer schemes*. 2017 8th International Renewable Energy Congress (IREC), 2017. 1-4 DOI: 10.1109/IREC.2017.7926005.

30. Chadee, X., N. Seegobin, and R. Clarke *Optimizing the Weather Research and Forecasting (WRF) Model for Mapping the Near-Surface Wind Resources over the Southernmost Caribbean Islands of Trinidad and Tobago*. *Energies*, 2017. **10**, 931 DOI: 10.3390/en10070931.
31. Cohen, A.E., et al. *A review of planetary boundary layer parameterization schemes and their sensitivity in simulating southeastern US cold season severe weather environments*. *Weather and forecasting*, 2015. **30**, 591-612 DOI: 10.1175/WAF-D-14-00105.1.
32. Banks, R.F., et al. *Sensitivity of boundary-layer variables to PBL schemes in the WRF model based on surface meteorological observations, lidar, and radiosondes during the HygrA-CD campaign*. *Atmospheric Research*, 2016. **176-177**, 185-201 DOI: <https://doi.org/10.1016/j.atmosres.2016.02.024>.
33. Mohammadpour Penchah, M., H. Malakooti, and M. Satkin *Evaluation of planetary boundary layer simulations for wind resource study in east of Iran*. *Renewable Energy*, 2017. **111**, 1-10 DOI: <https://doi.org/10.1016/j.renene.2017.03.040>.
34. Dudhia, J. *WRF (3.9) Modeling System Overview*. Available from: https://mcc2.org/wmogurmc/images/workshops/ASEAN/day2/WRF_overview.pdf [Accessed on 23/April/ 2019]
35. Stauffer, D.R. and N.L. Seaman *Multiscale Four-Dimensional Data Assimilation*. *Journal of Applied Meteorology*, 1994. **33**, 416-434 DOI: 10.1175/1520-0450(1994)033<0416:Mfdda>2.0.Co;2.
36. Liu, Y., et al. *The Operational Mesogamma-Scale Analysis and Forecast System of the U.S. Army Test and Evaluation Command. Part I: Overview of the Modeling System, the Forecast Products, and How the Products Are Used*. *Journal of Applied Meteorology and Climatology*, 2008. **47**, 1077-1092 DOI: 10.1175/2007jamc1653.1.
37. Barker, D., et al. *The weather research and forecasting model's community variational/ensemble data assimilation system: WRFDA*. *Bulletin of the American Meteorological Society*, 2012. **93**, 831-843.
38. Barker, D.M., et al. *A Three-Dimensional Variational Data Assimilation System for MM5: Implementation and Initial Results*. *Monthly Weather Review*, 2004. **132**, 897-914 DOI: 10.1175/1520-0493(2004)132<0897:Atvdas>2.0.Co;2.
39. Huang, X.-Y., et al. *Four-Dimensional Variational Data Assimilation for WRF: Formulation and Preliminary Results*. *Monthly Weather Review*, 2009. **137**, 299-314 DOI: 10.1175/2008mwr2577.1.
40. Misaki, T., et al. *Accuracy Comparison of Coastal Wind Speeds between WRF Simulations Using Different Input Datasets in Japan*. *Energies*, 2019. **12**, 2754.
41. Carvalho, D., et al. *WRF wind simulation and wind energy production estimates forced by different reanalyses: Comparison with observed data for Portugal*. *Applied Energy*, 2014. **117**, 116-126 DOI: 10.1016/j.apenergy.2013.12.001.
42. Santos-Alamillos, F.J., et al. *Analysis of WRF Model Wind Estimate Sensitivity to Physics Parameterization Choice and Terrain Representation in Andalusia (Southern Spain)*. *Journal of Applied Meteorology and Climatology*, 2013. **52**, 1592-1609 DOI: 10.1175/jamc-d-12-0204.1.
43. University Corporation for Atmospheric Research (UCAR). *Steps to run analysis nudging in WRF-ARW*. Available from: http://www2.mmm.ucar.edu/wrf/users/wrfv3.1/How_to_run_grid_fdda.html [Accessed on August 16 2018]
44. Ohsawa, T., et al., *Investigation of WRF configuration for offshore wind resource maps in Japan* In *Conference Proceedings. Wind Europe Summit, Hamburg Messe, Hamburg, Germany, 27 – 29 September 2016*
45. Center, E.R.O.a.S.E., *USGS EROS Archive - Digital Elevation - Global 30 Arc-Second Elevation (GTOPO30)*.
46. Danielson, J.J. and D.B. Gesch, *Global multi-resolution terrain elevation data 2010 (GMTED2010)*. 2011, US Geological Survey.
47. *WRF V3 Geographical Static Data Downloads Page Page*. Available from: http://www2.mmm.ucar.edu/wrf/users/download/get_sources_wps_geog_V3.html [Accessed on 30 Sep 2019]
48. *Available GRIB Datasets from NCAR*. Available from: http://www2.mmm.ucar.edu/wrf/users/download/free_data.html [Accessed on 30/09 2018]
49. Duda, M. *Running the WRF Preprocessing System*. *The WRF Users' Basic Tutorial* Available from: <https://pdfs.semanticscholar.org/presentation/bdd9/87db4d0661c5e8d5fd3157a14d106da56887.pdf> [Accessed on Dec 2018]
50. Chen, X., F. Hossain, and L.-Y. Leung, *Application of Numerical Atmospheric Models, in Resilience of Large Water Management Infrastructure: Solutions from Modern Atmospheric Science*, F. Hossain, Editor. 2020, Springer International Publishing: Cham. p. 45-60.

51. Carvalho, D., et al., *Wind resource modelling in complex terrain using different mesoscale–microscale coupling techniques*. Applied Energy, 2013. **108**: p. 493-504.
52. Carvalho, D., et al. *A sensitivity study of the WRF model in wind simulation for an area of high wind energy*. Environmental Modelling & Software, 2012. **33**, 23-34 DOI: 10.1016/j.envsoft.2012.01.019.
53. Mattar, C. and D. Borvarán *Offshore wind power simulation by using WRF in the central coast of Chile*. Renewable Energy, 2016. **94**, 22-31 DOI: 10.1016/j.renene.2016.03.005.
54. Gbode, I.E., et al., *Evaluation of Weather Research and Forecasting (WRF) model physics in simulating West African Monsoon (WAM)*. 2017, Presentation.
55. Emery, C., E. Tai, and G. Yarwood, *Enhanced meteorological modeling and performance evaluation for two Texas ozone episodes, in Prepared for the Texas Natural Resource Conservation Commission, by ENVIRON International Corporation*. 2001.
56. Kang, D., K. Ko, and J. Huh *Comparative Study of Different Methods for Estimating Weibull Parameters: A Case Study on Jeju Island, South Korea*. Energies, 2018. **11**, 356 DOI: 10.3390/en11020356.
57. Energy Commission of Ghana. *Summary Results Of Wind Energy Resource Assessment At 8 Locations Along The Coast Of Ghana Conducted By The Energy Commission Under GEDAP/MoEP*. Available from: <http://bit.do/e3WA4> [Accessed on 05/Aug/ 2019]
58. Wei Wang, C.B., Michael Duda, Jimmy Dudhia, Dave Gill, Michael Kavulich, Kelly Keene, Ming Chen, Hui-Chuan Lin, John Michalakes, Syed Rizvi, Xin Zhang, Judith Berner, Soyoung Ha and Kate Fossell, *ARW Version 3 Modeling System User's Guide*. 2016, NCAR: Colorado, USA.
59. *How to interpret WRF variables*. Available from: https://www.openwfm.org/wiki/How_to_interpret_WRF_variables [Accessed on 30/09 2018]
60. Ovens, D. *How to Properly Rotate WRF Winds to Earth-Relative Coordinates Using Python, GEMPAK, and NCL*. Available from: <http://www-k12.atmos.washington.edu/~ovens/wrfwinds.html> [Accessed on January 18 2019]
61. Giannakopoulou, E.-M. and R. Nhili *WRF Model Methodology for Offshore Wind Energy Applications*. Advances in Meteorology, 2014. **2014**, DOI: 10.1155/2014/319819.
62. Giannaros, T.M., D. Melas, and I. Ziomas *Performance evaluation of the Weather Research and Forecasting (WRF) model for assessing wind resource in Greece*. Renewable Energy, 2017. **102**, 190-198 DOI: 10.1016/j.renene.2016.10.033.
63. Ji-Hang, L., G. Zhen-Hai, and W. Hui-Jun *Analysis of Wind Power Assessment Based on the WRF Model*. Atmospheric and Oceanic Science Letters, 2014. **7**, 126-131 DOI: 10.3878/j.issn.1674-2834.13.0078.
64. Rogers, E., et al., *Changes to the NCEP Meso Eta Analysis and Forecast System: Increase in resolution, new cloud microphysics, modified precipitation assimilation, modified 3DVAR analysis*. NWS Technical Procedures Bulletin, 2001. **488**: p. 15.
65. Iacono, M.J., et al., *Impact of an improved longwave radiation model, RRTM, on the energy budget and thermodynamic properties of the NCAR community climate model, CCM3*. Journal of Geophysical Research: Atmospheres, 2000. **105**(D11): p. 14873-14890.
66. Dudhia, J. *Numerical study of convection observed during the winter monsoon experiment using a mesoscale two-dimensional model*. Journal of the atmospheric sciences, 1989. **46**, 3077-3107 DOI: 10.1175/1520-0469(1989)046<3077:NSOCOD>2.0.CO;2.
67. Janjić, Z.I., *Nonsingular implementation of the Mellor-Yamada level 2.5 scheme in the NCEP Meso model*. NCEP Office Note No. 437, 2002.
68. Janjić, Z., *The surface layer in the NCEP Eta model* In Conference Proceedings. Eleventh Conference on Numerical Weather Prediction, American Meteorological Society, Norfolk, VA.19–23 August1996
69. Janjić, Z.I., *The Step-Mountain Eta Coordinate Model: Further Developments of the Convection, Viscous Sublayer, and Turbulence Closure Schemes*. Monthly Weather Review, 1994. **122**(5): p. 927-945.
70. Mukul Tewari, N., et al., *Implementation and verification of the unified NOAA land surface model in the WRF model (Formerly Paper Number 17.5)* In Conference Proceedings. 20th Conference on Weather Analysis and Forecasting/16th Conference on Numerical Weather Prediction, 2004
71. Kain, J.S. *The Kain–Fritsch convective parameterization: an update*. Journal of Applied Meteorology, 2004. **43**, 170-181 DOI: 10.1175/1520-0450(2004)043<0170:TKCPAU>2.0.CO;2.

Paper I

Received:

20 November 2018

Revised:

8 February 2019

Accepted:

15 March 2019

Cite as: Denis E. K. Dzebre, Akwasi A. Acheampong, Joshua Ampofo, Muyiwa S. Adaramola. A sensitivity study of Surface Wind simulations over Coastal Ghana to selected Time Control and Nudging options in the Weather Research and Forecasting Model.

Heliyon 5 (2019) e01385.

doi: [10.1016/j.heliyon.2019.e01385](https://doi.org/10.1016/j.heliyon.2019.e01385)



A sensitivity study of Surface Wind simulations over Coastal Ghana to selected Time Control and Nudging options in the Weather Research and Forecasting Model

Denis E. K. Dzebre^{a,b,c,**}, Akwasi A. Acheampong^d, Joshua Ampofo^b,
Muyiwa S. Adaramola^{a,*}

^a Faculty of Environmental Sciences and Natural Resources, Norwegian University of Life Sciences, Ås, Norway

^b Department of Mechanical Engineering, Kwame Nkrumah University of Science and Technology, Kumasi, Ghana

^c The Brew-Hammond Energy Centre, Kwame Nkrumah University of Science and Technology, Kumasi, Ghana

^d Department of Geomatic Engineering, Kwame Nkrumah University of Science and Technology, Kumasi, Ghana

* Corresponding author.

** Corresponding author.

E-mail addresses: dekdzebre.coe@knust.edu.gh (D.E.K. Dzebre), muyiwa.adaramola@nmbu.no (M.S. Adaramola).

Abstract

Over the years, the Weather Research and Forecasting Model (WRF) has been gaining popularity as a low-cost alternative source of data for wind resource assessments. This paper investigates the impact of selected time control, and nudging options on wind simulations in WRF. We conducted 15 numerical experiments, combining 5 simulation run-times and 3 options for disabling nudging in the Planetary Boundary Layer (PBL) in WRF. Hourly wind speed and direction predictions were compared with actual measurements at 40 m, 50 m and 60 m a.g.l. From our results, we recommend that, for optimum performance, the method of disabling nudging in the PBL should be chosen with simulation run times in mind. For wind simulations in our study area, up to 2 days run-times with nudging disabled below 1600 m in model configurations

gives the best wind speed predictions. However, disabling nudging below the model-calculated PBL height offers more consistent results and produces relatively less prediction error with longer run times.

Keywords: Atmospheric science, Environmental science

1. Introduction

Assessments of wind resources is key to the successful development of wind power on a commercial scale. Data for such assessments have traditionally been from mast-mounted instruments. However, in recent times, Numerical Weather Prediction Models (NWP) such as the Weather Research and Forecasting Model (WRF) have been gaining popularity as low-cost alternative sources of data for these assessments. Like most numerical models, WRF offers a wide range of options that must be put together to form model configurations with which the model can be run. Model configurations are key contributors to model performance.

Among the options that have been found to significantly affect model performance in wind simulations with WRF; are the Time Control and Nudging options [1, 2]. The Time Control options are used to specify among other things, the simulation integration time or run time (which is basically the length of the period that is simulated by the model), as well as time intervals between the lateral boundary condition inputs and simulation output files. Nudging (Newtonian relaxation) is one of the options in the Four-Dimensional Data Assimilation (FDDA) system of WRF. The FDDA system comprises options for keeping simulations close to gridded analyses values and/or observed values (actual measurements) over the simulation run time. The former is often referred to as grid or analyses nudging, while the latter is termed observational nudging. Analysis nudging options in WRF include the nudging coefficients for the variables to be nudged, whether nudging should be applied for all vertical levels in the simulation domain, and if not, which levels it should be disabled for, and how. In this paper, we focus on the options of integration or run time, and the vertical levels for which nudging should be disabled. The combined effect of these two parameters has been found to improve model performance in wind simulations by reducing model divergence and error accumulation [2].

NWP models tend to diverge and accumulate approximation errors after running for some time. These situations get worse with increasing simulation run times [2, 3]. With the Time Control options alone, these errors can be reduced for simulations covering long periods. This can be achieved by performing relatively shorter segmented simulations, that together cover the desired (longer) period. However, using this option (of shorter segmented runs) requires more time and computing resources for simulations. This is because, in line with best practices, simulations run times in WRF must incorporate a model “spin-up” time (the average time it takes

for the model to adequately develop mesoscale processes). However, model outputs from this spin-up time are not considered as true representations of the state of the atmosphere and so, are often discarded [3, 4, 5, 6, 7, 8, 9]. Using shorter run times for simulations in studies covering longer periods, requires more of such model spin-up times, which in turn requires that, extra time and computing resources be spent on running simulations. For example, for a study that covers a period of one year, and uses 12 hours spin-up time per simulation, the total number of extra days that must be run and discarded as model spin-up are presented in Table 1. Therefore, though using shorter run times might improve wind predictions by WRF, it also increases the time and computational needs for studies and assessments. In addition, for study designs that are computationally expensive and span long study periods, the use of a short run times might not necessarily be worth the improvements in model performance. Nonetheless, the option has been used, often in combination with grid nudging in model configurations for sensitivity studies and model performance assessments of WRF for wind simulations [1, 2, 3, 4, 5, 6, 7, 8, 9, 10, 11, 12, 13]. Some of the run times (excluding model spin-up times) that have been used in wind simulation studies include, 12 hours [11], 1 day [3, 14], 2 days [2, 8], 7 days [7], 9 days [6], and 30 or 31 days [5, 12].

It is common practice in sensitivity studies of WRF for wind simulations, to apply nudging at heights above the Planetary Boundary Layer (PBL) only (in other words, disable nudging within the PBL). This is done with the intention of allowing meso-scale processes in the PBL to develop freely [11, 12, 13]. There are 3 ways by which analyses nudging within the PBL can be disabled in WRF [1, 15];

- i. by specifying the height (in model vertical levels) above which nudging should be applied (or below which nudging should be disabled).
- ii. by letting the model apply nudging above the model-calculated height of the PBL (The accuracy of this model-calculated PBL height depends on the PBL parameterisation scheme used in the model configuration).

Table 1. Effect of different run times on a study covering 1 year (assuming 12 hours model spin up time).

Run time (excluding model spin-up time)	Number of simulations required to cover study period	Total number of extra days required as spin up time	Extra time required for simulations
1 day	365	182.5 days	50%
2 days	183	91.5 days	25%
7 days	53	26.5 days	8%
31 days	12	6 days	2%

- iii. by letting the model choose the higher of a specified height, and the model-calculated PBL height, and applying Nudging above whichever is chosen (i.e. the highest).

The diversity in options available in the WRF model has always presented the challenge of identifying an optimum configuration for simulations, as model performance has been found to depend on many factors including, availability of computing resources, variables of interest, model configuration and prevailing climatic conditions. In addition, interaction between different options in WRF can sometimes be non-linear, and this calls for different possible combinations of options to be tested to determine an optimum configuration. It has been the practice to determine the optimum configuration for a variable of interest with sensitivity studies, which assess comparatively, the effects of different model configurations on model performance.

Carvalho et al. [2] found that, wind speed predictions by WRF are better, with a model configuration that includes the grid nudging option combined, with a run time of 2 days instead of 30 days. However, this study did not examine the possible effects of other integration times, nor the different methods of applying nudging or the possible interaction of the two options, on model performance. Ohsawa et al. [1] found that, applying nudging above PBL heights calculated by the Mellor-Yamada-Janjic (MYJ) PBL scheme produces better results as compared to applying nudging above a fixed height (of 1000 m) for offshore wind simulations in Japan. However, these options were not tested with different run times, nor the third option of disabling nudging in the PBL, tested. In addition, given the strong sensitivity PBL schemes often exhibit to different climatic conditions that pertain in different seasons and at different locations, the generalisability of the findings of Ohsawa et al., might be limited.

Against this background, in this study, we investigate sensitivity of winds (in an area of good wind energy potential in Ghana [16]), to different combinations of five simulation run times and three methods of disabling nudging in WRF. The accuracies of these different combinations are compared with actual field (ground) measurements at a selected location in the south-eastern part of Ghana (Section 2.1). The aim of this study is to recommend combinations of run time and nudging options that are suitable for model configurations for wind simulations with WRF in Ghana.

2. Methods

2.1. Study area and measured data

The study area, as depicted in Fig. 1, stretches approximately between longitudes 0° and 1° East, and latitudes 4.5° and 6° North, and covers the eastern coastal plains



Fig. 1. Map of Ghana showing its international borders and the study area (in yellow and red respectively).

of Ghana. This area was identified to have some of the best wind energy potential in Ghana in a study conducted in 2002 [16]. The Energy Commission of Ghana (EC) has conducted mast measurement exercises at selected sites in the area in the past. The observational (measured) data for this study, is from one of the masts in one such measurement exercise, at Anloga (Lat 5.79°N and Long. 0.91°E), a town along the coast in the study area. The data comprises hourly averages of wind speeds for December 2013, measured at heights of 40, 50, and 60 m above ground level, and wind directions, measured at 50 and 60 m.

2.2. Model and domain configuration

The simulation domains comprised three (3) one-way nested domains of resolutions 27 km, 9 km, and 3 km. The horizontal resolutions were chosen to achieve a recommended nesting ratio of 3 [17, 18]. The final horizontal resolution of 3 km was chosen because it has been found to be optimum for wind simulations in WRF. Increasing the final resolution beyond this value was found not to significantly improve model performance, despite being more computationally expensive [2, 5]. The outermost domain covers Ghana and its neighbouring countries as well as parts of the Sahel deserts to the north and the sea to the south of the country. Domain 2 covers the lower half of the country, and parts of its neighbouring countries to the east. Domain 3 covers the high wind energy potential coastal plains of South-East Ghana. Most of the EC's wind energy measurement masts as well as the sites of some planned wind farms in Ghana, are located in this domain (Domain 3). These domains are depicted in Fig. 2.

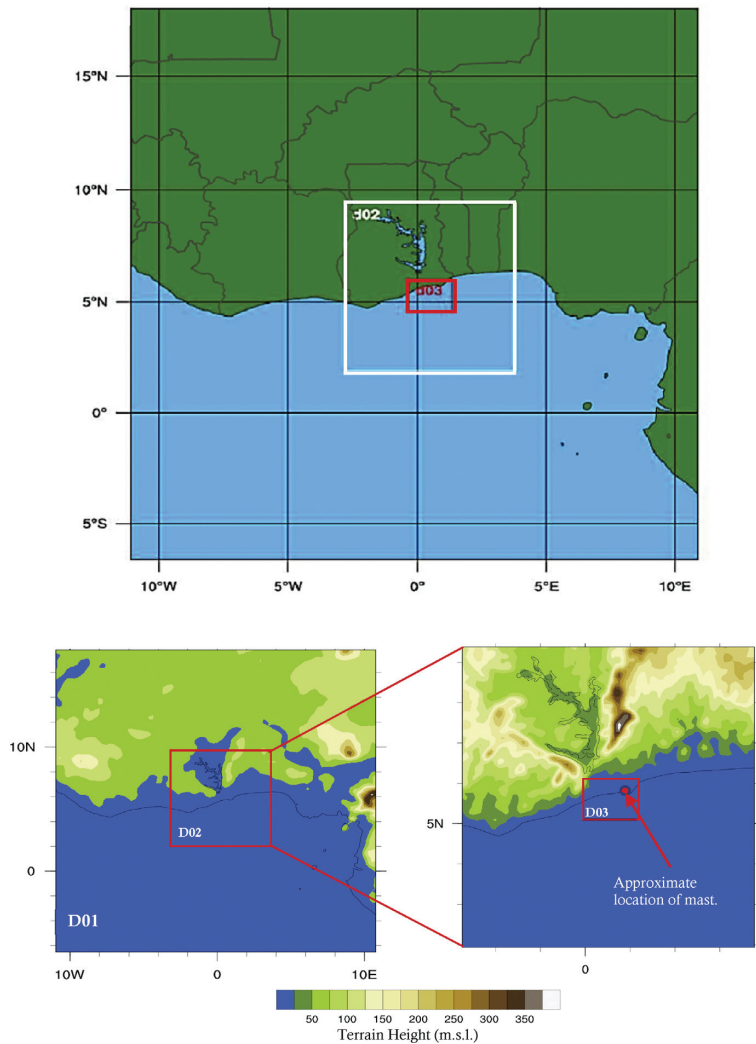


Fig. 2. Simulation domains.

The model configuration is summarised in Table 2. The Mercator Geographical Projection scheme was used as recommended by Wei Wang et al. [19]. The Mellor-Yamada Nakanishi and Nino Level 3 (MYNN3) PBL scheme was chosen for this study based on results of a preliminary evaluation of PBL parameterisation schemes for this area. Following recommendations on vertical level references for tests [19], and nested simulations in WRF [20], 40 vertical levels, (automatically set for a pressure of 5000 Pa at the top of the model) were chosen for all domains. Cumulus parameterisation was turned off for domain 3 as the horizontal resolution in this domain

Table 2. Model configuration for all experiments.

Model version	Advanced research WRF v3.8.1		
Driving data	NCEP FNL Operational Model Global Tropospheric Analyses at 1-degree spatial, 26 pressure levels, and 6 hourly temporal resolutions		
Land use data	24-category USGS		
Geographical projection scheme	Mercator		
Vertical resolution	40 levels		
Horizontal resolution (km)	27	9	3
Domain size (grid points)	91 × 103	82 × 94	64 × 55
Parameterization schemes:			
Cloud microphysics (MP)	Eta microphysics (ETA) scheme		
Long-wave radiation (LW-Rad)	Rapid Radiative Transfer Model scheme (RRTMG version)		
Short-wave radiation (SW-Rad)	Dudhia scheme		
Surface layer (SL)	Nakanishi and Nino PBL's surface layer scheme (MYNN)		
Land surface model (LSM)	Noah Land Surface Model		
Planetary boundary layer (PBL)	The Mellor Yamada Nakanishi Nino Level 3 (MYNN3.)		
Cumulus	Kain-Fritsch scheme (turned off for domain 3)		

is considered fine enough for adequate resolving of cumulus processes [2, 21]. All simulations were initialised with the NCEP FNL Operational Model Global Tropospheric Analyses (NCEP GFS-FNL) dataset at 1° horizontal, 26 mandatory pressure levels, and 6-hours temporal resolutions [22]. The same dataset was used for the analysis nudging.

2.3. Experimental design

Fifteen (15) numerical experiments were performed, testing all possible combinations of the five selected run times (1 day, 2 days, 7 days, 14 days, 31 days) and all the three methods of disabling nudging in the PBL. Except for 14 days integration time, all the other integration times tested in this study have been used in previous sensitivity studies on wind simulations in WRF; 1 day [3, 14], 2 days [2, 8], 7 days [7], 9 days [6], and 30 or 31 days [5, 12]. Each experiment involved the simulation of the entire month of December, 2013. For the five experiments in which the height below which nudging must be disabled had to be specified, 10 model vertical levels (corresponding to approximately 1600 m above sea level (asl) in our vertical grid configuration, which has lowest level at approximately 56 m asl) was specified. This number of levels is specified in model configurations similar to the one used in this study (i.e. pressure at the top of the model = 5000 Pa, vertical levels

automatically set) [15, 19]. The number of simulations and other details of each experiment are presented in Table 3. All simulations were run with a spin-up time of 12 hours.

2.4. Post-processing of wind data from WRF output files

A position (specified as latitude (i), longitude (j), and vertical level(k)) on the WRF grid corresponds to a cell [23]. Surface wind speeds and directions for a position in WRF were calculated from the U (x-component) and V (y-component) winds. As illustrated in Fig. 3, U winds are on at the centres of the left and right faces of the cell, while the V winds are on the middles of the front and back faces [23]. The observation data for verification comprises only surface winds (winds in the horizontal plane). Therefore, hourly simulated surface winds for a cell were calculated (for every hour) as:

$$WS = \left[\left(\frac{U_{i,j,k} + U_{i+1,j,k}}{2} \right)^2 + \left(\frac{V_{i,j,k} + V_{i,j+1,k}}{2} \right)^2 \right]^{0.5} \quad (1)$$

Table 3. Experimental Design (the run times specified exclude the spin-up time).

No.	Experiment designation	Simulation run time	Levels above which grid nudging should be applied (or below which nudging should be disabled)	Number of simulations
1	1 day_N-10l	1 day	10 model vertical levels	31
2	2 days_N-10l	2 days	10 model vertical levels	16
3	7 days_N-10l	7 days	10 model vertical levels	5
4	14 days_N-10l	14 days	10 model vertical levels	3
5	31 days_N-10l	31 days	10 model vertical levels	1
6	1 day_N-pblh	1 day	Model-calculated PBL height	31
7	2 days_N-pblh	2 days	Model-calculated PBL height	16
8	7 days_N-pblh	7 days	Model-calculated PBL height	5
9	14 days_N-pblh	14 days	Model-calculated PBL height	3
10	31 days_N-pblh	31 days	Model-calculated PBL height	1
11	1 day_N-a	1 day	The higher of 10 model vertical levels and PBL height	31
12	2 days_N-a	2 days	The higher of 10 model vertical levels and PBL height	16
13	7 days_N-a	7 days	The higher of 10 model vertical levels and PBL height	5
14	14 days_N-a	14 days	The higher of 10 model vertical levels and PBL height	3
15	31 days_N-a	31 days	The higher of 10 model vertical levels and PBL height	1

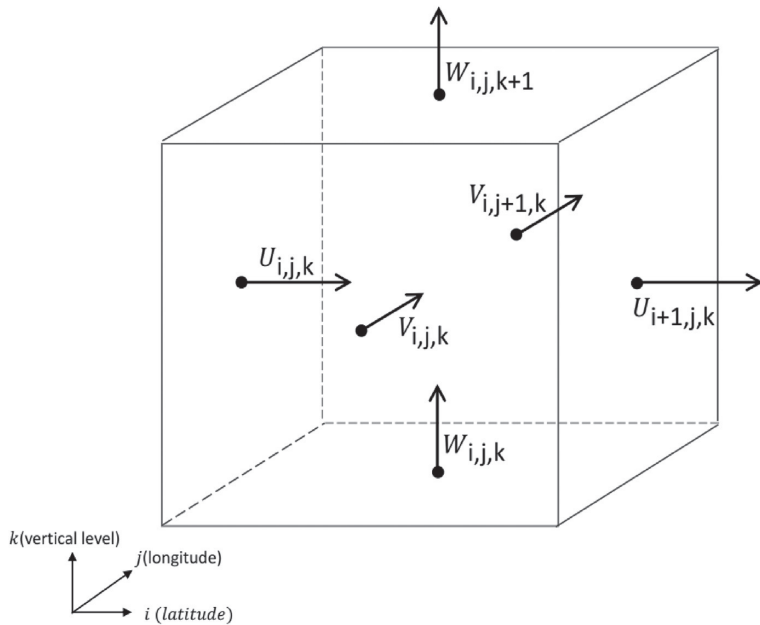


Fig. 3. Grid cell in WRF.

Direction was determined from the same U and V averages for each timestep using the four-quadrant inverse tangent function. Winds were not rotated in this study as with the Mercator projection (which was used in this study), the model grid aligns with earth coordinates and so rotation of the winds is not needed [24].

The wind speeds at heights of analysis (40 m, 50 m, and 60 m) were linearly interpolated from wind speeds for the levels immediately below and above them. While linear interpolation might not be the best approach to obtain the wind speeds for the heights of analysis, we believe this should not significantly affect the relative performance of the options being tested, once the same approach is used in processing the data for all the options tested in the study.

For the interpolation, the vertical levels in WRF were converted to height above ground level (in m) as [19];

$$Height(a.g.l) = \left(\frac{(PH + PHB)_{i,j,k} + (PH + PHB)_{i,j,k+1}}{2g} \right) - HGT \tag{2}$$

where PH is the perturbation geopotential height (m^2/s^2), PHB is the base-state geopotential height (m^2/s^2), g is acceleration due to gravity (m/s^2), and HGT represents the terrain height (m) [19]. Values for PH, PHB and HGT were all WRF simulation outputs.

2.5. Statistical metrics for validation

Hourly predictions of wind speeds and directions were compared with ground data measured hourly, at heights of 40, 50, and 60 m above ground level. The relative performances of the configuration options were evaluated using the comparative Prediction Skill Score measure [25], calculated from the sum of scaled (unity normalised) values of the following statistical metrics of simulated wind speeds and directions:

- i. the Root Mean Square Error (RMSE),
- ii. the Mean Error (ME),
- iii. Standard Error (STDE) and the
- iv. Correlation Coefficient (CC) between simulated and measured data.

The RMSE is a measure of the difference between simulated and measured values and is calculated as:

$$RMSE = \left(\frac{1}{N} \sum_i^N (\Delta)^2 \right)^{0.5} \quad (3)$$

where $\Delta = WS_{sim} - WS_{obs}$ and N is the number of data points.

The ME, like the RMSE, is a measure of error, but most importantly, helps determine whether the model was over-predicting or under-predicting winds. It was calculated as:

$$ME = \frac{1}{N} \sum_i^N (\Delta) \quad (4)$$

The STDE gives an indication of how spread out predictions are from the predicted mean. A smaller standard error is preferred. STDE is calculated from the RMSE and ME as:

$$STDE = (RMSE^2 - ME^2)^{0.5} \quad (5)$$

The linear dependence of simulated and measured wind speeds was assessed with the Pearson Correlation Coefficient (CC). It was calculated as [26].

$$CC = \frac{\sum (X - \bar{X})(Y - \bar{Y})}{\sqrt{\sum (X - \bar{X})^2 \sum (Y - \bar{Y})^2}} \quad (6)$$

where X and Y are the simulated and observed wind speeds respectively.

For angles, Δ was calculated as [11];

$$\Delta = \begin{cases} \theta_{sim} - \theta_{obs} & \text{when } |\theta_{sim} - \theta_{obs}| < 180^\circ \\ (\theta_{sim} - \theta_{obs}) \left(1 - \frac{360}{|\theta_{sim} - \theta_{obs}|} \right) & \text{when } |\theta_{sim} - \theta_{obs}| > 180^\circ \end{cases} \quad (7)$$

Angular mean was calculated according the circular statistics principles [27], and correlation between simulated and measured angles was determined with a Circular Correlation Coefficient [27].

Metrics were scaled (normalised) according to [25] as:

$$X_{SCALED} = \frac{X_i - X_{min}}{X_{max} - X_{min}} \quad (10)$$

where Xmax and Xmin refer to maximum and minimum values of the Metric (RMSE, STDE, ME, or CC) being scaled. Scaling is such that $0 \leq X_{SCALED} \leq 1$.

The Prediction Skill Score was then calculated as:

$$Skill\ Score = (1 - RMSE_{SCALED}) + (1 - |ME|_{SCALED}) + (1 - STDE_{SCALED}) + CC_{SCALED} \quad (9)$$

Such that $0 \leq Skill\ Score \leq 4$.

The scheme with the highest Skill Score was ranked as the best scheme and vice versa.

The fitted Weibull probability curves for measured and predicted data from the tested configurations were also compared. The Weibull distribution is widely used to represent wind speed distributions for wind energy applications, primarily because it accurately fits wind data well. Its probability function is [28];

$$f(W S) = \left(\frac{k}{c}\right) \left(\frac{W S}{c}\right)^{k-1} \exp\left[-\left(\frac{W S}{c}\right)^k\right] \quad (11)$$

where $f(W S)$ is the probability of observing wind speed ($W S$), k is dimensionless Weibull shape parameter, and c is the Weibull scale parameter. The two parameters can be determined as follows [28];

$$k = \left(\frac{\sigma}{W S_m}\right)^{-1.086} \quad (12)$$

$$c = \frac{W S_m k^{2.6674}}{0.184 + 0.816 k^{2.73855}} \quad (13)$$

where σ and $W S_m$ (m/s), are the standard deviation and the average respectively, of the wind speed data.

Effects of the tested model configurations on wind power estimation were evaluated by comparing the Average Wind Power Flux, estimated with measured and predicted data. The Average Wind Power Flux, assuming a rotor swept area of unity was estimated as [12].

$$WP_{flux} = \frac{1}{N} \sum_{i=1}^N 0.5 \times \rho \times WS_i^3 \tag{14}$$

where WS_i is the wind speed, and ρ , the air density. Due to a lack of access to local air density measurements, a value of 1.156 kg m^{-3} , based on findings of a study in the Caribbean was assumed [29] (based on the assumption that the Caribbean should have a similar climate as Ghana). In addition, estimates of local air density with data (Average Temperature, Relative Humidity and Pressure) from selected online sources [30, 31, 32], was found to average approximately 1.160 kg m^{-3} , producing less than 1% difference in the Average Power Flux estimated with the air density value from the Caribbean study.

3. Results and discussion

Fig. 4 shows the observed and predicted average wind speeds at 60 m for December 2013. It can be observed from the figure that, generally, the shorter run times gave better predictions, with 1 day runs giving the best predictions. We also see that, average wind speed predictions for experiments that were conducted with Nudging above 10 model vertical levels (the N-10l group) and those conducted with Nudging above the higher of 10 vertical levels or the model-calculated PBL height (the N-a group) are approximately the same. However, in contrast to the trend in the N-10l and N-a groups of experiments; average wind speed predictions for experiments from the N-pblh group, (in which nudging was below the model-calculated height of the PBL), though better with 1 day and 2 days run times, become almost constant with run times of 7 days or more. The better performance of this approach of disabling nudging (disabling it below the model calculated PBL height) for longer run times (7 days or more in this case) can also be seen from the figure.

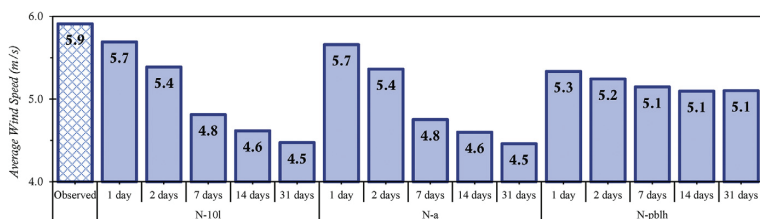


Fig. 4. Average wind speeds at 60 m a.g.l from experiments grouped by Nudging options tested.

The better predictions with the smaller run times can be attributed to the relatively lower model divergence and error accumulation that shorter run times achieve [2]. We observe this in Fig. 5, which shows the plots of daily average wind speeds (in December, 2013) for the 5 run times tested. We also observe that, the deviations of the predicted wind speeds from the observed wind speeds appear to be more pronounced in the plots for run times of 7, 14, and 31 days in Fig. 5(c), (d), and (e) respectively, pointing to relatively larger model divergence and error accumulation by experiments with these run times.

The similarity in results between the N-10l and N-a groups of experiments mentioned earlier, can again be seen in the plots in Fig. 5. There is little deviation between the lines for the daily average wind speeds plots for experiments from

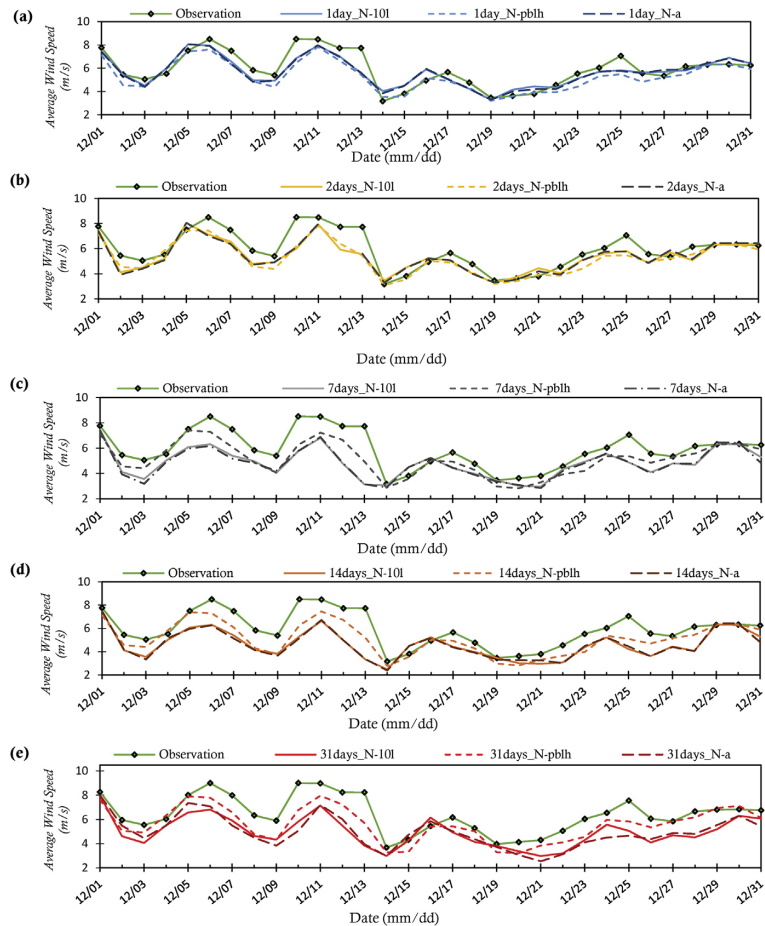


Fig. 5. Average wind speeds at 60 m a.g.l from experiments conducted with run times of; (a) 1 day, (b) 2 days, (c) 7 days, (d) 14 days, (e) 31 days.

the two groups, irrespective of simulation run time. This similarity suggests that, the calculated PBL height was either often close to, or less than the height at vertical level 10 (approximately 1600 m for our experimental setup). From Fig. 6, which depicts a plot of the daily maximum PBL heights at the location where our observational data was taken, we find this to be the latter. This means that, in the N-a group experiments, nudging was basically being disabled in the same manner as in the N-10l experiments; for the lower 10 vertical levels.

The more or less constant predictions of average wind speeds in experiments with 7, 14 and 31 days run times from the N-pblh group, can be explained by the relatively little deviation between the predicted wind speeds from the 3 experiments. This can be seen in Fig. 7(b). This result can also be taken as an indication of the consistency of this method of disabling nudging in the PBL in simulations with run times of 7 days or more. A possible contributing factor to the better performance of the experiments from the (N-pblh) group, might be the ability of that method (of disabling nudging) to determine more appropriately, the levels to nudge. With the N-10l experiments, levels above an assumed constant PBL height (of 1600 m) are nudged. However, this might not be best as, the PBL height tends to vary (as can be seen in Fig. 6), falling within the lowest 1000 m–3000 m of the atmosphere depending on the amount of ground friction and turbulent mixing present [14, 33].

3.1. Statistical metrics and prediction skill

The trends observed above are confirmed by the statistical metrics presented in Table 4. Generally, experiments with shorter run times had better RMSE, ME, and STDE than those with longer run times from the same experimental groups. The better consistency of disabling nudging below the model-calculated PBL height is seen in the fact that, there is comparatively less variation in RMSEs and MEs, for experiments from the N-pblh group. In addition, experiments from this group record some of the lowest STDEs. Low STDEs can be taken as an indication of consistency in model performance [2, 12]. The greater model divergence and error accumulation associated with longer run times is also seen in the greater RMSEs and MEs for experiments with run times of 7 days or more.

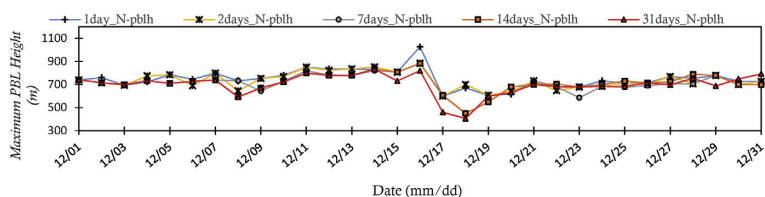


Fig. 6. Daily average PBL heights from N-pblh group of experiments.

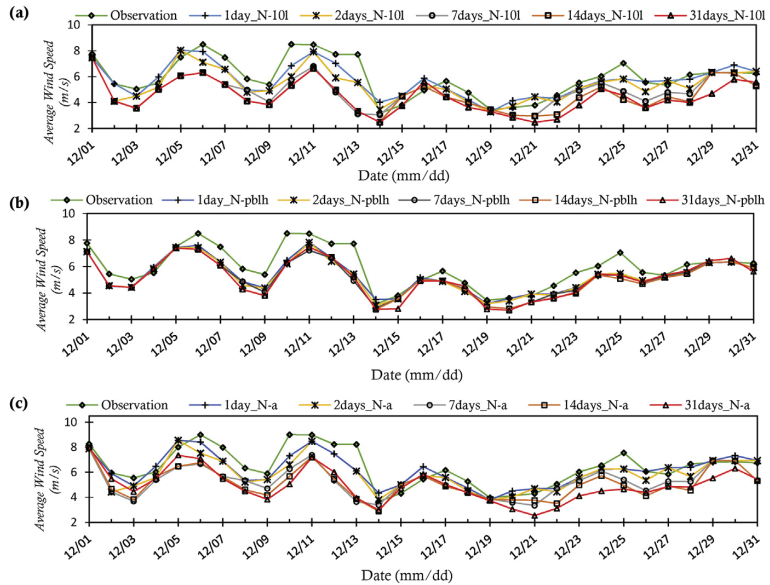


Fig. 7. Average wind speeds at 60 m a.g.l from experiments conducted with Nudging disabled; (a) below 10 vertical levels, (b) below the model-calculated PBL height, (c) below the higher of 10 vertical levels or PBL height.

Table 4. Statistical metrics for wind speed predictions at 60 m.

	Average wind speeds (m/s)	RMSE (m/s)	ME (m/s)	STDE (m/s)	CC	Prediction skill score
Observation	5.9					
1 day_N-10l	5.7	1.23	-0.22	1.21	0.7	3.5
1 day_N-pblh	5.3	1.25	-0.61	1.10	0.8	3.4
1 day_N-a	5.7	1.25	-0.25	1.22	0.7	3.4
2 days_N-10l	5.4	1.40	-0.52	1.30	0.7	2.8
2 days_N-pblh	5.2	1.30	-0.67	1.12	0.8	3.3
2 days_N-a	5.4	1.40	-0.55	1.29	0.7	2.8
7 days_N-10l	4.8	1.86	-1.10	1.49	0.6	1.2
7 days_N-pblh	5.1	1.38	-0.76	1.15	0.8	3.0
7 days_N-a	4.8	1.89	-1.16	1.49	0.6	1.1
14 days_N-10l	4.6	1.98	-1.29	1.50	0.6	0.8
14 days_N-pblh	5.1	1.42	-0.82	1.16	0.8	2.9
14 days_N-a	4.6	2.01	-1.31	1.52	0.6	0.7
31 days_N-10l	4.5	1.98	-1.44	1.37	0.7	1.1
31 days_N-pblh	5.1	1.48	-0.81	1.24	0.7	2.6
31 days_N-a	4.5	2.04	-1.45	1.43	0.6	0.8

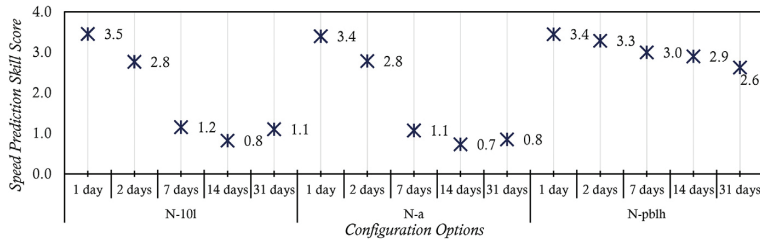


Fig. 8. Speed prediction skill scores at 60 m for configurations tested.

Combining the metrics into prediction skill scores, we find that configurations with the shorter run times generally record the highest skill scores as depicted in Fig. 8. In addition, disabling nudging below 1600 m (model vertical level 10), is best for 1 day and 2 days runs only. For the other run times tested, disabling nudging below the model-calculated PBL height offers better performance. Generally, nudging below the model-calculated PBL height offers the most consistent performance. Full results on the metrics and Skill Scores are presented in Annex-I.

3.2. Effect on wind power estimates

Fig. 9 depicts the Weibull probability distribution plots for observed data and data predicted with seven of the configuration options tested. Plots for the N-a group of experiments are not included because they are very similar to those of the N-10l group of experiments. Moreover, for the 7, 14, and 31 days run times, only experiments from the N-pblh group are plotted because they ranked better than those from the other groups. It can be seen from the figure that, apart from the 1day_N-10l configuration, all the other configurations overestimate and underestimate lower and

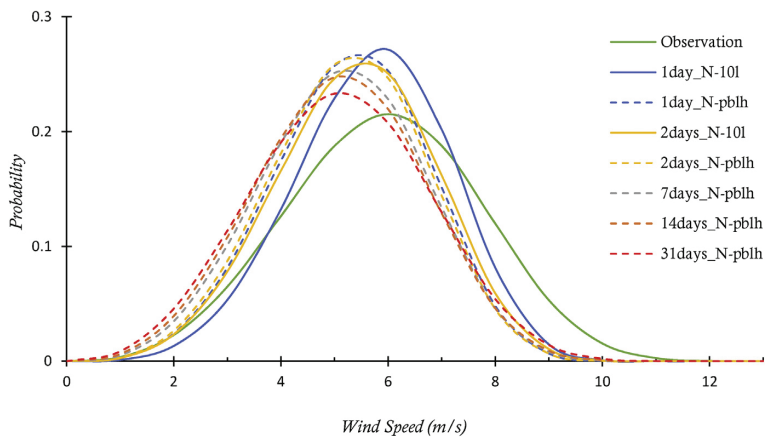


Fig. 9. Weibull P.D.F plots for data at 60 m from observations and seven of the options tested.

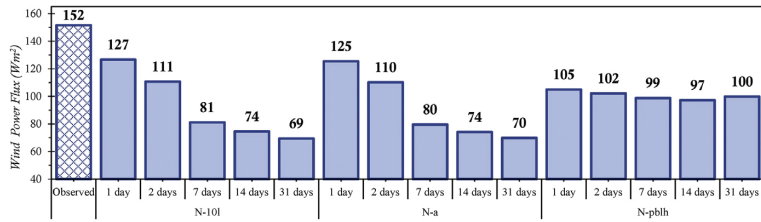


Fig. 10. Wind power estimates from observed and predicted data at 60 m.

higher speeds respectively; with deviation for lower speeds greatest for configurations with higher run times. Therefore, as can be observed in Fig. 10, the shorter run times generally gave better estimations of the power flux. Though there are deviations with the 1day_N-10l configuration as well, they are relatively less, and this configuration predicts the higher speeds better. The more accurate estimations by the 1day_N-10l resulted in a relatively better average wind speed prediction error of 4%, and a wind power estimation error of 16%, as can be seen from Table 5.

For the nudging options tested, disabling nudging below the model-calculated PBL height (experiments from the N-pblh group), produced more consistent results, producing errors ranging from approximately 10 to 13.7% of observed average wind

Table 5. Percentage error of estimated average wind speed and energy estimates at 60 m.

	Average wind speeds (m/s)	Wind speed prediction error (%)	Shape factor, k	Scale factor, c	Estimated power flux (W/m ²)	Power flux estimation error (%)
Observation	5.9		3.68	6.56	152	
1 day_N-10l	5.7	3.7	4.50	6.25	127	16
1 day_N-pblh	5.3	10.3	4.15	5.85	105	31
1 day_N-a	5.7	4.3	4.39	6.22	125	17
2 days_N-10l	5.4	8.9	4.09	5.95	111	27
2 days_N-pblh	5.2	11.3	4.07	5.79	102	33
2 days_N-a	5.4	9.3	3.98	5.93	110	27
7 days_N-10l	4.8	18.6	3.78	5.33	81	46
7 days_N-pblh	5.1	12.9	3.80	5.70	99	35
7 days_N-a	4.8	19.6	3.62	5.28	80	48
14 days_N-10l	4.6	21.9	3.45	5.14	74	51
14 days_N-pblh	5.1	13.8	3.67	5.66	97	36
14 days_N-a	4.6	22.2	3.42	5.13	74	51
31 days_N-10l	4.5	24.3	3.30	4.99	69	54
31 days_N-pblh	5.1	13.7	3.45	5.68	100	34
31 days_N-a	4.5	24.5	3.20	4.99	70	54

speeds, and 31–34% of power flux estimates from observed data (See Table 5). In contrast, though disabling nudging below 1600 m (model vertical level 10) gave the best result with the 1 day run time, it produced a wider error range when the run time is increased to 30 days; from approximately 4 to 24% of observed average wind speeds, and 16–54% of energy estimates from observed data. The same trend is found for experiments from the N-a group.

The trends discussed above are also observed in the shape and scale parameters for the fitted data, also presented in Table 5.

3.3. Wind direction predictions

We found no significant difference in the direction predictions of the various configuration options tested. Observed wind directions for this period was mostly from the

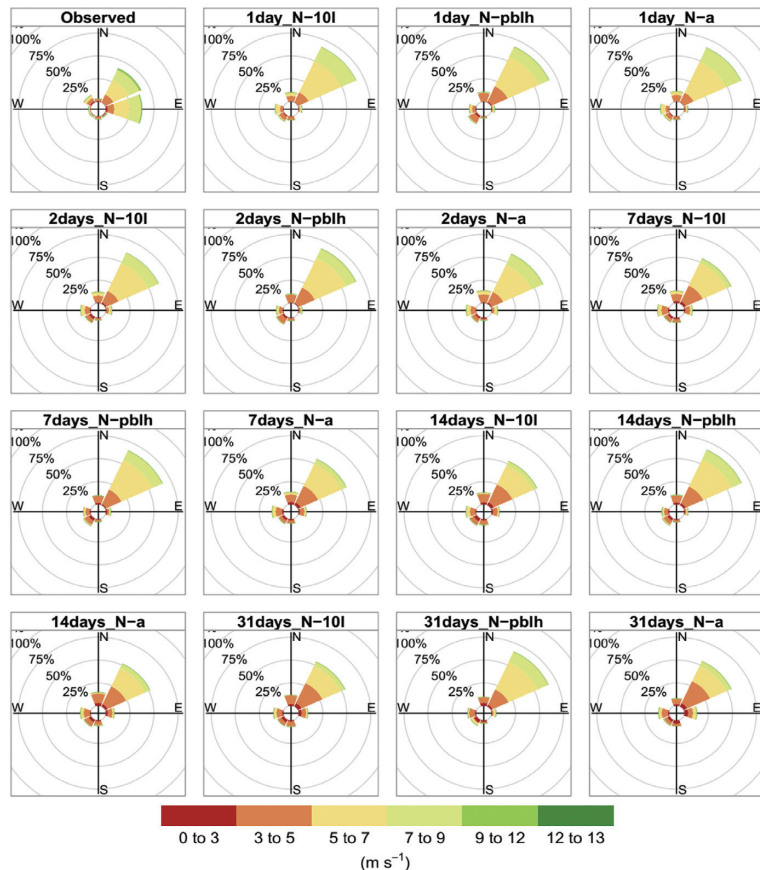


Fig. 11. Wind roses of observation data and scheme predictions at a height of 60 m.

North-East and the East. All the model configurations tested predicted the dominant direction to North-East. This can be seen in Fig. 11, which shows wind roses for observed and predicted wind directions at a height of 60 m. From the statistical metrics for direction prediction at 60 m, presented in Table 6, our analysis suggests the 1 day_N-pblh as the best ranked configuration. We also observe some of the trends in speed predictions being repeated in the direction predictions as well; the shorter run time options generally give better direction prediction skill scores. In addition, the N-pblh group of experiments exhibit the most consistent performance as compared to other groups. This can be explained by the fact that wind directions were calculated from the wind speed predictions. However, all the options tested predict the same direction (North-East), as the dominant wind direction for this site in December 2013.

3.4. Effect of elevation (height) on findings

We found no significant changes in ranking of the configurations tested in this study when the analysis was repeated for the other heights at which we had observational data (i.e. 50 m and 40 m). Configuration rankings remained the same, albeit with marginal drops in prediction skill scores for direction prediction, as can be seen from Fig. 12(b).

Table 6. Statistical metrics for wind speed predictions at 60 m.

	Average wind direction (degrees)	RMSE (degrees)	ME (degrees)	STDE (degrees)	CircC	Prediction skill score
Observation	55.8					
1 day_N-10l	39.6	47.3	-25.9	39.6	0.4	2.6
1 day_N-pblh	37.5	46.7	-27.6	37.7	0.5	3.2
1 day_N-a	39.4	47.2	-26.9	38.8	0.4	2.9
2 days_N-10l	37.7	47.6	-25.1	40.5	0.5	2.4
2 days_N-pblh	39.7	48.9	-27.0	40.7	0.4	2.6
2 days_N-a	38.9	47.1	-25.5	39.6	0.5	2.6
7 days_N-10l	41.0	56.6	-26.9	49.8	0.5	1.7
7 days_N-pblh	42.7	47.8	-26.0	40.1	0.4	2.5
7 days_N-a	38.7	56.2	-27.4	49.1	0.5	1.9
14 days_N-10l	40.4	61.0	-27.5	54.4	0.5	1.2
14 days_N-pblh	42.8	48.1	-25.6	40.8	0.4	2.3
14 days_N-a	37.0	59.8	-28.0	52.9	0.5	1.5
31 days_N-10l	44.2	62.0	-29.0	54.8	0.5	1.5
31 days_N-pblh	43.3	47.8	-24.9	40.8	0.4	2.3
31 days_N-a	50.5	59.0	-24.6	53.6	0.4	0.7

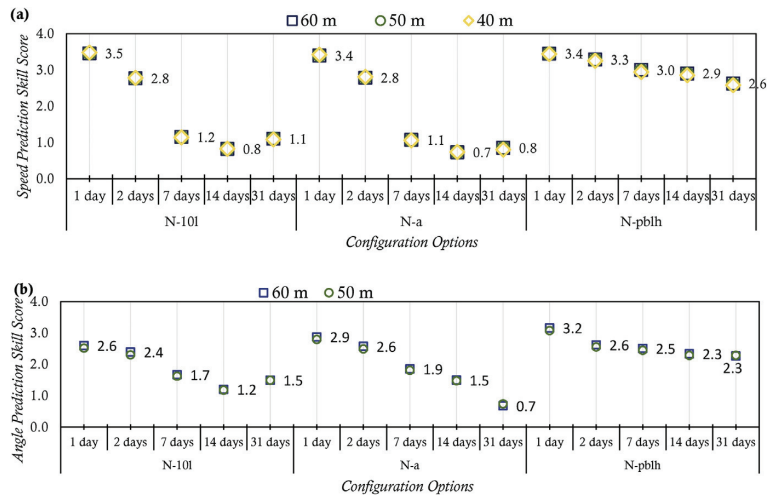


Fig. 12. Skill scores for; (a) Speed prediction (b) Direction prediction (Values are scores at 60 m height).

We also found no changes in the trends that were observed in the estimated power with data from the configurations. There were drops in estimated power at the lower heights, due to lower wind speeds at these heights. Full results on the estimated power for the lower heights can be found in the Annex-I.

4. Conclusion

This study investigated the effects of combining simulation run times of varying lengths with 3 different methods of disabling nudging in the PBL, on wind speed and direction predictions by WRF model. Effects of the configuration options on power estimated from the data they predicted was also examined. Five selected run times were each combined with three methods of disabling grid nudging within the PBL in WRF simulations.

We found that, shorter simulation run times generally offer better model performance over longer simulation run times. Consistent with findings of Carvalho et al. [2], 2 day runs offered better model performance over 30 day runs, when combined with an appropriate method of disabling grid nudging in the PBL. In this study, it was found that the 2 days runs reduced the average wind speed prediction error for the study area from 24% of observed wind speeds, to less than 10%. The error in wind power flux estimated with predicted data, reduced from 54% of estimates with observed data, to 27%. The simulated results were found to further improve, when simulation run time was reduced to 1 day; average wind speed prediction error dropped to less than 4% of the observed average, and error in power estimated with predicted data dropped to 16% of estimates from observed data. Furthermore, results

suggest that, where longer run times must be used for simulations (due to time constraint or computing constraints that the shorter run times require), the error from predictions can be reduced by choosing an appropriate method of applying grid nudging. In line with the findings of Ohsawa et al. [1], when nudging is disabled below the model-calculated PBL height instead of a fixed height, average prediction error is reduced, possibly because of the ability this approach of disabling nudging to better determine the appropriate levels at which winds should be nudged. In this study, this approach reduced speed prediction error from 24% to 14%. The error in power flux estimated with the predicted data also reduced from 54% to 34%. It must be noted that performance margins for this approach (disabling below model-calculated PBL height) might differ with different PBL schemes, as model estimation of the PBL height depends on the PBL scheme used for the simulations [14, 33]. In addition, this study does not examine the sensitivity of the options to seasonal variations conditions, which often affects model performance.

Based on our results, we recommend that, for optimum model performance, grid nudging options should be chosen with run times in mind. For our study area (and perhaps other areas with similar terrain and climatic conditions in Ghana and the West African sub-region), model configurations with shorter run times of 1 or 2 days, combined with grid nudging above a height of 1600 m give the best average wind speed predictions, and are therefore recommended for wind simulations. However, for longer run times (of 7 days or more), the more consistently performing approach of disabling nudging below the model-calculated PBL height, gives better results and is therefore recommended.

Declarations

Author contribution statement

Denis E.K. Dzebre: Conceived and designed the experiments; Performed the experiments; Analyzed and interpreted the data; Contributed reagents, materials, analysis tools or data; Wrote the paper.

Akwasi A. Acheampong: Conceived and designed the experiments.

Joshua Ampofo: Conceived and designed the experiments.

Muyiwa S. Adaramola: Conceived and designed the experiments; Contributed reagents, materials, analysis tools or data.

Funding statement

This work was supported by the Energy and Petroleum (EnPe) Project of the Norwegian Agency for Development Cooperation (Norad) and by the UPERCRET-

KNUST Program who supported Denis Edem Kwame Dzebre with a PhD scholarship.

Competing interest statement

The authors declare no conflict of interest.

Additional information

Supplementary content related to this article has been published online at <https://doi.org/10.1016/j.heliyon.2019.e01385>.

References

- [1] T. Ohsawa, et al., Investigation of WRF configuration for offshore wind resource maps in Japan, in: Wind Europe Summit, Hamburg Messe, Hamburg, Germany, 2016.
- [2] D. Carvalho, et al., A sensitivity study of the WRF model in wind simulation for an area of high wind energy, *Environ. Model. Softw.* 33 (2012) 23–34.
- [3] X. Chadee, N. Seegobin, R. Clarke, Optimizing the Weather Research and Forecasting (WRF) model for mapping the near-surface wind resources over the Southernmost Caribbean Islands of Trinidad and Tobago, *Energies* 10 (2017) 931.
- [4] S. Fernández-González, et al., Sensitivity analysis of the WRF model: wind-resource assessment for complex terrain, *J. Appl. Meteorol. Climatol.* (2017).
- [5] E.-M. Giannakopoulou, R. Nhili, WRF model methodology for offshore wind energy applications, *Adv. Meteorol.* (2014).
- [6] T.M. Giannaros, D. Melas, I. Ziomas, Performance evaluation of the Weather Research and Forecasting (WRF) model for assessing wind resource in Greece, *Renew. Energy* 102 (2017) 190–198.
- [7] L. Ji-Hang, G. Zhen-Hai, W. Hui-Jun, Analysis of wind power assessment based on the WRF model, *Atmos. Ocean. Sci. Lett.* 7 (2014) 126–131.
- [8] M. Mohammadpour Penchah, H. Malakooti, M. Satkin, Evaluation of planetary boundary layer simulations for wind resource study in east of Iran, *Renew. Energy* 111 (2017) 1–10.
- [9] M.O. Mughal, et al., Wind modelling, validation and sensitivity study using Weather Research and Forecasting model in complex terrain, *Environ. Model. Softw.* 90 (2017) 107–125.

- [10] C. Surussavadee, W. Wu, Evaluation of WRF planetary boundary layer schemes for high-resolution wind simulations in Northeastern Thailand, in: 2015 IEEE International Geoscience and Remote Sensing Symposium, IGARSS), 2015, pp. 3949–3952.
- [11] C. Surussavadee, Evaluation of WRF near-surface wind simulations in tropics employing different planetary boundary layer schemes, in: 2017 8th International Renewable Energy Congress (IREC), 2017, pp. 1–4.
- [12] D. Carvalho, et al., WRF wind simulation and wind energy production estimates forced by different reanalyses: comparison with observed data for Portugal, *Appl. Energy* 117 (2014) 116–126.
- [13] F.J. Santos-Alamillos, et al., Analysis of WRF model wind estimate sensitivity to physics parameterization choice and terrain representation in Andalusia (Southern Spain), *J. Appl. Meteorol. Climatol.* 52 (2013) 1592–1609.
- [14] R.F. Banks, et al., Sensitivity of boundary-layer variables to PBL schemes in the WRF model based on surface meteorological observations, lidar, and radiosondes during the HygrA-CD campaign, *Atmos. Res.* 176–177 (2016) 185–201.
- [15] University Corporation for Atmospheric Research (UCAR), Steps to Run Analysis Nudging in WRF-ARW, 2018 [cited 2018 August 16]; Available from: http://www2.mmm.ucar.edu/wrf/users/wrfv3.1/How_to_run_grid_fdda.html.
- [16] E.O. Essandoh, E.Y. Osei, F.W. Adam, Prospects of wind power generation in Ghana, *Int. J. Mech. Eng. Technol.* 5 (10) (2014) 156–179.
- [17] D. Gill, M. Pyle, Nesting in WRF, 2012. Presentation.
- [18] M. Duda, Running the WRF Preprocessing System, 2016. Presentation.
- [19] C.B. Wei Wang, Michael Duda, Jimy Dudhia, Dave Gill, Michael Kavulich, Keene Kelly, Ming Chen, Hui-Chuan Lin, John Michalakes, Syed Rizvi, Xin Zhang, Judith Berner, Soyoung Ha, Kate Fossell, ARW Version 3 Modeling System User's Guide, 2016.
- [20] W. Wang, Considerations for Designing an Numerical Experiment, 2017.
- [21] W.C. Skamarock, A description of the advanced research WRF version 3, *Tech. Note* (2008) 1–96.
- [22] NCEP FNL Operational Model Global Tropospheric Analyses, Continuing from July 1999, 2000.

- [23] J. Mandel, J. Beezley, A. Kochanski, Coupled atmosphere-wildland fire modeling with WRF 3.3 and SFIRE 2011, *Geosci. Model Dev.* 4 (2011) 591–610.
- [24] Ovens, D. How to Properly Rotate WRF Winds to Earth-Relative Coordinates Using Python, GEMPAK, and NCL. [cited 2019 January 18]; Available from: <http://www-k12.atmos.washington.edu/~ovens/wrfwinds.html>.
- [25] J. Dudhia, et al., Evaluation of Weather Research and Forecasting (WRF) Model Physics in Simulating West African Monsoon, WAM), 2017.
- [26] Statistical Computation Laboratory. Computing the Pearson Correlation Coefficient. [cited 2018 27/05]; Available from: <http://www.stat.wmich.edu/s216/book/node122.html>.
- [27] C. Agostinelli, U. Lund, R Package ‘Circular’: Circular Statistics (Version 0.4-7), 2013.
- [28] M.S. Adaramola, M. Agelin-Chaab, S.S. Paul, Assessment of wind power generation along the coast of Ghana, *Energy Convers. Manag.* 77 (2014) 61–69.
- [29] X.T. Chadee, R.M. Clarke, Air density climate of two caribbean tropical islands and relevance to wind power, *ISRN Renew. Energy* 2013 (2013) 7.
- [30] Cedar Lake Ventures Inc, Average Weather in Accra, Ghana, Year Round – Weather Spark, 2018 [cited 2018 07/06]; Available from: <https://weatherspark.com/y/42322/Average-Weather-in-Accra-Ghana-Year-Round>.
- [31] Climate and Average Monthly Weather in Accra, Ghana, World Weather and Climate Information, Accra,Ghana, 2019 [cited 2019 January 24]; Available from: <https://weather-and-climate.com/average-monthly-Rainfall-Temperature-Sunshine>.
- [32] The World Bank Group, Climate Change Knowledge Portal, 2019 [cited 2019 January 24]; Available from: http://sdwebx.worldbank.org/climateportal/index.cfm?page=country_historical_climate&ThisRegion=Africa&ThisCCCode=GHA.
- [33] R. Boadh, et al., Sensitivity of PBL schemes of the WRF-ARW model in simulating the boundary layer flow parameters for its application to air pollution dispersion modeling over a tropical station, *Atmósfera* 29 (2016) 61–81.

Annex-I: Full Statistical Metrics from Analyses

AVERAGE SPEEDS AND RAW METRICS

	60 m				50 m				40 m						
	Average Wind Speeds (m/s)	RMSE (m/s)	ME (m/s)	STDE (m/s)	CC	Average Wind Speeds (m/s)	RMSE (m/s)	ME (m/s)	STDE (m/s)	CC	Average Wind Speeds (m/s)	RMSE (m/s)	ME (m/s)	STDE (m/s)	CC
Observation	5.9					5.8					5.8				
1day_N-10l	5.7	1.23	-0.22	1.21	0.7	5.7	1.2	-0.2	1.2	0.7	5.6	1.2	-0.1	1.2	0.7
1day_N-pblh	5.3	1.25	-0.61	1.10	0.8	5.3	1.2	-0.6	1.1	0.8	5.2	1.2	-0.5	1.1	0.8
1day_N-a	5.7	1.25	-0.25	1.22	0.7	5.6	1.2	-0.2	1.2	0.7	5.6	1.2	-0.2	1.2	0.7
2days_N-10l	5.4	1.40	-0.52	1.30	0.7	5.4	1.4	-0.5	1.3	0.7	5.3	1.3	-0.4	1.3	0.7
2days_N-pblh	5.2	1.30	-0.67	1.12	0.8	5.2	1.3	-0.6	1.1	0.8	5.2	1.3	-0.6	1.1	0.8
2days_N-a	5.4	1.40	-0.55	1.29	0.7	5.3	1.4	-0.5	1.3	0.7	5.3	1.3	-0.5	1.3	0.7
7days_N-10l	4.8	1.86	-1.10	1.49	0.6	4.8	1.8	-1.0	1.5	0.6	4.8	1.8	-1.0	1.5	0.6
7days_N-pblh	5.1	1.38	-0.76	1.15	0.8	5.1	1.4	-0.7	1.1	0.8	5.1	1.3	-0.7	1.1	0.8
7days_N-a	4.8	1.89	-1.16	1.49	0.6	4.7	1.8	-1.1	1.5	0.6	4.7	1.8	-1.1	1.5	0.6
14days_N-10l	4.6	1.98	-1.29	1.50	0.6	4.6	1.9	-1.2	1.5	0.6	4.6	1.9	-1.2	1.5	0.6
14days_N-pblh	5.1	1.42	-0.82	1.16	0.8	5.1	1.4	-0.8	1.1	0.8	5.0	1.4	-0.7	1.2	0.8
14days_N-a	4.6	2.01	-1.31	1.52	0.6	4.6	2.0	-1.3	1.5	0.6	4.6	1.9	-1.2	1.5	0.6
31days_N-10l	4.5	1.98	-1.44	1.37	0.7	4.5	1.9	-1.4	1.3	0.7	4.4	1.9	-1.3	1.4	0.7
31days_N-pblh	5.1	1.48	-0.81	1.24	0.7	5.1	1.4	-0.8	1.2	0.7	5.0	1.4	-0.7	1.2	0.7
31days_N-a	4.5	2.04	-1.45	1.43	0.6	4.4	2.0	-1.4	1.4	0.6	4.4	2.0	-1.4	1.4	0.6

SCALED METRICS AND PREDICTION SKILL SCORES

	60 m				50 m				40 m						
	RMSE _D ^{SCALED} (m/s)	ME _D ^{SCALED} (m/s)	STDE _D ^{SCALED} (m/s)	CC	Skill Score	RMSE _D ^{SCALED} (m/s)	ME _D ^{SCALED} (m/s)	STDE _D ^{SCALED} (m/s)	CC	Skill Score	RMSE _D ^{SCALED} (m/s)	ME _D ^{SCALED} (m/s)	STDE _D ^{SCALED} (m/s)	CC	Skill Score
1day_N-10l	0	0	0.3	0.7	3.5	0	0	0.3	0.7	3.5	0	0	0.3	0.7	3.5
1day_N-pblh	0.0	0.3	0	0.8	3.4	0.0	0.3	0	0.8	3.4	0.0	0.3	0	0.8	3.4
1day_N-a	0.0	0.0	0.3	0.7	3.4	0.0	0.0	0.3	0.7	3.4	0.0	0.0	0.3	0.7	3.4
2days_N-10l	0.2	0.2	0.5	0.7	2.8	0.2	0.2	0.5	0.7	2.8	0.2	0.2	0.5	0.7	2.8
2days_N-pblh	0.1	0.4	0.0	0.8	3.3	0.1	0.4	0.1	0.8	3.3	0.1	0.4	0.1	0.8	3.2
2days_N-a	0.2	0.3	0.4	0.7	2.8	0.2	0.3	0.4	0.7	2.8	0.2	0.3	0.4	0.7	2.8
7days_N-10l	0.8	0.7	0.9	0.6	1.2	0.8	0.7	0.9	0.6	1.1	0.8	0.7	0.9	0.6	1.1
7days_N-pblh	0.2	0.4	0.1	0.8	3.0	0.2	0.5	0.1	0.8	3.0	0.2	0.5	0.2	0.8	2.9
7days_N-a	0.8	0.8	0.9	0.6	1.1	0.8	0.8	0.9	0.6	1.1	0.8	0.8	0.9	0.6	1.1
14days_N-10l	0.9	1.0	1.0	0.6	0.8	0.9	0.9	1.0	0.6	0.8	0.9	0.9	1.0	0.6	0.8
14days_N-pblh	0.2	0.5	0.2	0.8	2.9	0.2	0.5	0.2	0.8	2.9	0.2	0.5	0.2	0.8	2.9
14days_N-a	1.0	0.9	1	0.6	0.7	1.0	0.9	1	0.6	0.7	1.0	0.9	1	0.6	0.7
31days_N-10l	0.9	1.0	0.6	0.7	1.1	0.9	1.0	0.6	0.7	1.1	0.9	1.0	0.6	0.7	1.1
31days_N-pblh	0.3	0.5	0.3	0.7	2.6	0.3	0.5	0.3	0.7	2.6	0.3	0.5	0.3	0.7	2.6
31days_N-a	1	1	0.8	0.6	0.8	1	1	0.8	0.6	0.8	1	1	0.8	0.6	0.8

AVERAGE DIRECTION PREDICTIONS AND RAW METRICS

	60 m						50 m					
	Average Wind Direction (degrees)	RMSE (degrees)	ME (degrees)	STDE (degrees)	CircC		Average Wind Direction (degrees)	RMSE (degrees)	ME (degrees)	STDE (degrees)	CircC	
Observation	55.8						54.5					
1day_N-10l	39.6	47.3	-25.9	39.6	0.4		39.5	46.3	-23.9	39.6	0.4	
1day_N-pblh	37.5	46.7	-27.6	37.7	0.5		37.4	45.5	-25.6	37.6	0.5	
1day_N-a	39.4	47.2	-26.9	38.8	0.4		39.3	46.0	-24.9	38.7	0.4	
2days_N-10l	37.7	47.6	-25.1	40.5	0.5		37.9	46.5	-22.9	40.4	0.5	
2days_N-pblh	39.7	48.9	-27.0	40.7	0.4		39.6	47.8	-25.0	40.7	0.4	
2days_N-a	38.9	47.1	-25.5	39.6	0.5		39.3	45.9	-23.4	39.5	0.5	
7days_N-10l	41.0	56.6	-26.9	49.8	0.5		41.3	55.7	-24.7	49.9	0.5	
7days_N-pblh	42.7	47.8	-26.0	40.1	0.4		42.7	46.6	-23.9	40.0	0.4	
7days_N-a	38.7	56.2	-27.4	49.1	0.5		38.6	55.3	-25.2	49.1	0.5	
14days_N-10l	40.4	61.0	-27.5	54.4	0.5		40.9	60.2	-25.3	54.6	0.5	
14days_N-pblh	42.8	48.1	-25.6	40.8	0.4		42.8	47.0	-23.5	40.7	0.4	
14days_N-a	37.0	59.8	-28.0	52.9	0.5		37.2	59.1	-25.9	53.1	0.5	
31days_N-10l	44.2	62.0	-29.0	54.8	0.5		43.0	62.0	-27.3	55.7	0.5	
31days_N-pblh	43.3	47.8	-24.9	40.8	0.4		43.5	46.4	-23.0	40.3	0.4	
31days_N-a	50.5	59.0	-24.6	53.6	0.4		50.0	58.4	-22.8	53.8	0.4	

SCALED METRICS AND MODEL SKILL SCORE FOR DIRECTION PREDICTION

	60 m						50 m					
	RMSE ^{SCALED} (degrees)	ME ^{SCALED} (degrees)	STDE ^{SCALED} (degrees)	CircC	Skill Score		RMSE ^{SCALED} (degrees)	ME ^{SCALED} (degrees)	STDE ^{SCALED} (degrees)	CircC	Skill Score	
1day_N-10l	0.04	0.70	0.11	0.4	2.6		0.05	0.76	0.11	0.4	2.5	
1day_N-pblh	0	0.31	0	0.5	3.2		0	0.38	0	0.5	3.1	
1day_N-a	0.03	0.47	0.06	0.4	2.9		0.03	0.54	0.06	0.4	2.8	
2days_N-10l	0.06	0.88	0.16	0.5	2.4		0.06	0.97	0.16	0.5	2.3	
2days_N-pblh	0.14	0.44	0.18	0.4	2.6		0.14	0.51	0.17	0.4	2.6	
2days_N-a	0.03	0.79	0.11	0.5	2.6		0.02	0.88	0.10	0.5	2.5	
7days_N-10l	0.65	0.47	0.71	0.5	1.7		0.62	0.58	0.68	0.5	1.6	
7days_N-pblh	0.07	0.69	0.14	0.4	2.5		0.06	0.76	0.13	0.4	2.4	
7days_N-a	0.62	0.35	0.67	0.5	1.9		0.59	0.46	0.64	0.5	1.8	
14days_N-10l	0.93	0.35	0.98	0.5	1.2		0.89	0.45	0.94	0.5	1.2	
14days_N-pblh	0.09	0.78	0.18	0.4	2.3		0.09	0.84	0.17	0.4	2.3	
14days_N-a	0.86	0.22	0.89	0.5	1.5		0.83	0.30	0.86	0.5	1.5	
31days_N-10l	1	0	1	0.5	1.5		1	0	1	0.5	1.5	
31days_N-pblh	0.07	0.93	0.18	0.4	2.3		0.05	0.96	0.15	0.4	2.3	
31days_N-a	0.80	1	0.93	0.4	0.7		0.78	1	0.90	0.4	0.7	

SUMMARY OF ESTIMATED POWER AT DIFFERENT HEIGHTS

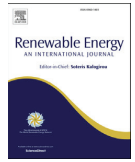
	60 m		50 m		40 m	
	Estimated Power Flux (Wm ⁻²)	Power Flux Estimation Error (%)	Estimated Power Flux (Wm ⁻²)	Power Flux Estimation Error (%)	Estimated Power Flux (Wm ⁻²)	Power Flux Estimation Error (%)
Observation	152		145		141	
1day_N-10l	127	16	124	15	122	14
1day_N-pblh	105	31	103	29	100	29
1day_N-a	125	17	123	15	121	15
2days_N-10l	111	27	109	25	107	25
2days_N-pblh	102	33	100	31	98	31
2days_N-a	110	27	108	26	106	25
7days_N-10l	81	46	80	45	78	45
7days_N-pblh	99	35	96	34	94	33
7days_N-a	80	48	78	46	77	46
14days_N-10l	74	51	73	50	72	49
14days_N-pblh	97	36	95	35	93	34
14days_N-a	74	51	73	50	72	49
31days_N-10l	69	54	68	53	67	52
31days_N-pblh	100	34	97	33	95	33
31days_N-a	70	54	69	53	67	52

Paper II



Contents lists available at ScienceDirect

Renewable Energy

journal homepage: www.elsevier.com/locate/renene

A preliminary sensitivity study of Planetary Boundary Layer parameterisation schemes in the weather research and forecasting model to surface winds in coastal Ghana



Denis E.K. Dzebre^{a, b, c}, Muyiwa S. Adaramola^{a, *}

^a Faculty of Environmental Sciences and Natural Resources, Norwegian University of Life Sciences, Ås, Norway

^b Department of Mechanical Engineering, Kwame Nkrumah University of Science and Technology, Kumasi, Ghana

^c The Brew-Hammond Energy Centre, Kwame Nkrumah University of Science and Technology, Kumasi, Ghana

ARTICLE INFO

Article history:

Received 22 August 2018

Received in revised form

20 March 2019

Accepted 21 June 2019

Available online 22 June 2019

Keywords:

Wind energy

Planetary boundary layer (PBL)

parameterisation schemes

Weather research and forecasting model

(WRF)

Sensitivity study

Ghana

Tropics

ABSTRACT

There is growing interest in the use of Weather Researching and Forecasting (WRF) model for assessment of wind energy potential. The influence of parameterisation schemes in these models depends on meteorological processes, which tend to differ with geographic regions. In this paper, we test the sensitivity of surface winds in an area in Ghana, to 11 of the Planetary Boundary Layer schemes available in WRF. Thirty-six days were simulated with the schemes. Hourly simulated wind speeds and directions were compared with measurements taken at 40, 50, and 60m above ground level, and the schemes ranked according to a prediction skill score calculated according to how well their predictions compared to observations. The local closure MYNN schemes offered consistently good performance; often predicting the average wind speed with a Root Mean Square Error of less than <2 m/s, indicating good performance. However, the GBM and UW schemes produced relatively better results for days selected from a period in which monthly average winds at this location are highest. Based on our results, we recommend the MYNN3 (and the GBM, depending on the season of the year) for wind simulations in this area, and areas with similar topography and climate in Ghana.

© 2019 The Authors. Published by Elsevier Ltd. This is an open access article under the CC BY-NC-ND license (<http://creativecommons.org/licenses/by-nc-nd/4.0/>).

1. Introduction

1.1. Background

Ranking of potential wind farm sites based on wind energy potential is an important step toward the development of the wind resources on a national scale. This involves the assessment of the wind energy potential at the candidate sites, with local wind speed and direction measurements, often taken over at least, one year, so that the local wind climatology can be realistically represented [1,2]. However, mast measurements can be expensive and time-consuming. As a result, there is growing interest in wind simulations with Numerical Weather Prediction (NWP) models, which offer a relatively low-cost alternative source of data for assessments of wind resources. The Weather Research and Forecasting Model (WRF), is one such model which has proven to be a reference in

research and operational regional wind resource assessment over the years [3,4].

NWP models rely on parameterisation schemes to adequately represent processes that cannot be explicitly resolved by the models. In WRF, these schemes fall into the Microphysics (MP), Cumulus, Long-wave Radiation (Rad-L), Short-wave Radiation (Rad-S), Land Surface Model (LSM), Surface Layer (SL), and Planetary Boundary Layer (PBL) categories [3]. Studies have reported significant sensitivities of WRF surface wind simulations, to PBL schemes in particular [1,2,4–13].

1.2. Turbulence parameterisation

The influence of the earth's surface is transferred to the free atmosphere through several processes that take place in the lower atmosphere (turbulent or boundary layer). Atmospheric

* Corresponding author.

E-mail addresses: dekdzbre.coe@knust.edu.gh (D.E.K. Dzebre), muyiwa.adaramola@mmbu.no (M.S. Adaramola).

turbulence, caused by irregular swirls of fluids and heat energy in the atmosphere, is responsible for the vertical and horizontal dispersion of substances such as water vapour, smoke and energy in the atmosphere, and plays a very important role in these processes occurring in the turbulent layer. Atmospheric turbulence is a mix of mechanical and thermal turbulence. Mechanical turbulence comes mainly from wind shear, which is caused mainly by frictional drag from the earth's surface, resulting in slower winds near the surface than aloft. It can also be caused by wind swirls behind obstacles such as trees, buildings and islands (wake turbulence). Thermal or convective turbulence on the other hand, results from plumes of warm, more buoyant air rising and cold, denser air descending to replace it when solar radiation heats the earth's surface. When the vertical movement of air, combines with flow disturbances due to mechanical turbulence, surface wind flow becomes irregular, deviating from mean flow [14].

Turbulence can often not be completely resolved by NWP models. Therefore, turbulence parameterisation in NWP models, approximates (parameterizes) unresolved turbulence, so that time derivatives of variables (such as three-dimensional wind velocity components; u , v , and w) can be predicted using the models. To achieve this, finite numbers of (lower order) unknowns in prognostic (prediction) equations are predicted or solved for, while the remaining (higher order) unknowns are approximated. Closure orders are named after the highest order unknowns that are predicted. Therefore, a first order closure for instance, predicts moments (or means) of up to the first order, and approximates the second moments (which are covariance terms that are basically averages of products of two departures (variability due to turbulence) from the mean (e.g., $\overline{u'v'}$)). Similarly, second order closure predicts all moments up to the second moments, and approximates the third and higher moments, and so on and so forth. Sometimes, some higher order moments may be predicted while others, of the same order, are approximated, in which case the order of closure is a non-integer. For instance, a closure that predicts all first moments and some second moments, while approximating other second moments will be a 1.5 order closure [15]. Second-order or higher order closures of wind components can be used to quantify the Turbulent Kinetic Energy (TKE) associated with the transfer processes that occur in the boundary layer [16,17]. Higher-order closures have often been found to be more accurate, as they are able solve for higher moments [16]. However, they are more computationally expensive.

Regardless of the order of closure, two main approaches are used for closure approximations; the local and non-local (mixed layer) approaches. Local closure parameterizes unknown quantities in terms of values of known quantities, or close vertical derivatives of these quantities at the same grid point. Non-local closure on the other hand, parameterizes in terms of quantities at other grid points in the vertical grid. A common closure approximation technique is the K-theory or gradient-transport theory, in which the second moments are approximated in terms of turbulent flux. With this theory, if the approximation term in the general prognostic equation for a variable ξ is

$$\frac{\partial}{\partial z} \bar{\xi} = \dots - \frac{\partial}{\partial x_j} (\overline{\xi' u_j'}) \quad (1)$$

then a closure approximation of the flux, $\overline{\xi' u_j'}$, is given by

$$\overline{\xi' u_j'} = -K \frac{\partial}{\partial x_j} (\bar{\xi}) \quad (2)$$

where K is a scalar associated with the transfer process of the variable [16]. Its polarity indicates whether the turbulent flux is

down or up the local gradient of ξ , and it can be expressed in terms of the TKE and length-scale (mixing length) or specified from a profile. The different methods for getting K , gives rise to different TKE closure schemes [9,18]. The schemes can also differ in how the TKE is obtained, with some schemes solving additional prognostic equations to predict the TKE [19]. Local closures work best in stable climatic conditions, where turbulent eddies (departures from the local variable mean) are small and locally generated [16].

Non-local closure approaches recognise the presence of non-localised and large eddies whose vertical dimension is approximately that of the entire boundary-layer depth, and assume that these eddies are generated from turbulence that is not localised, but spans the entire boundary layer [16]. Diagnostic non-local schemes in WRF account for non-local transport by large eddies with the inclusion of either a mass-flux profile, $M\Delta T$, or a non-gradient term, I , in the prognostic equation of a variable [19]. The closure approximation term in the prognostic equation therefore becomes (with the counter gradient term);

$$\frac{\partial}{\partial z} K \left(\frac{\partial}{\partial z} \xi + I \right) \quad (3)$$

and with the mass-flux term;

$$\frac{\partial}{\partial z} \left(K \frac{\partial}{\partial z} \xi + M\Delta T \right) \quad (4)$$

where ΔT represents the difference in temperatures at some vertical level in the boundary layer, and at the top of the surface layer, and M , a function of the surface heat flux [16,19].

Turbulence is parameterised in WRF by PBL parameterisation schemes with direct inputs from SL and LSM parameterisation schemes. The twelve (12) PBL parameterisation schemes available in the Advanced Research WRF (ARW) v3.8.1 are presented in Table 1. The YSU is an improved version of the MRF scheme [9]. It can be run with two wind-bias correction methods for terrain effects. The methods are set with the "topo_wind" option (topo_wind = 1 or 2 in the "bl_pbl_physics" section of the WRF namelist. input file). All these schemes, except the SH scheme are recommended for horizontal grid resolutions greater than 1 km. For horizontal grid resolutions between 200 m and 1 km, the SH scheme is recommended. And for horizontal grid resolutions less than 100 m, Large Eddy Simulations (without a PBL parameterisation) are recommended [19]. It should be noted that simulations with finer resolutions in WRF are more computationally expensive, and the improvement in results this achieves in wind simulations, has not always been found to be worth the extra computational power [2,5]. Descriptions of the schemes, (their pros and cons) and appropriate references are available in number of studies [20, 21] and on the physics section of the WRF Users page.

Performance of parameterisation schemes often depends significantly on the meteorological processes that prevail in a specific geographic region [16]. So, sensitivity studies of parameterisation schemes are recommended to determine the optimum schemes to use in a climatic region. Studies examining the sensitivity of wind simulations by WRF for wind energy assessment purposes to PBL schemes in the tropics are few. We came across only one such study for sub-Saharan Africa in open literature. In that study, which was over a site with complex terrain in East Africa, the YSU scheme was found to be the better scheme, when it was tested against the ACM2 scheme for wind speeds and directions at heights of 38, 39, and 46 m [8]. In other sensitivity studies aimed at wind energy assessments in other areas in the

Table 1
Summary of PBL schemes available in the AR-WRF v3.8.1 [19–23].

Scheme	Order	Closure Method	Year Added
Mellor–Yamada–Janjic (MYJ)	1.5	Local	2000
Medium Range Forecast (MRF)	1	Non-local	2000
Yonsei University (YSU)	1	Non-local	2004
Asymmetric Convective Model (ACM2)	1	Local + Non-local	2008
Mellor–Yamada Nakanishi and Niino Level 2.5 (MYNN2)	1.5	Local	2009
Mellor–Yamada Nakanishi and Niino Level 3 (MYNN3)	2	Local	2009
Bougeault–Lacarrère (BL)	1.5	Local	2009
University of Washington - TKE (UW)	1.5	Local	2011
Total Energy - Mass Flux (TEMF)	1.5	Local + Non-local	2011
Quasi-Normal Scale Elimination (QNSE)	1.5	Local	2012
Grenier–Bretherton–McCa (GBM)	1.5	Local	2013
Shin–Hong (SH)		Non-local	2015

tropics, the YSU scheme was again found to produce the best simulations in a test of six (6) other schemes (MYJ, ACM2, UW, TEMF, MYNN2, and QNSE) over Trinidad and Tobago [18]. However, in simulations of wind speeds and directions at 65 and 90 m over North-Eastern Thailand, the UW and GBM schemes were found to produce the best results, while the QNSE, YSU and MYNN3 were the worst among 9 schemes tested in one study [7]. In addition, in another study for winds at the same heights (at 65 and 90 m), the YSU, and MYNN3 performed well for speeds above 2 m/s, while the ACM2 and GMB were the worst among the 7 schemes that were tested [6]. Other studies in other tropical areas for other applications have tested all the schemes except the sub-grid SH scheme, with the MYJ, MYNN, QNSE, YSU and ACM2 schemes being tested more often. The ACM2, YSU and MYNN2 have often been found to produce better simulations of wind speeds and directions at 10 m height, while the MYJ and QNSE schemes tended to often produce the worst results, considerably overestimating wind speeds [9,13,24–26]. Some studies also found all these schemes to be sensitive to seasons, with the MYNN2 and ACM2 schemes being best in the winter and summer periods respectively [26](Gunwani & Mohan, 2017).

Ghana's Renewable Energy (RE) Policy targets 10% of total electricity consumption from (non-large hydro) RE sources by 2020. As at the end of 2017, the country's RE electricity generation is mainly from solar PV generation, and stood at less than the 10% target [27]. The country has potential for utility wind power [28], but development is currently faced with various challenges, including limited data for resource assessments. This lack of wind data can be mitigated with numerical simulations of surface winds with NWP models such as WRF. Towards this, this study investigates the sensitivity of surface winds at a potential wind farm site in the country to simulations with all applicable PBL schemes in the AR-WRF. The aim of this study is to determine comparatively, the performance of the schemes and make recommendations on which schemes are likely to be suitable for wind simulations over this area and other areas with similar climate and topographic conditions in the country.

2. Data and method

2.1. Study area and measured data

The study area covers the eastern coastal plains of Ghana. The area stretches, approximately, between longitudes 0° and 1°E as well as latitudes 4.5°N and 6°N. According to a wind map of Ghana (shown in Fig. 2) that was developed as part of the Solar

and Wind Energy Resource Assessment (SWERA) [29], and based on measurement campaigns by the Energy Commission of Ghana (EC), the study area has wind resources good enough to make a wind power project viable. The Energy Commission of Ghana (EC), based on this study, has been conducting mast measurements at selected sites, mostly along the coast of the area. The observational (measured) data for this study, which comprise hourly averages of wind speeds for 2013, were measured at heights of 40, 50, and 60 m above ground level, and wind directions, at 50 and 60 m only, are from one of such EC masts, located at Anloga. Anloga is in the coastal strip between the Keta Lagoon and the sea, in the Keta Municipality of Volta Region in Ghana (see Fig. 1(b)). Most of the areas in the study area have low-lying coastal plains covered in savanna grass vegetation (see Fig. 1(c)). As can be seen from the terrain map in Fig. 1(a), the study area generally has a smooth terrain. The highest point in the Keta municipality is about 53 m above sea level [30].

The southern parts of Ghana experience two main seasons in a year; a relatively dry Harmattan season and a bimodal Rainy season that ends in November. The Harmattan season is dominated by dry and dusty desert winds from the North-East, between December and March, while Monsoon winds from the south, over the sea, dominate the Rainy season [31].

2.2. Model and domain configuration

The simulation domain comprised three (3) one-way nested domains of resolutions 27 km, 9 km, and 3 km. Fig. 3 illustrates the domains. The horizontal resolutions were chosen to achieve a recommended nesting ratio of less than 5 [20]. The final horizontal resolution of 3 km was chosen because it has been found to be optimum for wind simulations in (earlier versions of) WRF. Increasing the resolution beyond this was found not to significantly improve model performance, despite being more computationally expensive [2,5]. The outermost domain covers Ghana and its immediate neighbouring countries as well as parts of the Sahel deserts to the north and the sea to the south of the country. Domain 2 covers the part of the country, and parts of its immediate neighbouring countries to the east. Domain 3 covers the high wind energy potential coastal plains of Southeast Ghana. Most of the EC's wind energy measurement masts, as well as the sites of some planned wind farms in Ghana, are in the area captured by this domain. Based on recommended vertical level references for tests [20], a vertical resolution of 40 levels was used for all domains. The levels were automatically set by the model. The model configuration is summarised in Table 2.

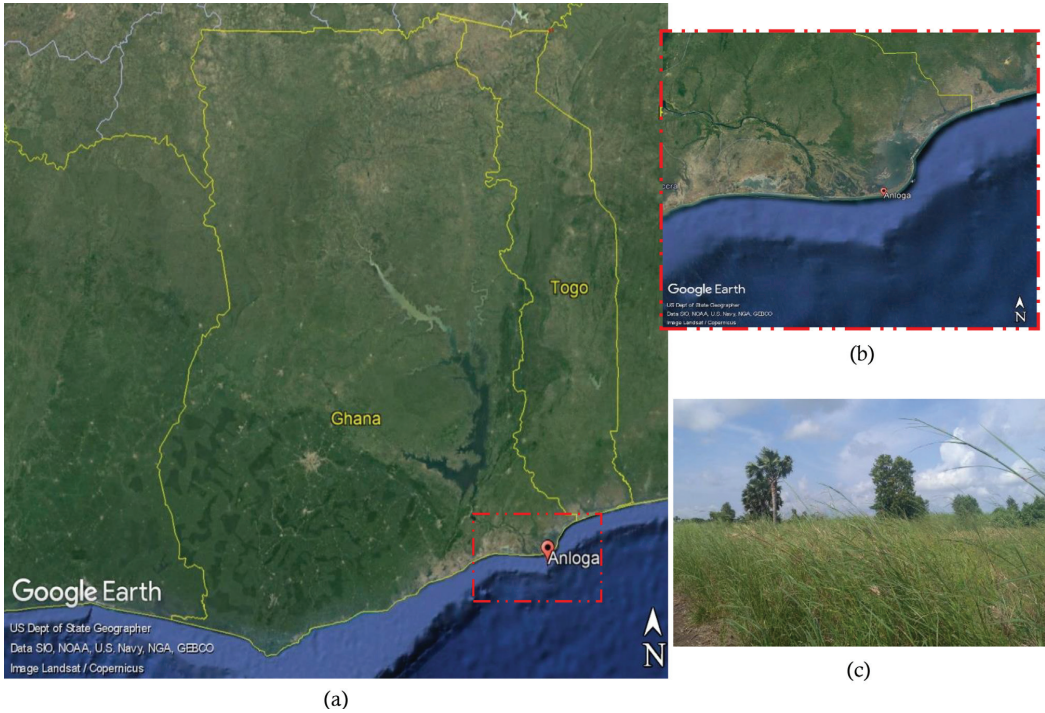


Fig. 1. (a): Map of Ghana showing study area (in broken red borders). (b): Study area (c): Typical vegetation cover in the study; grassland dotted with date palms and trees.

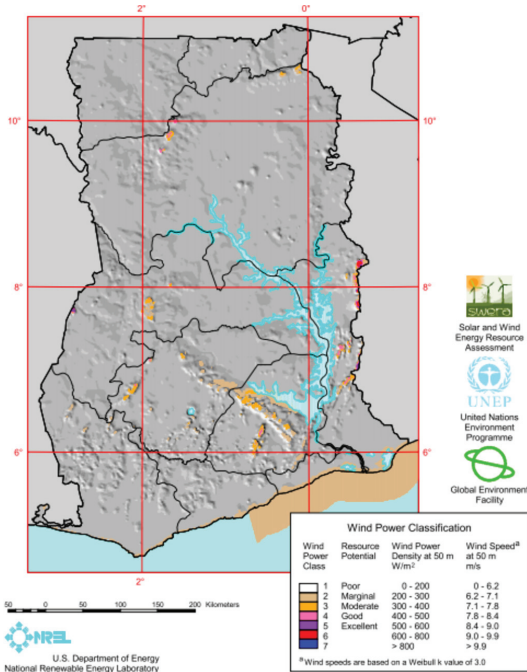


Fig. 2. Ghana wind power classification map (at 50m) [29].

2.2.1. Scheme configurations

Eleven (11) scheme configurations, which are presented in Table 3, were tested. The Shin-Hong (SH) scheme was not tested as it is not recommended for the final horizontal resolution chosen for this study [19]. The Medium Range Forecast (MRF) scheme was also not tested, as the YSU is considered an improved version of it [20]. The YSU scheme was run in two configurations; based on the two wind-bias correction methods for terrain effects [20]. SL, LSM and other parameterisation schemes (apart from the PBL schemes) were selected based on recommendations of [3,20] and similar researches in the tropics (mentioned earlier). Cumulus parameterisation was turned off for domain 3 as the horizontal resolution in this domain is considered fine enough for adequate resolving of cumulus processes [2,3].

2.3. Experimental approach

The experimental approach in this study is slightly different from what has been used in other studies, where a whole year or several months are simulated in order to choose the best scheme for an area. In the approach used for this study, we assume that the parameterisation scheme configuration that best predicts extreme (the highest and lowest) wind events consistently, should be able to predict other wind events well. Against this assumption, the scheme configurations were tested on “sets” of test days, selected for their relatively high or low daily average wind speeds, and their representativeness of the two main seasons in this part of Ghana; the Rainy season (spanning April to November), and the Harmattan

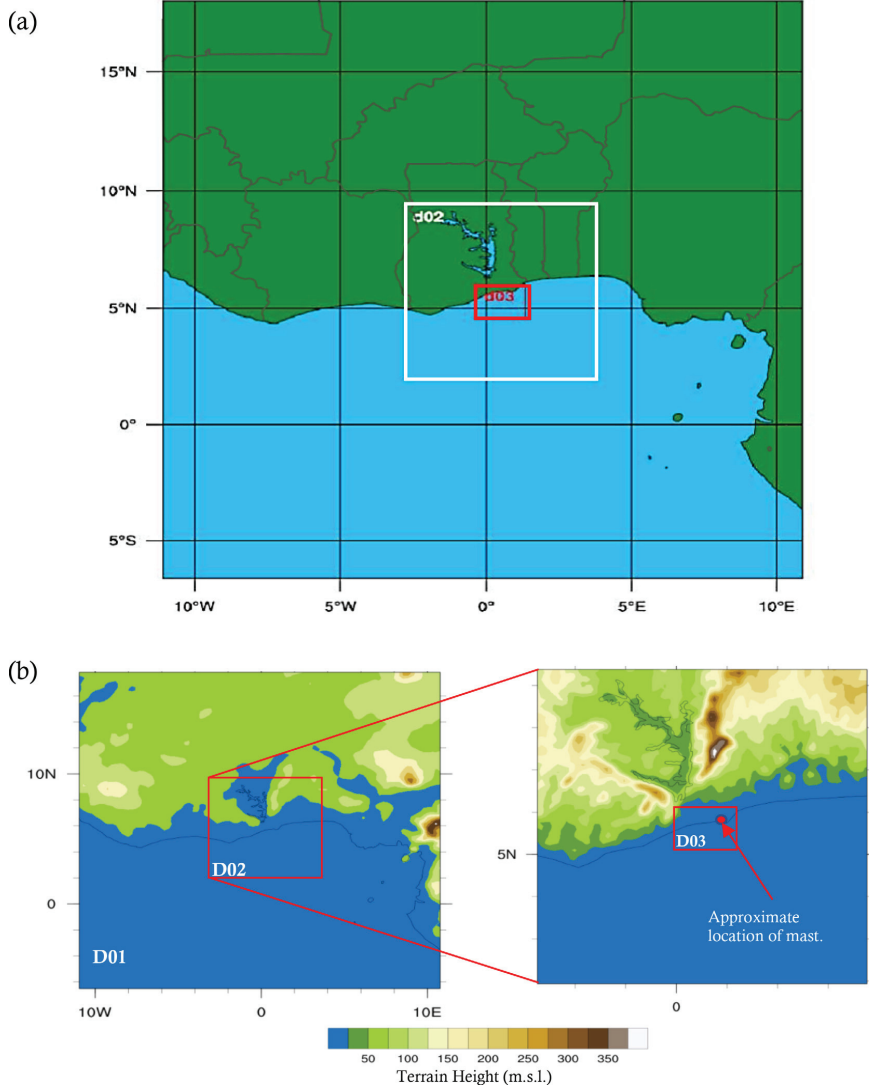


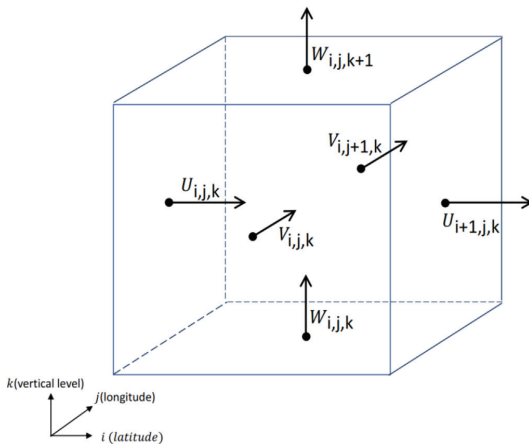
Fig. 3. Simulation domains.

Table 2
Model Configuration.

Model Version: ARW 3.8.1			
Nudging	Grid Nudging; turned off for lower 10 model levels.		
Initial and boundary conditions	NCEP Final Analysis (GFS-FNL): 1-degree spatial and 6 hourly temporal resolutions.		
Land Use data	30-arc-second USGS		
Geographical Projection scheme	Mercator		
Vertical Resolution	40 levels (automatically set)		
Horizontal resolution (km)	27	9	3
Domain size (grid points)	91 × 103	82 × 94	64 × 55
Parameterisation Schemes:			
Cloud Microphysics (MP)	Eta microphysics (ETA) scheme		
Long-wave Radiation (LW-Rad)	Rapid Radiative Transfer Model scheme (RRTMG)		
Short-wave Radiation (SW-Rad)	Dudhia scheme		
Surface Layer (SL)	Revised MM5 similarity scheme (R-MM5), Eta similarity scheme (ETA), Quasi-Normal Scale Elimination PBL's surface layer scheme (QNSE), Nakanishi and Nino PBL's surface layer scheme (MYNN), Pleim-Xiu surface layer scheme (PX), Total Energy – Mass Flux surface layer scheme (TEMF).		
Land Surface Model (LSM)	Noah Land Surface Model, Pleim-Xiu Land Surface Model.		
Planetary Boundary Layer (PBL)	YSU, MYJ, ACM2, QNSE, MYNN2, MYNN3, BL, UW, TEMF, GBM.		
Cumulus	Kain-Fritsch scheme – turned off for domain 3		

Table 3
Parameterisation Scheme configurations that were tested.

Designation	MP	LW - Rad	SW - Rad	SL	LSM	PBL	Cumulus
YSU(1)	ETA	RRTMG	Dudhia	R-MM5	Noah	YSU (topo_wind = 1)	Kain-Fritsch
YSU(2)	ETA	RRTMG	Dudhia	R-MM5	Noah	YSU (topo_wind = 2)	Kain-Fritsch
MYJ	ETA	RRTMG	Dudhia	ETA	Noah	MYJ	Kain-Fritsch
QNSE	ETA	RRTMG	Dudhia	QNSE	Noah	QNSE	Kain-Fritsch
MYNN2	ETA	RRTMG	Dudhia	MYNN	Noah	MYNN2	Kain-Fritsch
MYNN3	ETA	RRTMG	Dudhia	MYNN	Noah	MYNN3	Kain-Fritsch
ACM2	ETA	RRTMG	Dudhia	PX	PX	ACM2	Kain-Fritsch
UW	ETA	RRTMG	Dudhia	R-MM5	Noah	UW	Kain-Fritsch
GBM	ETA	RRTMG	Dudhia	R-MM5	Noah	GBM	Kain-Fritsch
BL	ETA	RRTMG	Dudhia	R-MM5	Noah	BL	Kain-Fritsch
TEMF	ETA	RRTMG	Dudhia	TEMF	Noah	TEMF	Kain-Fritsch

**Fig. 4.** Grid cell in WRF.

Season (spanning December to March). A three month “High Winds” season (spanning July to September) within the Rainy Season was also considered, because the highest monthly average wind speeds at this site are usually recorded during this (High Winds) period [32]. Each set of test days comprised six (6) selected days; from each season. The first set of test day comprises the day

with the lowest daily wind speed average, and that with the highest daily wind speed average from each of the 3 seasons. The second set of test days comprised the days with the second highest and second lowest average wind speeds from each of the seasons, and so on.

All the scheme configurations were used to simulate the first and second sets of test days. Scheme configurations that consistently ranked worst after simulations of the first twelve test days, were dropped from subsequent tests, in which the remaining schemes were tested with simulations of more selected days. Consistently poorly ranked schemes continued to be eliminated after each subsequent test, until a consistently best-ranked scheme was identified and selected as the best scheme for the simulations. The advantage of this approach is that, it enabled us to test seasonal sensitivity of the scheme configurations without having to run a full year of simulations, as has been the practice in some previous studies. In all, a total of 36 days (i.e. six sets of six days) were used in this study. A successful simulation for each of the test days covered a period of 36 h. The first 12 h (from noon of the previous day) was considered as spool up time for the model and discarded as per recommendations of [1,2,18]. A plot of the daily wind speed averages for this site in the year 2013 and the selected days used in this study are available in [Appendix 1](#).

2.4. Post-processing of wind data from WRF result files

A position (specified as latitude (i), longitude (j), and vertical level (k)) on the WRF grid corresponds to a cell. Surface wind speeds and directions for a position in WRF were calculated from the U (x-component) and V (y-component) winds. The U winds are

on at the centres of the left and right faces of the cell, while the V winds are on the middles of the front and back faces as illustrated in Fig. 4. The simulated winds that were used for analysis was calculated (on an hourly basis) using a vector approach as:

$$Speed = \left[\left(\frac{U_{i,j,k} + U_{i+1,j,k}}{2} \right)^2 + \left(\frac{V_{i,j,k} + V_{i+1,j,k}}{2} \right)^2 \right]^{0.5} \quad (5)$$

Direction was determined from the same hourly U and V averages using the four-quadrant inverse tangent formular.

The wind speeds at heights of analysis (40m, 50m, 60m) were interpolated from wind speeds for the levels immediately below and above them. For this, the vertical levels in WRF had to be converted to height above ground level (in m). These were calculated hourly according to Ref. [20] as;

$$Height(a.g.l) = \left(\frac{(PH + PHB)_{i,j,k} + (PH + PHB)_{i,j,k+1}}{2g} \right) - HGT \quad (6)$$

where PH is the perturbation geopotential height, PHB the base-state geopotential height, and HGT, the terrain height [20]. Values for PH, PHB and HGT were all obtained from the simulation results.

2.5. Statistical metrics for validation

WRF predictions of wind speeds at heights of 40, 50, and 60 m above ground level, and direction predictions at 50 and 60 m were evaluated with the comparative Prediction Skill Score measure [33]. This was calculated from the sum of scaled (unity normalised) values of the following Statistical Metrics of evaluated simulated wind speeds and directions:

- (i) Root Mean Square Error (RMSE),
- (ii) Mean Error (ME),
- (iii) Standard Error (STDE) and
- (iv) Correlation Co-efficient between simulated and measured speeds and directions.

The RMSE is a measure of the difference between simulated and measured values. However, it is often criticised for “punishing” small errors by exaggerating them and making bad predictions appear worse than they are; something we consider to be conservative in this case. It is calculated as:

$$RMSE = \left(\frac{1}{N} \sum_i^N (\Delta)^2 \right)^{0.5} \quad (7)$$

where $\Delta = Speed_{simulated} - Speed_{measured}$ and N , the number of data points.

The Mean Error (ME), like the RMSE, is a measure of error, but more importantly, helps determine whether the model was over-predicting or under-predicting winds. It is calculated as:

$$ME = \frac{1}{N} \sum_i^N (\Delta) \quad (8)$$

The Standard Error (STDE) gives an indication of how spread out predictions are from the predicted mean. A smaller standard error is preferred. It is calculated from the RMSE and ME as;

$$STDE = \left(RMSE^2 - ME^2 \right)^{0.5} \quad (9)$$

The linear dependence of simulated and measured wind speeds

was assessed with the Pearson Correlation Coefficient given as [34].

$$CC = \frac{\sum (X - \bar{X})(Y - \bar{Y})}{\sqrt{\sum (X - \bar{X})^2 \sum (Y - \bar{Y})^2}} \quad (10)$$

where X and Y are the simulated and observed wind speeds respectively.

For angles (wind directions), Δ was calculated as follows [7];

$$\Delta = \begin{cases} \theta_{sim} - \theta_{obs} & \text{when } |\theta_{sim} - \theta_{obs}| < 180^\circ \\ (\theta_{sim} - \theta_{obs}) \left(1 - \frac{360}{|\theta_{sim} - \theta_{obs}|} \right) & \text{when } |\theta_{sim} - \theta_{obs}| > 180^\circ \end{cases} \quad (11)$$

Angular mean was calculated using vector notation approach [35], and correlation between simulated and measured angles was determined with a Circular Correlation Coefficient, calculated as [35]:

$$CircC = \frac{\sum \sin(\alpha - \bar{\alpha}) \sin(\beta - \bar{\beta})}{\sqrt{\sum \sin^2(\alpha - \bar{\alpha}) \sum \sin^2(\beta - \bar{\beta})}} \quad (12)$$

where α and β are the simulated and observed wind direction angles respectively.

The Prediction Skill Score was calculated as [33]:

$$Skill\ Score = (1 - RMSE_{SCALED}) + (1 - |ME|_{SCALED}) + (1 - STDE_{SCALED}) + CC_{SCALED} \quad (13)$$

Such that, $0 \leq Skill\ Score \leq 4$

Metrics were scaled according to Ref. [33] as;

$$X_{SCALED} = \frac{X_i - X_{min}}{X_{max} - X_{min}} \quad (14)$$

Such that, $0 \leq X_{SCALED} \leq 1$

The scheme with the highest Skill Score was ranked as the best scheme and vice versa.

3. Results

We exclude the TEMF scheme configuration from this initial analysis as we could not simulate all the first twelve test days, with that scheme. The model kept crashing when we attempted to simulate four of those days (February 17th, June 20th, March 15th, and April 10th) with this configuration (using the same model timestep as had been used in all the other simulations).

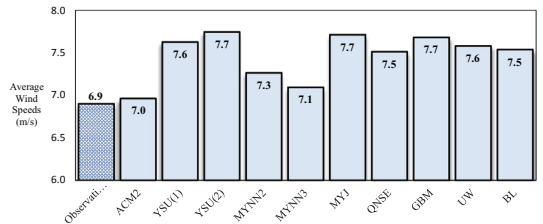


Fig. 5. Average wind speeds for all schemes for first six (6) test days at 60 m height.

Table 4
Statistical metrics at 60 m for 6 test days for all schemes.

PBL Scheme	RMSE (m/s)	ME (m/s)	STDE (m/s)	CC
ACM2	2.2	0.1	2.2	0.8
YSU(1)	2.1	0.7	2.0	0.9
YSU(2)	2.1	0.8	1.9	0.9
MYNN2	2.1	0.4	2.0	0.9
MYNN3	2.0	0.2	2.0	0.9
MYJ	2.3	0.8	2.1	0.8
QNSE	2.4	0.6	2.3	0.8
GBM	2.2	0.8	2.0	0.9
UW	2.1	0.7	2.0	0.9
BL	2.2	0.6	2.1	0.8

3.1. Wind speed prediction for first 6 test days

Fig. 5 shows the average simulated wind speed for the first 6 days for all but the TEMF scheme configuration. As can be observed from this figure, the ACM2, MYNN3, and MYNN2 scheme configurations give the best three estimations of average wind speeds for the first 6 selected test days. Among the worst predictors are the YSU(2), MYJ and GBM schemes.

Statistical metrics at 60 m are presented in Table 4. All the scheme configurations overestimated the wind speeds. The ACM2 scheme configuration exhibited the least estimation bias while the YSU(2), the least Standard Error. Most of the schemes exhibited good prediction-observation correlation. However, only the MYNN3 scheme exhibited good prediction with $RMSE \leq 2$ m/s, as recommended by Refs. [8,36], for this period. Combining the metrics into Prediction Skill Scores and ranking the schemes with the scores, the MYNN3, MYNN2 and ACM2 rank as the top 3 scheme configurations for this period. This can be observed from Fig. 6, which illustrates the wind speed prediction skill scores of the scheme configurations tested. Despite not having the worst prediction of the average wind speed for the first 6 test days, the QNSE scheme configuration scores lowest in prediction skill score, and therefore ranks worst. This is because it performs relatively poorly in almost all the metrics, except for the ME. The YSU(2) scheme, despite having one of the worst average speed predictions ranks 5, above the QNSE scheme, which had a better prediction. And this is because the YSU(2) is relatively better than the QNSE in terms of almost all the metrics. It can also be observed from Fig. 6 that the performance of the scheme configurations remained consistent, even when they were analysed for the two other heights at which we had measured data. Full results of the analyses at 50 m and 40 m are available in Appendix 2.

3.2. Direction prediction for first six (6) test days

All the schemes predicted North-East to be the dominant wind

direction, as can be observed in Fig. 7, which comprises wind roses for measured and predicted wind directions at a height of 60 m. Direction prediction was almost the same by all schemes. Measured wind directions for this period was mostly from the north-east and the east. Since the predicted angles were calculated from the predicted wind speeds, differences in the angle predictions can be attributed to differences in the wind speed predictions by the different scheme configurations. Similarly, we found no significant differences in angle predictions by the scheme configurations when the analysis was conducted at 50 m. Details of average measured and predicted directions, statistical metrics and skill scores are available in Appendix 2.

3.3. Sensitivity to seasons

The best scheme configurations for the entire 6 days test period largely remained the best in the two main seasons: the Harmattan season, and Rainy season. However, this changed for the “High Winds” season, where the two YSU schemes and GBM scheme configurations were now the best 3 schemes. It however must be noted that, for the entire rainy season (which includes this High Winds season) the MYNN schemes remained two of the top three schemes. This can be observed from Table 5, which comprises measured and predicted average wind speeds (from the days in the various seasons), as well prediction skill scores for scheme configurations at a height of 60 m.

3.4. Consistency of scheme predictions

We increased the number of test days to 36 in increments of 6, eliminating the consistently poorly ranked schemes with each increment. After the first increment to 12 test days, the BL, MYJ and QNSE schemes, having consistently ranked poor among the schemes, as illustrated in Fig. 7, were dropped. The GBM, YSU(1) and UW were also dropped after 18 test days, for similar reasons. As can be observed from Fig. 8, the top 3 scheme configurations for up

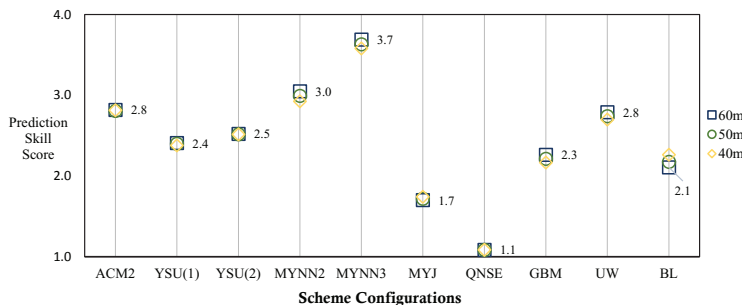


Fig. 6. Speed prediction Skill Scores at all heights for first 6 test days (Values are Scores at 60 m).

Table 5
Seasonal average Wind speeds and speed prediction skill scores at 60 m for first 6 test days.

	Harmattan		Entire Rainy Season		High Winds	
	Average Wind Speed (m/s)	Skill Score	Average Wind Speed (m/s)	Skill Score	Average Wind Speed (m/s)	Skill Score
Measurements	6.59		7.05		8.06	
ACM2	7.30	3.3	6.79	1.9	7.52	1.8
YSU(1)	7.89	1.9	7.49	2.6	7.94	3.5
YSU(2)	8.07	2.5	7.59	2.6	8.01	3.8
MYNN2	7.43	2.9	7.18	3.1	7.59	2.4
MYNN3	7.10	3.5	7.09	3.7	7.51	2.0
MYJ	8.13	1.0	7.50	2.2	7.93	3.5
QNSE	8.13	1.3	7.20	1.5	7.57	1.0
GBM	8.09	1.8	7.47	2.7	7.92	3.8
UW	7.96	2.2	7.39	3.3	7.73	2.9
BL	7.80	1.7	7.41	2.3	7.72	2.1

to 24 test days consistently remained MYNN3, MYNN2 and ACM2 schemes, and the MYNN2 scheme always ranked after the MYNN3 scheme. However, neither the MYNN3 nor ACM2 scheme was consistently ranking best, for which reason the two (ACM2 and MYNN3) were tested further for 12 extra test days, bringing the total number of test days (for the two) to 36. The MYNN3 scheme emerged the most consistently best scheme of the two after the extra testing. Full results are available in Appendix 2.

The seasonal test after increasing the number of test days to 12,

produced similar trends as the seasonal test for the first 6 test days, in that the best schemes again for the whole period dominated the two main seasons, but different schemes dominated predictions in the “High Winds” season. This can be observed in Table 6, which presents seasonal sensitivity results for the schemes for 12 days of simulations. Therefore, subsequently, we analysed scheme performance in the High Winds season only, with increasing test days, to determine the best scheme for this season. Fig. 9 illustrates the ranking of the schemes in the (High Winds) season with increasing

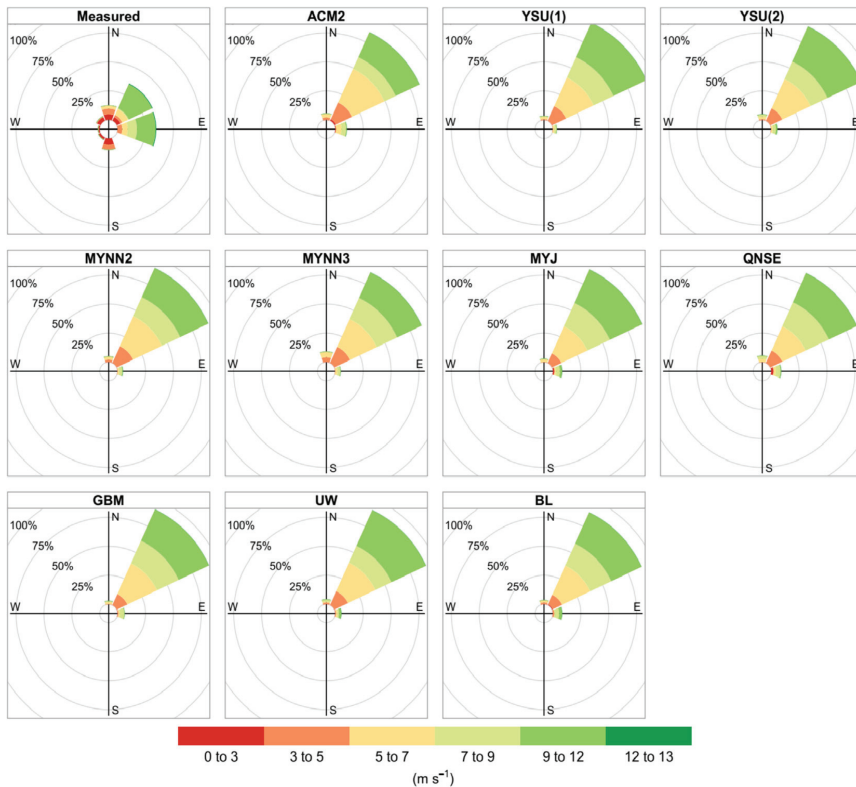


Fig. 7. Wind roses of observation data and scheme predictions at a height of 60 m.

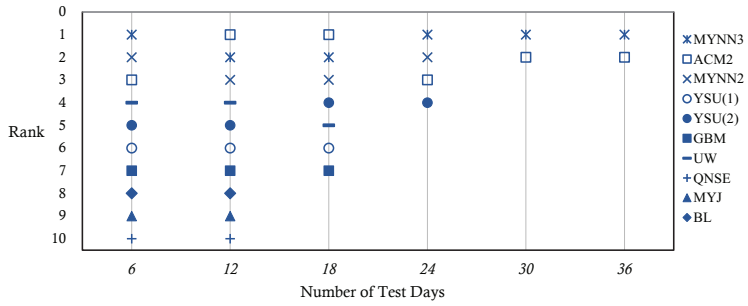


Fig. 8. Scheme Rankings for predictions at 60 m.

Table 6
Seasonal average wind speeds and speed prediction skill for first 12 test days.

	Harmattan		Entire Rainy Season		High Winds	
	Average Wind Speed (m/s)	Skill Score	Average Wind Speed (m/s)	Skill Score	Average Wind Speed (m/s)	Skill Score
Measurements	6.26		6.80		7.58	
ACM2	6.59	3.2	6.83	3.5	7.18	2.4
YSU(1)	7.15	2.1	7.53	2.7	7.74	3.2
YSU(2)	7.30	2.7	7.64	2.4	7.82	3.3
MYNN2	6.68	3.2	7.11	3.1	7.31	2.3
MYNN3	6.43	3.3	6.99	3.2	7.16	1.5
MYJ	7.40	0.9	7.56	1.8	7.76	3.1
QNSE	7.37	1.3	7.27	1.2	7.29	1.2
GBM	7.28	2.5	7.55	2.1	7.67	3.7
UW	7.14	2.6	7.38	3.2	7.52	3.7
BL	7.20	1.8	7.42	2.2	7.56	2.8

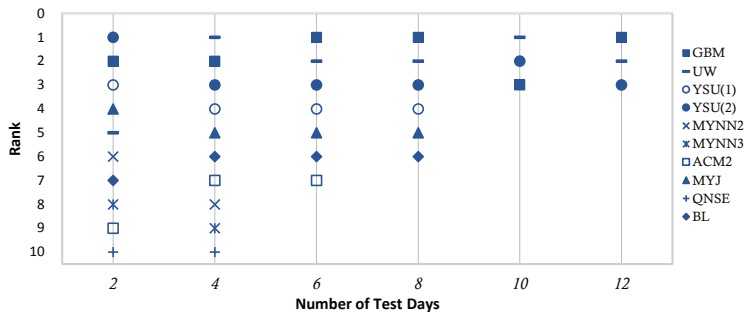


Fig. 9. Scheme Rankings in the "High Winds" season for predictions at 60 m.

test days at a height of 60 m. It can be seen from the figure that, the GBM scheme consistently ranks best or second best in simulating winds from the days selected from this season. The UW and YSU also rank consistently well. However, at lower heights, the UW sometimes outranked the GBM scheme (see full results in [Appendix 2](#)).

3.5. Results with TEMF scheme

With TEMF scheme, some days in the first 12 days (February 17th, June 20th, March 15th, April 10th) could not be simulated and therefore, all results for this scheme were excluded from the analysis and results already presented in this work. Notwithstanding, when this scheme was included in an analysis that was restricted to the days that it could fully simulate, we found it to be one of the relatively worst schemes, and it had no significant influence on the ranking of the best schemes, be it across all seasons or in the High Winds season. For this reason, it was not included in subsequent tests. Detailed results for this analysis (that included the TEMF scheme) are available in [Appendix 2](#).

4. Discussion

When we rank the PBL schemes tested in this study based on their prediction skill scores, the second order MYNN3 local closure approximation scheme appears to be the best scheme for wind simulations across all major seasons. It consistently often ranked best at all the heights that were considered for analysis. It is followed by the 1.5 order hybrid closure ACM2, and local closure MYNN2 schemes. These three schemes consistently predicted with the best prediction skills irrespective of the number of simulated days. Judging from the terrain and pertaining vegetation cover in the study area, the main source of turbulence over the study area should be thermal turbulence, as there is little elevation or the kind of vegetation cover that can cause significant mechanical turbulence. The good performance of the local MYNN schemes, suggests the turbulent eddies generated by thermal turbulence over this site are more often small and localised in nature; conditions that are generally better resolved by local closure techniques [16]. As a second order scheme, the MYNN3 scheme predicts Turbulent Kinetic Energy (TKE) and other second moment terms, instead of approximating them like the lower order schemes would have done. This probably explains why the MYNN3 scheme consistently ranked better than MYNN2 scheme which does a limited prediction of TKE at “sub-grid” level [20]. The ACM2 scheme is a hybrid scheme that combines non-local upward closure with local downward closure techniques. Its good performance suggests that some eddies that were generated on some of the days tested, were large enough to be considered non-localised, presenting conditions that it could resolve better than the MYNN schemes.

The GBM and UW schemes generally simulate winds better, in the “High Winds” season. These two schemes are similar and were designed to better depict the influence of clouds in the PBL and better resolve conditions comparable to large eddy simulation conditions. A major difference between the two is that the UW scheme diagnosis TKE (approximates by relating it to the state of other variables) instead of predicting it [23]. The consistency of the top four (4) ranked schemes, which are GBM, UW and the two non-local YSU schemes, suggests that the cloud cover that this part of

the country tends to experience around this time of the year [37], combined with the high winds during this period, produces conditions that are more similar to non-localised large eddy conditions during this time of the year compared to the rest of the year. Where a full year's simulation, comprising shorter runs like the type used in this study will be conducted at this site, it might make sense to run this period with the GBM or UW schemes for better results, though we cannot tell at this stage how much improvement in overall wind energy estimate this might bring.

Generally, our findings agree with findings of other similar studies we found in open literature. The QNSE and MYJ schemes were often the worst schemes for speed prediction [9]. The TEMF scheme was one of the worst schemes when it was included in the analysis [18]. The best schemes include MYNN2, YSU and ACM2 schemes [6,8,24,26], as well as the UW and GBM schemes [7]. Compared with the ACM2 scheme, the YSU scheme is better [8]. However, we find that performance of the PBL schemes depends on the prevailing weather conditions of period they are used to simulate. Overall, the MYNN3 appears to be the best scheme for simulations over this area.

5. Conclusion

In this paper, we investigated the sensitivity of selected BPL schemes in the AR-WRF v3.8.1 to winds at a site with high wind energy potential in South-Eastern Ghana. From our findings, we conclude that generally, the higher local closure schemes with TKE prediction, and hybrid schemes (combining local and non-local closure) best simulate all year winds at this site, with the former being more consistent. We believe the local, second order, MYNN3 scheme is best for wind simulations in this area (and perhaps other parts of the country and West African sub-region with similar terrain and climate), due to its consistently good performance ranking in our tests. We also find that the local 1.5 order GBM and UW schemes simulate winds better during a “High Winds” period but do not give the kind of all-year performance that the MYNN3 exhibited. We recommend tests covering longer periods to determine if the comparative performance of the schemes remains same. We also recommend tests to determine if estimated energy with combined data simulated by different schemes for the different periods in which each performs best, would have any advantages over energy estimations with data from just one scheme.

Acknowledgements

Denis Dzebre acknowledges the PhD scholarship support by the UPERCRET Program with fund from the Energy and Petroleum (EnPe) Project of the Norwegian Agency for Development Cooperation (Norad).

Appendix 1

Daily Wind Speed Averages at Anloga for 2013

Appendix 2. Analyses Results

Average speeds and metrics for speed prediction (first 6 test days)

	50 m				40 m					
	Average Wind Speeds (m/s)	RMSE (m/s)	ME (m/s)	STDE (m/s)	CC	Average Wind Speeds (m/s)	RMSE (m/s)	ME (m/s)	STDE (m/s)	CC
Observations	6.9					6.7				
ACM2	7.0	2.2	0.1	2.2	0.8	6.9	6.8	2.1	0.1	0.8
YSU(1)	7.6	2.1	0.7	2.0	0.9	7.6	6.7	2.1	0.8	0.9
YSU(2)	7.7	2.1	0.8	1.9	0.9	7.7	7.5	2.1	0.8	0.9
MYNN2	7.3	2.1	0.4	2.0	0.9	7.2	7.0	2.0	0.4	0.9
MYNN3	7.1	2.0	0.2	2.0	0.9	7.0	6.9	1.9	0.2	0.9
WJ1	7.7	2.3	0.8	2.1	0.8	7.6	7.6	2.2	0.9	0.8
QNSE	7.5	2.4	0.6	2.3	0.8	7.4	7.4	2.3	0.7	0.8
GRM	7.7	2.2	0.8	2.0	0.9	7.6	7.6	2.1	0.9	0.9
UW	7.6	2.1	0.7	2.0	0.9	7.5	7.5	2.0	0.7	0.8
BL	7.5	2.2	0.6	2.1	0.8	7.5	7.4	2.1	0.7	0.8

Scaled metrics and model mean scores for speed prediction (first 6 test days)

	50m				40m			
	ME _{SCALED} (m/s)	STDE _{SCALED} (m/s)	CC	Skill Score	ME _{SCALED} (m/s)	STDE _{SCALED} (m/s)	CC	Skill Score
ACM2	0.0	0.6	0.8	2.8	0.4	0.6	0.8	2.8
YSU(1)	0.4	0.8	0.9	2.4	0.4	0.2	0.9	2.4
YSU(2)	0.4	1.0	0.0	2.5	0.4	1.0	0.0	2.5
MYNN2	0.2	0.4	0.2	3.0	0.2	0.3	0.9	3.0
MYNN3	0.0	0.2	0.0	3.7	0.0	0.1	0.9	3.6
WJ1	0.7	1.0	0.5	1.7	0.7	0.9	0.8	1.7
QNSE	1.0	0.7	1.0	1.1	1.0	1.0	0.8	1.1
GRM	0.5	0.9	0.2	2.3	0.5	0.9	0.2	2.2
UW	0.3	0.8	0.0	2.8	0.3	0.1	0.9	2.7
BL	0.6	0.7	0.5	2.1	0.5	0.7	0.4	2.2

60 m

	50 m				40 m					
	Average Wind Direction (degrees)	RMSE (degrees)	ME (degrees)	STDE (degrees)	CircC	Average Wind Direction (degrees)	RMSE (degrees)	ME (degrees)	STDE (degrees)	CircC
Observations	38.7					36.4				
ACM2	48.9	56.6	-7.6	56.1	0.5	49.0	57.1	-5.7	56.9	0.5
YSU(1)	45.5	58.1	-11.4	56.9	0.5	45.5	58.5	-9.5	57.7	0.5
YSU(2)	45.8	58.0	-11.1	56.9	0.5	45.9	58.4	-9.1	57.7	0.5
MYNN2	45.0	58.9	-10.3	57.9	0.4	45.0	59.3	-8.4	58.7	0.4
MYNN3	45.2	58.9	-8.8	58.1	0.5	45.2	59.2	-6.9	58.8	0.5
WJ1	47.3	57.5	-11.4	56.4	0.5	47.3	58.1	-9.5	57.3	0.5
QNSE	49.1	56.0	-9.5	55.2	0.5	49.1	56.6	-7.7	56.1	0.5
GRM	46.6	57.8	-10.3	56.9	0.5	46.6	58.3	-8.4	57.7	0.5
UW	47.2	58.0	-9.4	57.2	0.5	47.2	58.4	-8.4	57.9	0.5
BL	47.4	57.8	-10.5	56.9	0.4	47.4	58.4	-8.6	57.8	0.5

Scaled metrics and model skill score for direction prediction (first 6 test days)

	50m				40m			
	ME _{SCALED} (degrees)	STDE _{SCALED} (degrees)	CC	Skill Score	ME _{SCALED} (degrees)	STDE _{SCALED} (degrees)	CC	Skill Score
ACM2	0.2	1.0	0.3	2.0	0.2	1.0	0.3	2.0
YSU(1)	0.7	0.0	0.6	2.2	0.7	0.0	0.6	2.2
YSU(2)	0.7	0.1	0.6	2.1	0.7	0.1	0.6	2.1
MYNN2	1.0	0.3	1.0	1.2	1.0	0.3	1.0	1.2
MYNN3	1.0	0.7	1.0	0.8	1.0	0.7	1.0	0.8

(continued on next page)

(continued)

		50 m					
		Average Wind Direction (degrees)	RMSE (degrees)	ME (degrees)	STDE (degrees)	CircC	
60 m		Average Wind Direction (degrees)	RMSE (degrees)	ME (degrees)	STDE (degrees)	CircC	
MYJ	0.5	0.0	0.0	0.4	0.5	2.5	0.5
QNSE	0.0	0.5	0.0	0.0	0.5	3.0	0.0
GRM	0.6	0.3	1.9	0.6	0.5	1.6	0.5
UW	0.7	0.5	0.7	0.7	0.5	0.7	0.5
BL	0.6	0.2	0.2	0.6	0.4	2.0	0.5
60 m							
Average Wind Speeds		RMSE (m/s)	ME (m/s)	STDE (m/s)	CC	STDE (m/s)	CC
Average Wind Speeds		RMSE (m/s)	ME (m/s)	STDE (m/s)	CC	STDE (m/s)	CC
Observations	6.6						
ACM2	6.7	1.9	0.1	1.9	0.8	6.6	0.8
YSU(1)	7.5	2.0	0.9	1.8	0.9	7.4	0.9
YSU(2)	7.5	2.0	0.9	1.8	0.9	7.4	0.9
MYNN2	7.0	1.9	0.4	1.9	0.8	6.9	0.8
MYNN3	6.8	1.9	0.2	1.9	0.8	6.6	0.8
MYJ	7.5	2.2	0.9	2.0	0.8	7.4	0.8
QNSE	7.3	2.2	0.7	2.1	0.8	7.2	0.8
GRM	7.5	2.1	0.8	1.9	0.8	7.4	0.8
UW	7.3	2.0	0.7	1.8	0.8	7.2	0.8
BL	7.3	2.1	0.7	1.9	0.8	7.2	0.8
40 m							
Average Wind Speeds		RMSE (m/s)	ME (m/s)	STDE (m/s)	CC	STDE (m/s)	CC
Average Wind Speeds		RMSE (m/s)	ME (m/s)	STDE (m/s)	CC	STDE (m/s)	CC
Observations	6.4						
ACM2	6.4	1.9	0.2	1.9	0.8	6.6	0.8
YSU(1)	7.5	2.0	1.0	1.8	0.9	7.4	0.9
YSU(2)	7.5	2.0	1.0	1.8	0.9	7.4	0.9
MYNN2	7.0	1.9	0.4	1.9	0.8	6.9	0.8
MYNN3	6.8	1.9	0.2	1.9	0.8	6.6	0.8
MYJ	7.5	2.1	0.9	1.9	0.8	7.4	0.8
QNSE	7.3	2.2	0.7	2.0	0.8	7.2	0.8
GRM	7.5	2.0	0.8	1.8	0.8	7.4	0.8
UW	7.3	1.9	0.7	1.8	0.8	7.2	0.8
BL	7.3	2.0	0.8	1.9	0.8	7.2	0.8
60m							
Average Wind Speeds		RMSE _{SCALED} (m/s)	ME _{SCALED} (m/s)	STDE _{SCALED} (m/s)	CC	Skill Score	
Average Wind Speeds		RMSE _{SCALED} (m/s)	ME _{SCALED} (m/s)	STDE _{SCALED} (m/s)	CC	Skill Score	
Observations	6.4						
ACM2	0.0	0.0	0.4	0.0	0.4	0.0	0.4
YSU(1)	0.4	0.8	0.2	0.4	0.2	0.8	0.2
YSU(2)	0.4	1.0	0.0	0.9	0.2	0.5	0.0
MYNN2	0.1	0.3	0.4	0.9	0.5	3.0	0.2
MYNN3	0.1	0.1	0.4	0.9	0.5	3.2	0.1
MYJ	0.9	1.0	0.6	0.8	1.3	1.0	0.6
QNSE	1.0	0.7	1.0	0.8	1.1	1.0	0.7
GRM	0.5	0.9	0.2	0.6	0.9	0.2	0.3
UW	0.1	0.7	0.1	0.7	0.1	0.7	0.1
BL	0.6	0.8	0.5	0.8	0.2	0.5	0.7
50m							
Average Wind Direction		RMSE (degrees)	ME (degrees)	STDE (degrees)	CC	STDE (degrees)	CC
Average Wind Direction		RMSE (degrees)	ME (degrees)	STDE (degrees)	CC	STDE (degrees)	CC
Observations	48.7						
ACM2	43.6	51.4	-15.2	49.1	0.5	43.6	50.6
YSU(1)	42.8	52.4	-16.7	49.7	0.6	42.8	51.2
YSU(2)	43.2	52.6	-16.4	50.0	0.5	43.3	51.4
MYNN2	41.2	53.3	-17.9	50.2	0.5	41.1	51.4
MYNN3	47.4	54.7	-19.0	51.3	0.4	47.4	52.2
MYJ	45.1	51.7	-14.5	49.6	0.5	45.1	51.4
QNSE	46.6	53.3	-15.2	51.1	0.5	46.6	52.6
GRM	43.5	52.2	-15.9	49.8	0.5	43.5	51.3
UW	44.9	53.7	-15.3	51.5	0.5	44.9	52.9
BL	45.6	54.8	-15.8	52.4	0.4	45.5	53.8
50 m							
Average Wind Direction		RMSE (degrees)	ME (degrees)	STDE (degrees)	CC	STDE (degrees)	CC
Average Wind Direction		RMSE (degrees)	ME (degrees)	STDE (degrees)	CC	STDE (degrees)	CC
Observations	48.7						
ACM2	43.6	51.4	-15.2	49.1	0.5	43.6	50.6
YSU(1)	42.8	52.4	-16.7	49.7	0.6	42.8	51.2
YSU(2)	43.2	52.6	-16.4	50.0	0.5	43.3	51.4
MYNN2	41.2	53.3	-17.9	50.2	0.5	41.1	51.4
MYNN3	47.4	54.7	-19.0	51.3	0.4	47.4	52.2
MYJ	45.1	51.7	-14.5	49.6	0.5	45.1	51.4
QNSE	46.6	53.3	-15.2	51.1	0.5	46.6	52.6
GRM	43.5	52.2	-15.9	49.8	0.5	43.5	51.3
UW	44.9	53.7	-15.3	51.5	0.5	44.9	52.9
BL	45.6	54.8	-15.8	52.4	0.4	45.5	53.8

Scaled metrics and model mean scores for speed prediction (12 test days)

Scaled metrics and models mean scores for direction prediction (12 test days)

	60m					50m					Skill Score	CircC	STDESCALED (degrees)	MESCALED (degrees)	RMSESCALED (degrees)	Skill Score	CircC	STDESCALED (degrees)	MESCALED (degrees)	RMSESCALED (degrees)	Skill Score
	RMSESCALED (degrees)	MESCALED (degrees)	STDESCALED (degrees)	CircC	Skill Score	RMSESCALED (degrees)	MESCALED (degrees)	STDESCALED (degrees)	CircC	Skill Score											
ACM2	0.0	0.8	0.0	0.5	2.7	0.0	0.0	0.0	0.5	2.7	0.0	0.0	0.9	0.5	2.7	0.5	0.5	0.0	0.9	0.5	2.7
YSU(1)	0.5	0.5	0.3	0.5	2.3	0.4	0.4	0.3	0.5	2.3	0.4	0.3	0.5	0.5	2.3	0.5	0.5	0.3	0.6	0.5	2.3
YSU(2)	0.3	0.6	0.2	0.5	2.4	0.3	0.3	0.2	0.5	2.4	0.3	0.2	0.6	0.5	2.4	0.3	0.2	0.2	0.6	0.5	2.4
MYNN2	0.5	0.3	0.3	0.5	2.4	0.4	0.4	0.3	0.5	2.4	0.4	0.3	0.6	0.5	2.4	0.4	0.3	0.2	0.6	0.5	2.4
MYNN3	1.0	0.6	0.6	0.4	1.8	0.8	0.8	0.6	0.4	1.8	0.8	0.6	1.0	0.4	1.8	0.8	0.6	0.5	1.0	0.4	1.8
MYJ	0.1	1.0	0.2	0.5	2.3	0.2	0.2	0.1	0.5	2.3	0.2	0.2	0.1	0.5	2.3	0.2	0.2	0.1	0.5	2.3	0.2
ONSE	0.6	0.6	0.6	0.5	1.5	0.6	0.6	0.6	0.5	1.5	0.6	0.6	0.6	0.5	1.5	0.6	0.6	0.6	0.6	0.5	1.5
GRM	0.3	0.7	0.2	0.5	2.4	0.3	0.3	0.2	0.5	2.4	0.3	0.2	0.7	0.5	2.4	0.3	0.2	0.2	0.7	0.5	2.4
UW	0.7	0.8	0.7	0.5	1.2	0.7	0.7	0.7	0.5	1.2	0.7	0.7	0.8	0.5	1.2	0.7	0.7	0.7	0.8	0.5	1.2
BL	1.0	0.7	1.0	0.4	0.7	1.0	1.0	1.0	0.4	0.7	1.0	1.0	0.8	0.4	0.7	1.0	1.0	0.7	0.8	0.4	0.8

	60m					50m					40m					Skill Score	CC	STDE (m/s)	
	ME (m/s)	RMSE (m/s)	STDE (m/s)	CC	Average Wind Speeds (m/s)	ME (m/s)	RMSE (m/s)	STDE (m/s)	CC	Average Wind Speeds (m/s)	ME (m/s)	RMSE (m/s)	STDE (m/s)	CC	Average Wind Speeds (m/s)				ME (m/s)
Observations	6.5	6.4	6.4	6.4	6.4	6.4	6.4	6.4	6.4	6.4	6.4	6.4	6.4	6.4	6.4	6.4	6.4	6.4	6.4
ACM2	1.8	0.2	1.8	0.8	1.8	0.3	0.3	1.8	0.8	1.8	0.8	0.6	6.6	1.8	0.4	1.8	0.8	1.8	0.8
YSU(1)	7.4	2.0	0.9	1.7	0.8	7.4	7.4	2.0	1.0	1.7	0.8	7.3	2.0	1.0	1.7	0.8	7.3	2.0	1.0
YSU(2)	7.5	2.0	1.0	1.7	0.9	7.5	7.5	2.0	1.1	1.7	0.8	7.4	2.0	1.2	1.7	0.8	7.4	2.0	1.2
MYNN2	7.0	1.8	0.4	1.8	0.8	6.9	6.9	1.8	0.5	1.8	0.8	6.8	1.9	0.5	1.8	0.8	6.8	1.9	0.5
MYNN3	6.8	1.8	0.3	1.8	0.8	6.7	6.7	1.8	0.3	1.8	0.8	6.6	1.8	0.4	1.8	0.8	6.6	1.8	0.4
GRM	7.5	2.0	0.9	1.8	0.8	7.4	7.4	2.0	1.0	1.7	0.8	7.4	2.1	1.1	1.7	0.8	7.4	2.1	1.1
UW	7.3	1.9	0.8	1.8	0.8	7.3	7.3	1.9	0.9	1.7	0.8	7.2	2.0	0.9	1.7	0.8	7.2	2.0	0.9

	60m					50m					40m					Skill Score	CC	STDESCALED (degrees)	MESCALED (degrees)	RMSESCALED (degrees)	Skill Score
	ME (degrees)	RMSE (degrees)	STDESCALED (degrees)	CC	Average Wind Direction (degrees)	ME (degrees)	RMSE (degrees)	STDESCALED (degrees)	CC	Average Wind Direction (degrees)	ME (degrees)	RMSE (degrees)	STDESCALED (degrees)	CC	Average Wind Direction (degrees)						
Observations	55.8	53.5	53.5	53.5	53.5	53.5	53.5	53.5	53.5	53.5	53.5	53.5	53.5	53.5	53.5	53.5	53.5	53.5	53.5		
ACM2	0.0	0.0	0.8	2.9	0.0	0.0	0.0	0.8	2.9	0.0	0.8	2.9	0.0	0.8	2.9	0.0	0.8	2.9	0.0		
YSU(1)	0.7	0.8	0.4	0.8	1.8	0.7	0.7	0.4	0.8	1.8	0.7	0.7	0.4	0.8	1.8	0.7	0.4	0.8	1.8		
YSU(2)	0.8	1.0	0.0	0.9	2.0	0.8	0.8	0.0	0.8	2.0	0.8	0.8	0.0	0.8	2.0	0.8	0.0	0.8	2.0		
MYNN2	0.2	0.3	0.9	0.8	2.6	0.2	0.2	0.9	0.8	2.5	0.2	0.2	0.9	0.8	2.5	0.2	0.2	0.9	0.8		
MYNN3	0.1	0.0	1.0	0.8	2.8	0.1	0.1	1.0	0.8	2.8	0.1	1.0	0.8	2.8	0.1	1.0	0.8	2.8	0.1		
GRM	1.0	0.9	0.7	0.8	1.2	1.0	1.0	0.6	0.8	1.3	1.0	1.0	0.6	0.8	1.3	1.0	1.0	0.6	0.8		
UW	0.6	0.7	0.5	0.8	2.0	0.6	0.6	0.5	0.8	2.0	0.6	0.6	0.5	0.8	2.0	0.6	0.5	0.7	0.8		

	60m					50m					Skill Score	CC	STDESCALED (degrees)	MESCALED (degrees)	RMSESCALED (degrees)	Skill Score	CC	STDESCALED (degrees)	MESCALED (degrees)	RMSESCALED (degrees)	Skill Score
	ME (degrees)	RMSE (degrees)	STDESCALED (degrees)	CC	Average Wind Direction (degrees)	ME (degrees)	RMSE (degrees)	STDESCALED (degrees)	CC	Average Wind Direction (degrees)											
Observations	55.8	53.5	53.5	53.5	53.5	53.5	53.5	53.5	53.5	53.5	53.5	53.5	53.5	53.5	53.5	53.5	53.5	53.5	53.5		
ACM2	42.9	52.2	-18.1	48.9	0.5	42.9	42.9	52.2	48.9	0.5	42.9	42.9	52.2	48.9	0.5	42.9	42.9	52.2	48.9		
YSU(1)	42.2	51.1	-19.3	47.3	0.5	42.2	42.2	51.1	47.3	0.5	42.2	42.2	51.1	47.3	0.5	42.2	42.2	51.1	47.3		
YSU(2)	42.6	51.1	-18.8	47.5	0.5	42.7	42.7	51.1	47.5	0.5	42.7	42.7	51.1	47.5	0.5	42.7	42.7	51.1	47.5		
MYNN2	40.7	51.9	-20.1	47.9	0.5	40.7	40.7	51.9	47.9	0.5	40.7	40.7	51.9	47.9	0.5	40.7	40.7	51.9	47.9		
MYNN3	45.4	55.9	-20.9	51.8	0.3	45.2	45.2	55.9	51.8	0.3	45.2	45.2	55.9	51.8	0.3	45.2	45.2	55.9	51.8		
GRM	42.9	51.1	-18.2	47.7	0.5	42.9	42.9	51.1	47.7	0.5	42.9	42.9	51.1	47.7	0.5	42.9	42.9	51.1	47.7		
UW	44.2	51.6	-17.7	48.4	0.5	44.2	44.2	51.6	48.4	0.5	44.2	44.2	51.6	48.4	0.5	44.2	44.2	51.6	48.4		

	60m					50m					Skill Score	CC	STDESCALED (degrees)	MESCALED (degrees)	RMSESCALED (degrees)	Skill Score	CC	STDESCALED (degrees)	MESCALED (degrees)	RMSESCALED (degrees)	Skill Score
	ME (degrees)	RMSE (degrees)	STDESCALED (degrees)	CC	Average Wind Direction (degrees)	ME (degrees)	RMSE (degrees)	STDESCALED (degrees)	CC	Average Wind Direction (degrees)											
Observations	55.8	53.5	53.5	53.5	53.5	53.5	53.5	53.5	53.5	53.5	53.5	53.5	53.5	53.5	53.5	53.5	53.5	53.5	53.5		
ACM2	0.2	0.9	0.4	0.5	2.0	0.3	0.3	0.9	0.5	2.0	0.3	0.3	0.9	0.5	2.0	0.3	0.3	0.9	0.5		
YSU(1)	0.0	0.5	0.0	0.5	3.0	0.0	0.0	0.5	3.0	0.0	0.0	0.5	3.0	0.0	0.5	3.0	0.0	0.5	3.0		

(continued on next page)

(continued)

60 m														
Average Wind Direction				Average Wind Speeds				Average Wind Direction						
RMSE (degrees)	ME (degrees)	STDE (degrees)	CircC	RMSE (degrees)	ME (m/s)	STDE (m/s)	CC	RMSE (degrees)	ME (degrees)	STDE (degrees)	CircC			
YSU(2)	0.0	0.6	0.0	0.5	2.8	0.0	0.0	0.7	0.0	0.5	2.8			
MYNN2	0.2	0.2	0.1	0.5	2.9	0.2	0.2	0.2	0.1	0.5	2.9			
MYNN3	1.0	1.0	1.3	0.3	1.0	1.0	1.0	0.0	1.0	0.3	1.3			
GBM	0.0	0.9	0.1	0.5	2.6	0.0	0.0	0.9	0.1	0.5	2.5			
UW	0.1	1.0	0.3	0.5	2.1	0.1	0.1	1.0	0.3	0.5	2.0			
50 m														
Average Wind Speeds				Average Wind Speeds				Average Wind Speeds						
RMSE (m/s)	ME (m/s)	STDE (m/s)	CC	RMSE (m/s)	ME (m/s)	STDE (m/s)	CC	RMSE (m/s)	ME (m/s)	STDE (m/s)	CC			
Observations	6.5	6.4	6.4	6.4	6.2	6.2	6.2	6.2	6.2	6.2	6.2			
ACM2	1.8	0.1	1.80	0.8	1.8	0.1	1.8	0.8	1.8	0.2	1.8			
YSU(2)	1.9	0.8	1.66	0.8	7.3	0.9	1.6	0.8	7.2	1.9	1.0			
MYNN2	1.8	0.3	1.76	0.8	6.7	1.8	0.4	1.8	0.8	6.6	1.7			
MYNN3	6.6	1.8	1.75	0.8	6.6	1.8	0.2	1.7	0.8	6.5	1.7			
Scaled metrics and model mean scores for speed prediction (24 test days)														
60m				50m				40m						
RMSE _{SCALED} (m/s)	ME _{SCALED} (m/s)	STDE _{SCALED} (m/s)	CC	Skill Score	RMSE _{SCALED} (m/s)	ME _{SCALED} (m/s)	STDE _{SCALED} (m/s)	CC	Skill Score	RMSE _{SCALED} (m/s)	ME _{SCALED} (m/s)	STDE _{SCALED} (m/s)	CC	Skill Score
ACM2	0.5	0.0	1.0	0.8	2.3	0.3	0.0	1.0	0.8	2.5	0.3	0.0	1.0	0.8
YSU(2)	1.0	1.0	0.0	0.8	1.8	1.0	1.0	0.0	0.8	1.8	1.0	1.0	0.0	0.8
MYNN2	0.3	0.3	0.7	0.8	2.5	0.3	0.3	0.8	2.4	0.3	0.3	0.8	0.8	2.4
MYNN3	0.0	0.1	0.6	0.8	3.1	0.0	0.1	0.7	0.8	3.1	0.0	0.1	0.7	0.8
50 m														
Average Wind Direction				Average Wind Direction				Average Wind Direction						
RMSE (degrees)	ME (degrees)	STDE (degrees)	CircC	RMSE (degrees)	ME (degrees)	STDE (degrees)	CircC	RMSE (degrees)	ME (degrees)	STDE (degrees)	CircC			
Observations	55.7	53.4	53.4	53.4	52.5	52.5	52.5	52.5	52.5	52.5	52.5			
ACM2	43.8	51.9	49.3	0.5	43.8	49.3	0.5	43.8	0.5	43.8	0.5			
YSU(2)	43.7	52.2	49.2	0.5	43.7	49.2	0.5	43.7	0.5	43.7	0.5			
MYNN2	43.9	54.3	50.4	0.4	43.9	50.4	0.4	43.9	0.4	43.9	0.4			
MYNN3	48.2	57.8	54.0	0.3	48.0	54.0	0.3	48.0	0.3	48.0	0.3			
Scaled metrics and models mean scores for direction prediction (24 test days)														
60m				50m				40m						
RMSE _{SCALED} (degrees)	ME _{SCALED} (degrees)	STDE _{SCALED} (degrees)	CircC	Skill Score	RMSE _{SCALED} (degrees)	ME _{SCALED} (degrees)	STDE _{SCALED} (degrees)	CircC	Skill Score	RMSE _{SCALED} (degrees)	ME _{SCALED} (degrees)	STDE _{SCALED} (degrees)	CircC	Skill Score
ACM2	0.0	1.0	0.0	2.4	0.0	1.0	0.0	2.4	0.0	1.0	0.0	2.4	0.0	2.4
YSU(2)	0.1	0.6	0.1	2.8	0.1	0.7	0.1	2.8	0.1	0.7	0.1	2.8	0.1	2.8
MYNN2	0.4	0.1	0.3	2.6	0.4	0.1	0.4	2.6	0.4	0.2	0.4	2.6	0.4	2.6
MYNN3	1.0	0.0	1.0	1.3	1.0	1.0	1.0	1.0	1.0	1.0	1.0	1.0	1.0	1.3
50 m														
Average Wind Speeds				Average Wind Speeds				Average Wind Speeds						
RMSE (m/s)	ME (m/s)	STDE (m/s)	CC	RMSE (m/s)	ME (m/s)	STDE (m/s)	CC	RMSE (m/s)	ME (m/s)	STDE (m/s)	CC			
Observations	6.5	6.3	6.3	6.3	6.2	6.2	6.2	6.2	6.2	6.2	6.2			
ACM2	1.7	0.0	1.7	0.8	6.4	1.7	0.8	6.4	1.7	0.8	6.4			
MYNN2	6.5	1.7	0.1	1.7	0.8	6.5	1.7	0.8	6.4	1.7	0.8			
MYNN3	6.5	1.7	0.1	1.7	0.8	6.5	1.7	0.8	6.4	1.7	0.8			
Scaled metrics and model mean scores for speed prediction (30 test days)														
60m				50m				40m						
RMSE _{SCALED} (m/s)	ME _{SCALED} (m/s)	STDE _{SCALED} (m/s)	CC	Skill Score	RMSE _{SCALED} (m/s)	ME _{SCALED} (m/s)	STDE _{SCALED} (m/s)	CC	Skill Score	RMSE _{SCALED} (m/s)	ME _{SCALED} (m/s)	STDE _{SCALED} (m/s)	CC	Skill Score
ACM2	1.7	0.0	1.7	0.8	6.4	1.7	0.8	6.4	1.7	0.8	6.4	1.7	0.8	6.4
MYNN2	6.5	1.7	0.1	1.7	0.8	6.5	1.7	0.8	6.4	1.7	0.8	6.4	1.7	0.8
MYNN3	6.5	1.7	0.1	1.7	0.8	6.5	1.7	0.8	6.4	1.7	0.8	6.4	1.7	0.8

		50 m						40 m							
Average Wind Direction (degrees)		RMSE (degrees)	ME (degrees)	STDE (degrees)	CircC	Average Wind Direction (degrees)	RMSE (degrees)	ME (degrees)	STDE (degrees)	CircC	Average Wind Speeds (m/s)	ME (m/s)	RMSE (m/s)	STDE (m/s)	CC
ACM2	1.0	0.0	1.0	0.8	1.8	1.0	0.8	1.8	1.0	0.0	52.0	0.0	55.4	52.8	0.4
MYNN3	0.0	1.0	0.0	0.8	2.8	0.0	0.8	2.8	0.0	1.0	44.9	0.4	58.1	54.5	0.2
											54.2	0.2			
Scaled metrics and models mean scores for direction prediction (30 test days)															
60m		50m						40m							
Average Wind Direction (degrees)		RMSE (degrees)	ME (degrees)	STDE (degrees)	CircC	Average Wind Direction (degrees)	RMSE (degrees)	ME (degrees)	STDE (degrees)	CircC	Average Wind Speeds (m/s)	ME (m/s)	RMSE (m/s)	STDE (m/s)	CC
Observations	54.6					52.0					6.2				
ACM2	44.9	55.2	-18.6	51.9	0.4	44.9	55.4	-16.6	52.8	0.4	6.4	1.7	6.4	1.7	0.8
MYNN3	50.1	58.5	-22.1	54.2	0.2	49.9	58.1	-20.2	54.5	0.2	6.4	1.7	6.4	1.7	0.8
Scaled metrics and model mean scores for speed prediction (36 test days)															
60m		50m						40m							
Average Wind Direction (degrees)		RMSE (degrees)	ME (degrees)	STDE (degrees)	CircC	Average Wind Direction (degrees)	RMSE (degrees)	ME (degrees)	STDE (degrees)	CircC	Average Wind Speeds (m/s)	ME (m/s)	RMSE (m/s)	STDE (m/s)	CC
Observations	6.4					6.3					6.2				
ACM2	6.5	1.8	0.1	1.8	0.8	6.4	1.8	0.8	6.4	0.1	6.2	0.1	6.4	1.7	0.8
MYNN3	6.5	1.7	0.1	1.7	0.8	6.5	1.7	0.8	6.4	0.2	6.4	0.2	6.4	1.7	0.8
Scaled metrics and model mean scores for direction prediction (36 test days)															
60m		50m						40m							
Average Wind Direction (degrees)		RMSE (degrees)	ME (degrees)	STDE (degrees)	CircC	Average Wind Direction (degrees)	RMSE (degrees)	ME (degrees)	STDE (degrees)	CircC	Average Wind Speeds (m/s)	ME (m/s)	RMSE (m/s)	STDE (m/s)	CC
Observations	58.0					55.6					6.2				
ACM2	44.9	56.4	-20.0	52.7	0.4	45.0	56.6	-18.0	53.7	0.4	6.4	1.7	6.4	1.7	0.8
MYNN3	49.5	60.5	-22.6	56.2	0.2	49.3	60.4	-20.7	56.7	0.2	6.4	1.7	6.4	1.7	0.8
Scaled metrics and models mean scores for direction prediction (36 test days)															
60m		50m						40m							
Average Wind Direction (degrees)		RMSE (degrees)	ME (degrees)	STDE (degrees)	CircC	Average Wind Direction (degrees)	RMSE (degrees)	ME (degrees)	STDE (degrees)	CircC	Average Wind Speeds (m/s)	ME (m/s)	RMSE (m/s)	STDE (m/s)	CC
Observations	58.0					55.6					6.2				
ACM2	44.9	56.4	-20.0	52.7	0.4	45.0	56.6	-18.0	53.7	0.4	6.4	1.7	6.4	1.7	0.8
MYNN3	49.5	60.5	-22.6	56.2	0.2	49.3	60.4	-20.7	56.7	0.2	6.4	1.7	6.4	1.7	0.8
Scaled metrics and models mean scores for direction prediction (36 test days)															
60m		50m						40m							
Average Wind Direction (degrees)		RMSE (degrees)	ME (degrees)	STDE (degrees)	CircC	Average Wind Direction (degrees)	RMSE (degrees)	ME (degrees)	STDE (degrees)	CircC	Average Wind Speeds (m/s)	ME (m/s)	RMSE (m/s)	STDE (m/s)	CC
Observations	6.09					5.99					5.88				
ACM2	6.20	2.00	0.11	2.00	0.82	6.13	2.00	0.82	6.13	1.96	6.06	0.14	6.06	1.96	0.82
YSU(1)	6.91	2.04	0.82	1.87	0.86	6.86	2.02	0.86	6.81	2.02	6.81	0.86	6.81	1.82	0.86
YSU(2)	6.96	2.03	0.87	1.84	0.86	6.92	2.01	0.92	6.88	2.01	6.88	0.92	6.88	1.77	0.86
MYNN2	6.51	1.96	0.42	1.92	0.86	6.42	1.94	0.43	6.33	1.94	6.33	0.43	6.33	1.79	0.86
MYNN3	6.34	1.89	0.25	1.87	0.87	6.26	1.86	0.26	6.18	1.86	6.18	0.26	6.18	1.89	0.86
MY1	7.03	2.19	0.94	1.98	0.83	6.96	2.16	0.97	6.90	2.16	6.90	0.97	6.90	1.93	0.82
QNSE	6.67	2.26	0.58	2.18	0.76	6.62	2.22	0.62	6.57	2.22	6.57	0.62	6.57	2.13	0.76

(continued on next page)

(continued)

	60 m				50 m				40 m						
	Average Wind Speeds (m/s)	RMSE (m/s)	ME (m/s)	STDE (m/s)	CC	Average Wind Speeds (m/s)	RMSE (m/s)	ME (m/s)	STDE (m/s)	CC	Average Wind Speeds (m/s)	RMSE (m/s)	ME (m/s)	STDE (m/s)	CC
GBM	6.85	2.03	0.76	1.88	0.85	6.82	2.01	0.83	1.83	0.85	6.79	2.03	0.90	1.82	0.85
UW	6.73	1.94	0.64	1.83	0.86	6.68	1.91	0.69	1.78	0.86	6.64	1.93	0.76	1.78	0.85
BL	6.86	2.11	0.77	1.96	0.83	6.79	2.06	0.79	1.91	0.83	6.71	2.06	0.83	1.89	0.83
TEMF	6.88	2.53	0.79	2.40	0.69	6.77	2.49	0.77	2.36	0.69	6.65	2.46	0.77	2.34	0.69

Scaled metrics and model mean scores															
	60m				50m				40m				Skill Score		
	RMSE(SCALED) (m/s)	MESCALED (m/s)	STDE(SCALED) (m/s)	CC	RMSE(SCALED) (m/s)	MESCALED (m/s)	STDE(SCALED) (m/s)	CC	RMSE(SCALED) (m/s)	MESCALED (m/s)	STDE(SCALED) (m/s)	CC			
ACM2	0.17	0.00	0.29	0.82	0.16	0.00	0.30	0.82	0.31	0.00	0.31	0.82	3.37		
YSU(1)	0.24	0.85	0.08	0.86	0.25	0.87	0.08	0.86	0.28	0.89	0.07	0.86	2.62		
YSU(2)	0.23	0.92	0.02	0.86	0.24	0.94	0.01	0.86	0.27	0.97	0.00	0.86	2.62		
MYNN2	0.11	0.38	0.15	0.86	0.12	0.35	0.19	0.86	0.14	0.32	0.23	0.85	3.16		
MYNN3	0.00	0.17	0.08	0.87	0.00	0.15	0.10	0.87	0.00	0.14	0.14	0.87	3.59		
MYJ	0.47	1.00	0.26	0.83	0.48	1.00	0.26	0.82	0.29	0.51	0.00	0.82	2.05		
QNSE	0.57	0.80	0.61	0.76	0.57	0.83	0.59	0.76	2.01	0.59	0.60	0.76	1.97		
GRM	0.22	0.79	0.10	0.85	0.24	0.83	0.09	0.85	2.70	0.27	0.85	0.08	2.63		
UW	0.07	0.64	0.00	0.86	0.08	0.66	0.00	0.86	3.12	0.09	0.68	0.00	3.08		
BL	0.34	0.80	0.23	0.83	0.33	0.78	0.22	0.83	2.50	0.32	0.77	0.21	2.53		
TEMF	1.00	0.82	1.00	0.69	0.87	1.00	0.76	1.00	0.69	0.93	1.00	0.70	0.69	0.99	

	Entire Rainy Season				High Winds			
	Average Wind Speed (m/s)	Skill Score	Average Wind Speed (m/s)	Skill Score	Average Wind Speed (m/s)	Skill Score	Average Wind Speed (m/s)	Skill Score
Measurements	3.16	2.3	7.07	2.8	7.58	2.7	7.18	2.7
ACM2	4.36	1.7	6.81	2.8	7.18	3.5	7.76	3.5
YSU(1)	5.07	1.7	7.57	2.7	7.82	3.3	7.76	3.3
YSU(2)	5.03	2.9	7.61	3.5	7.31	2.9	7.31	2.9
MYNN2	4.66	2.9	7.13	3.6	7.16	2.4	7.16	2.4
MYNN3	4.35	3.1	7.00	3.6	7.76	3.3	7.76	3.3
MYJ	5.22	1.4	7.53	2.6	7.29	2.5	7.29	2.5
QNSE	5.27	0.8	7.14	2.9	7.29	3.7	7.29	3.7
GRM	5.05	2.1	7.46	2.9	7.67	3.7	7.67	3.7
UW	4.84	2.2	7.36	3.4	7.52	3.7	7.52	3.7
BL	5.22	2.0	7.41	2.8	7.56	3.5	7.56	3.5
TEMF	5.19	1.3	7.44	1.0	7.71	1.5	7.71	1.5

	60 m				50 m				40 m						
	Average Wind Speeds (m/s)	RMSE (m/s)	ME (m/s)	STDE (m/s)	CC	Average Wind Speeds (m/s)	RMSE (m/s)	ME (m/s)	STDE (m/s)	CC	Average Wind Speeds (m/s)	RMSE (m/s)	ME (m/s)	STDE (m/s)	CC
Observations 8.1						7.9					7.8				
ACM2	7.5	1.6	-0.5	1.5	0.9	7.4	1.5	-0.5	1.4	0.9	7.3	1.5	-0.4	1.4	0.9
YSU(1)	7.9	1.3	-0.1	1.3	0.9	7.9	1.3	0.0	1.3	0.9	7.8	1.3	0.0	1.3	0.9
YSU(2)	8.0	1.3	-0.1	1.3	0.9	8.0	1.2	0.0	1.2	0.9	7.9	1.2	0.1	1.2	0.9
MYNN2	7.6	1.5	-0.5	1.4	0.9	7.4	1.5	-0.5	1.4	0.9	7.3	1.5	-0.5	1.4	0.9
MYNN3	7.5	1.5	-0.6	1.4	0.9	7.4	1.5	-0.5	1.4	0.9	7.2	1.6	-0.5	1.5	0.9
MYJ	7.9	1.3	-0.1	1.3	0.9	7.8	1.3	-0.1	1.3	0.9	7.7	1.3	0.0	1.3	1.0
QNSE	7.6	1.8	-0.5	1.7	0.9	7.5	1.7	-0.4	1.6	0.9	7.4	1.7	-0.3	1.6	0.9
GRM	7.9	1.3	-0.1	1.2	0.9	7.9	1.2	0.0	1.2	0.9	7.8	1.2	0.0	1.2	0.9
UW	7.7	1.4	-0.3	1.3	0.9	7.7	1.3	-0.3	1.3	0.9	7.6	1.3	-0.2	1.3	0.9
BL	7.7	1.6	-0.3	1.5	0.9	7.6	1.5	-0.3	1.5	0.9	7.5	1.5	-0.3	1.5	0.9

Scaled metrics and model mean scores for speed prediction (2 high winds test days)

	60m				50m				40m			
	RMSE _{SCALED} (m/s)	ME _{SCALED} (m/s)	STDE _{SCALED} (m/s)	Skill Score	RMSE _{SCALED} (m/s)	ME _{SCALED} (m/s)	STDE _{SCALED} (m/s)	Skill Score	RMSE _{SCALED} (m/s)	ME _{SCALED} (m/s)	STDE _{SCALED} (m/s)	Skill Score
ACM2	0.6	1.0	0.5	0.9	1.8	0.6	0.6	0.9	0.5	0.5	0.6	1.9
YSU(1)	0.1	0.1	0.2	0.9	3.5	0.1	0.0	0.2	0.2	0.0	0.2	3.6
YSU(2)	0.0	0.0	0.1	0.9	3.8	0.1	0.0	0.1	0.1	0.0	0.0	3.6
MYNN2	0.4	0.8	0.3	0.9	2.4	0.5	0.4	0.9	0.4	0.9	0.5	1.9
MYNN3	0.6	1.0	0.4	0.9	2.0	0.7	1.0	0.5	0.8	1.0	0.6	1.6
MVJ	0.2	0.1	0.2	0.9	3.5	0.1	0.1	0.9	0.1	0.0	0.1	3.8
QNSE	1.0	0.9	1.0	0.9	1.0	1.0	1.0	0.9	1.2	1.0	0.6	1.3
GRM	0.0	0.2	0.0	0.9	3.8	0.0	0.0	0.9	0.0	0.0	0.0	3.9
UW	0.2	0.6	0.2	0.9	2.9	0.3	0.4	0.2	0.2	0.3	0.3	3.1
BL	0.6	0.6	0.6	0.9	2.1	0.6	0.5	0.6	0.6	0.5	0.6	2.2

Average speeds and metrics for speed prediction (4 high winds test days)

	60 m				50 m				40 m			
	Average Wind Speeds (m/s)	RMSE (m/s)	ME (m/s)	STDE (m/s)	Average Wind Speeds (m/s)	RMSE (m/s)	ME (m/s)	STDE (m/s)	Average Wind Speeds (m/s)	RMSE (m/s)	ME (m/s)	STDE (m/s)
Observations	7.6				7.4				7.0			
ACM2	7.2	1.4	-0.4	1.3	0.9	7.1	1.4	-0.3	1.3	0.9	7.6	1.4
YSU(1)	7.7	1.3	0.2	1.3	0.9	7.7	1.3	0.3	1.3	0.9	7.7	1.4
YSU(2)	7.8	1.3	0.2	1.3	0.9	7.8	1.3	0.3	1.3	0.9	7.1	1.4
MYNN2	7.3	1.4	-0.3	1.4	0.9	7.2	1.4	-0.2	1.4	0.9	7.0	1.5
MYNN3	7.2	1.5	-0.4	1.4	0.9	7.1	1.5	-0.4	1.4	0.9	7.6	1.5
MVJ	7.8	1.4	0.2	1.3	0.9	7.7	1.3	0.3	1.3	0.9	7.2	1.4
QNSE	7.3	1.6	-0.3	1.5	0.9	7.2	1.5	-0.2	1.5	0.9	7.6	1.5
GRM	7.7	1.3	0.1	1.3	0.9	7.6	1.3	0.2	1.3	0.9	7.4	1.3
UW	7.5	1.3	-0.1	1.3	0.9	7.5	1.3	0.0	1.3	0.9	7.4	1.3
BL	7.6	1.4	0.0	1.4	0.9	7.5	1.4	0.1	1.4	0.9	0.0	1.4

Scaled metrics and model mean scores for speed prediction (4 high winds test days)

	60m				50m				40m			
	RMSE _{SCALED} (m/s)	ME _{SCALED} (m/s)	STDE _{SCALED} (m/s)	Skill Score	RMSE _{SCALED} (m/s)	ME _{SCALED} (m/s)	STDE _{SCALED} (m/s)	Skill Score	RMSE _{SCALED} (m/s)	ME _{SCALED} (m/s)	STDE _{SCALED} (m/s)	Skill Score
ACM2	0.4	0.9	0.2	0.9	2.4	0.3	0.2	0.9	0.2	0.2	0.2	3.1
YSU(1)	0.2	0.4	0.2	0.9	3.2	0.2	0.2	0.9	0.2	0.8	0.2	2.6
YSU(2)	0.1	0.5	0.0	0.9	3.3	0.1	0.0	0.9	0.0	1.0	0.0	2.7
MYNN2	0.5	0.6	0.5	0.9	2.3	0.6	0.6	0.9	0.6	0.3	0.7	2.2
MYNN3	0.8	1.0	0.6	0.9	1.5	0.9	1.0	0.7	0.9	0.6	0.8	1.6
MVJ	0.2	0.4	0.2	0.9	3.1	0.2	0.2	0.9	0.2	0.7	0.2	2.8
QNSE	1.0	0.7	1.0	0.9	1.2	1.0	1.0	0.5	1.0	1.0	1.0	1.9
GRM	0.0	0.2	0.0	0.9	3.7	0.0	0.0	0.9	0.0	0.6	0.0	3.2
UW	0.0	0.1	0.0	0.9	3.7	0.0	0.1	0.9	0.1	0.2	0.1	3.6
BL	0.5	0.0	0.6	0.9	2.8	0.5	0.6	0.9	0.6	0.1	0.6	2.6

Average speeds and metrics for speed prediction (6 high winds test days)

	60 m				50 m				40 m			
	Average Wind Speeds (m/s)	RMSE (m/s)	ME (m/s)	STDE (m/s)	Average Wind Speeds (m/s)	RMSE (m/s)	ME (m/s)	STDE (m/s)	Average Wind Speeds (m/s)	RMSE (m/s)	ME (m/s)	STDE (m/s)
Observations	7.4				7.2				7.0			
ACM2	7.0	1.3	-0.4	1.2	0.9	6.9	1.3	-0.3	1.2	0.9	6.9	1.3
YSU(1)	7.5	1.3	0.1	1.3	0.9	7.5	1.3	0.3	1.3	0.9	7.4	1.4
YSU(2)	7.6	1.2	0.2	1.2	0.9	7.6	1.3	0.4	1.2	0.9	7.5	1.4
MVJ	7.5	1.3	0.1	1.3	0.9	7.4	1.3	0.4	1.3	0.9	7.4	1.4
GRM	7.5	1.2	0.1	1.2	0.9	7.4	1.2	0.2	1.2	0.9	7.4	1.3
UW	7.3	1.2	-0.1	1.2	0.9	7.2	1.2	0.0	1.2	0.9	7.2	1.3
BL	7.4	1.3	0.0	1.3	0.9	7.3	1.3	0.1	1.3	0.8	7.2	1.4

(continued on next page)

(continued)

	60 m					50 m					40 m				
	Average Wind Speeds (m/s)	RMSE (m/s)	ME (m/s)	STDE (m/s)	CC	Average Wind Speeds (m/s)	RMSE (m/s)	ME (m/s)	STDE (m/s)	CC	Average Wind Speeds (m/s)	RMSE (m/s)	ME (m/s)	STDE (m/s)	CC
Scaled metrics and model mean scores for speed prediction (6 high winds test days)															
60m	RMSE _{SCALED} (m/s)	ME _{SCALED} (m/s)	STDE _{SCALED} (m/s)	CC	Skill Score	RMSE _{SCALED} (m/s)	ME _{SCALED} (m/s)	STDE _{SCALED} (m/s)	CC	Skill Score	RMSE _{SCALED} (m/s)	ME _{SCALED} (m/s)	STDE _{SCALED} (m/s)	CC	Skill Score
ACM2	0.8	1.0	0.3	0.9	1.8	0.4	0.7	0.3	0.9	2.5	0.0	0.1	0.9	3.7	
YSU(1)	0.5	0.2	0.5	0.9	2.7	0.5	0.7	0.4	0.9	2.2	0.6	0.7	0.0	1.4	
YSU(2)	0.3	0.5	0.2	0.9	2.9	0.4	1.0	0.1	0.9	2.3	0.7	1.0	0.1	1.3	
MYJ	0.7	0.2	0.7	0.9	2.3	0.7	0.6	0.6	0.9	1.9	0.8	0.5	0.6	0.0	
GRM	0.0	0.0	0.0	0.9	3.8	0.0	0.5	0.0	0.9	3.3	0.2	0.6	0.0	2.2	
UW	0.3	0.2	0.3	0.9	3.0	0.2	0.0	0.3	0.9	3.3	0.2	0.1	0.3	2.4	
BL	1.0	0.0	1.0	0.9	1.9	1.0	0.1	1.0	0.8	1.7	1.0	0.1	1.0	0.0	
Average speeds and metrics for speed prediction (8 high winds test days)															
60 m	Average Wind Speeds (m/s)	RMSE (m/s)	ME (m/s)	STDE (m/s)	CC	Average Wind Speeds (m/s)	RMSE (m/s)	ME (m/s)	STDE (m/s)	CC	Average Wind Speeds (m/s)	RMSE (m/s)	ME (m/s)	STDE (m/s)	CC
Observations	7.3					7.1					7.0				
YSU(1)	7.4	1.3	0.1	1.3	0.9	7.4	1.3	0.2	1.3	0.9	7.3	1.3	0.4	1.3	0.8
YSU(2)	7.5	1.2	0.2	1.2	0.9	7.5	1.3	0.3	1.2	0.9	7.4	1.3	0.5	1.2	0.9
MYJ	7.1	1.3	0.1	1.3	0.9	7.4	1.3	0.2	1.3	0.9	7.4	1.4	0.3	1.3	0.8
GRM	7.4	1.2	0.0	1.2	0.9	7.3	1.2	0.2	1.2	0.9	7.3	1.3	0.3	1.3	0.8
UW	7.3	1.3	-0.1	1.2	0.9	7.2	1.3	0.0	1.3	0.9	7.1	1.3	0.2	1.3	0.8
BL	7.4	1.3	0.0	1.3	0.9	7.3	1.3	0.1	1.3	0.8	7.2	1.4	0.2	1.4	0.8
Scaled metrics and model mean scores for speed prediction (8 high winds test days)															
60m	RMSE _{SCALED} (m/s)	ME _{SCALED} (m/s)	STDE _{SCALED} (m/s)	CC	Skill Score	RMSE _{SCALED} (m/s)	ME _{SCALED} (m/s)	STDE _{SCALED} (m/s)	CC	Skill Score	RMSE _{SCALED} (m/s)	ME _{SCALED} (m/s)	STDE _{SCALED} (m/s)	CC	Skill Score
YSU(1)	0.4	0.4	0.4	0.9	2.6	0.5	0.7	0.4	0.9	2.4	0.4	0.7	0.3	0.8	2.5
YSU(2)	0.1	1.0	0.0	0.9	2.7	0.2	1.0	0.0	0.9	2.6	0.3	1.0	0.0	0.9	2.6
MYJ	0.6	0.5	0.6	0.9	2.1	0.7	0.6	0.6	0.9	1.9	0.8	0.6	0.7	0.8	1.8
GRM	0.0	0.0	0.0	0.9	3.9	0.0	0.5	0.0	0.9	3.4	0.0	0.5	0.1	0.8	3.2
UW	0.4	0.3	0.4	0.9	2.8	0.3	0.0	0.4	0.9	3.2	0.1	0.0	0.3	0.8	3.4
BL	1.0	0.0	1.0	0.9	1.8	1.0	0.1	1.0	0.8	1.7	1.0	0.1	1.0	0.8	1.8
Average speeds and metrics for speed prediction (10 high winds test days)															
60 m	Average Wind Speeds (m/s)	RMSE (m/s)	ME (m/s)	STDE (m/s)	CC	Average Wind Speeds (m/s)	RMSE (m/s)	ME (m/s)	STDE (m/s)	CC	Average Wind Speeds (m/s)	RMSE (m/s)	ME (m/s)	STDE (m/s)	CC
Observations	7.3					7.1					6.9				
YSU(2)	7.6	1.2	0.3	1.2	0.9	7.6	1.3	0.5	1.2	0.9	7.5	1.3	0.6	1.2	0.9
GRM	7.5	1.2	0.2	1.2	0.9	7.4	1.2	0.3	1.2	0.9	7.4	1.3	0.5	1.2	0.8
UW	7.4	1.2	0.1	1.2	0.9	7.3	1.2	0.2	1.2	0.9	7.2	1.3	0.3	1.2	0.8
Scaled metrics and model mean scores for speed prediction (10 high winds test days)															
60m	RMSE _{SCALED} (m/s)	ME _{SCALED} (m/s)	STDE _{SCALED} (m/s)	CC	Skill Score	RMSE _{SCALED} (m/s)	ME _{SCALED} (m/s)	STDE _{SCALED} (m/s)	CC	Skill Score	RMSE _{SCALED} (m/s)	ME _{SCALED} (m/s)	STDE _{SCALED} (m/s)	CC	Skill Score
YSU(2)	0.8	1.0	0.0	0.9	2.1	1.0	1.0	1.2	0.9	0.7	1.0	1.0	0.0	0.9	1.9
GRM	1.0	0.5	0.7	0.9	1.6	0.8	0.6	1.2	0.9	1.3	0.9	0.6	0.8	0.8	1.5
UW	0.0	0.0	1.0	0.9	2.9	0.0	0.0	1.2	0.9	2.6	0.0	0.0	1.0	0.8	2.8

Average speeds and metrics for speed prediction (12 high winds test days)

	60 m				50 m				40 m						
	Average Wind Speeds (m/s)	RMSE (m/s)	ME (m/s)	STDE (m/s)	CC	Average Wind Speeds (m/s)	RMSE (m/s)	ME (m/s)	STDE (m/s)	CC	Average Wind Speeds (m/s)	RMSE (m/s)	ME (m/s)	STDE (m/s)	CC
Observations	7.3					7.1					6.9				
YSU(2)	7.6	1.3	0.3	1.3	0.8	7.5	1.3	0.4	1.3	0.8	7.5	1.4	0.6	1.3	0.8
GBM	7.4	1.3	0.2	1.3	0.8	7.4	1.3	0.3	1.3	0.8	7.3	1.4	0.4	1.3	0.8
UW	7.3	1.3	0.0	1.3	0.8	7.2	1.3	0.2	1.3	0.8	7.2	1.4	0.3	1.3	0.8

	60m				50m				40m			
	RMSE _{SCALED} (m/s)	ME _{SCALED} (m/s)	STDE _{SCALED} (m/s)	Skill Score	RMSE _{SCALED} (m/s)	ME _{SCALED} (m/s)	STDE _{SCALED} (m/s)	Skill Score	RMSE _{SCALED} (m/s)	ME _{SCALED} (m/s)	STDE _{SCALED} (m/s)	Skill Score
YSU(2)	1.0	1.0	0.2	0.8	1.0	1.0	0.0	0.8	1.0	1.0	0.0	0.8
GBM	0.0	0.5	0.0	0.8	0.1	0.5	0.2	0.8	0.4	0.5	0.4	0.8
UW	0.5	0.0	1.0	0.8	0.0	0.0	1.0	0.8	2.8	0.0	1.0	2.8

Scaled metrics and model mean scores for speed prediction (12 high winds test days)

References

- [1] D. Carvalho, et al., WRF wind simulation and wind energy production estimates forced by different reanalyses: comparison with observed data for Portugal, *Appl. Energy* 117 (2014) 116–126.
- [2] D. Carvalho, et al., A sensitivity study of the WRF model in wind simulation for an area of high wind energy, *Environ. Model. Softw.* 33 (2012) 23–34.
- [3] W.C. Skamarock, A description of the advanced research WRF version 3, *Tech. Note* (2008) 1–96.
- [4] F.J. Santos-Alamillos, et al., Analysis of WRF model wind estimate sensitivity to physics parameterization choice and terrain representation in andalusia (southern Spain), *Journal of Applied Meteorology and Climatology* 52 (2013) 1592–1609, <https://doi.org/10.1175/jamc-d-12-0204.1>.
- [5] E.-M. Giannakopoulou, R. Nhili, WRF model methodology for offshore wind energy applications, *Advances in Meteorology* 2014 (2014), 319819, 14 pages, <https://doi.org/10.1155/2014/319819>.
- [6] C. Surussavadee, W. Wu, Evaluation of WRF planetary boundary layer schemes for high-resolution wind simulations in Northeastern Thailand, in: *IEEE International Geoscience and Remote Sensing Symposium, IGARSS*, 2015, pp. 3949–3952, <https://doi.org/10.1109/IGARSS.2015.7326689>, 2015.
- [7] C. Surussavadee, Evaluation of WRF near-surface wind simulations in tropics employing different planetary boundary layer schemes, in: *8th International Renewable Energy Congress (IREC)*, 2017, pp. 1–4, <https://doi.org/10.1109/IREC.2017.7926005>, 2017.
- [8] M.O. Mughal, et al., Wind modelling, validation and sensitivity study using Weather Research and Forecasting model in complex terrain, *Environ. Model. Softw.* 90 (2017) 107–125, <https://doi.org/10.1016/j.envsoft.2017.01.009>.
- [9] K.B.R.R. Hariprasad, et al., Numerical simulation and intercomparison of boundary layer structure with different PBL schemes in WRF using experimental observations at a tropical site, *Atmos. Res.* 145–146 (2014) 27–44, <https://doi.org/10.1016/j.atmosres.2014.03.023>.
- [10] T. Ohsawa, et al., Investigation of WRF configuration for offshore wind resource maps in Japan, in: *Wind Europe Summit, Hamburg Messe, Hamburg, Germany*, 2016.
- [11] M. Mohammadpour Penchah, H. Malakooti, M. Satkin, Evaluation of planetary boundary layer simulations for wind resource study in east of Iran, *Renew. Energy* 111 (2017) 1–10, <https://doi.org/10.1016/j.renene.2017.03.040>.
- [12] C. Mattar, D. Borvarán, Offshore wind power simulation by using WRF in the central coast of Chile, *Renewable Energy*, 2016, pp. 22–31.
- [13] R. Boadh, et al., Sensitivity of PBL schemes of the WRF-ARW model in simulating the boundary layer flow parameters for its application to air pollution dispersion modeling over a tropical station, *Atmosfera* 29 (2016) 61–81, <https://doi.org/10.20937/ATM.2016.29.01.05>.
- [14] J.M. Wallace, P.V. Hobbs, *Atmospheric Science: an Introductory Survey*, vol. 92, Elsevier, 2006.
- [15] R.B. Stull, *An Introduction to Boundary Layer Meteorology*, vol. 13, Springer Science & Business Media, 2012.
- [16] T.T. Warner, *Numerical Weather and Climate Prediction*, Cambridge University Press, 2011.
- [17] F. Dominguez, *ATMO 579 Boundary Layer Meteorology and Surface Processes*, 2010.
- [18] X. Chadee, N. Seegobin, R. Clarke, Optimizing the weather research and forecasting (WRF) model for mapping the near-surface wind resources over the southernmost caribbean islands of Trinidad and Tobago, *Energies* 10 (2017) 931, <https://doi.org/10.3390/en10070931>.
- [19] J. Dudhia, Overview of WRF Physics, 2017.
- [20] C.B. Wei Wang, Michael Duda, Jimmy Dudhia, Dave Gill, Michael Kavulich, Keene Kelly, Ming Chen, Hui-Chuan Lin, John Michalakes, Syed Rizvi, Xin Zhang, Judith Berner, Soyoung, Ha and Kate Fossell, *ARW Version 3 Modeling System User's Guide*, 2016.
- [21] R.F. Banks, et al., Sensitivity of boundary-layer variables to PBL schemes in the WRF model based on surface meteorological observations, lidar, and radiosondes during the HyGRA-CD campaign, *Atmos. Res.* 176–177 (2016) 185–201, <https://doi.org/10.1016/j.atmosres.2016.02.024>.
- [22] S.-Y. Hong, Y. Noh, J. Dudhia, A new vertical diffusion package with an explicit treatment of entrainment processes, *Mon. Weather Rev.* 134 (9) (2006) 2318–2341.
- [23] A.E. Cohen, et al., A review of planetary boundary layer parameterization schemes and their sensitivity in simulating southeastern US cold season severe weather environments, *Weather Forecast.* 30 (2015) 591–612, <https://doi.org/10.1175/WAF-D-14-00105.1>.
- [24] S. Madala, et al., Mesoscale atmospheric flow-field simulations for air quality modeling over complex terrain region of Ranchi in eastern India using WRF, *Atmos. Environ.* 107 (2015) 315–328, <https://doi.org/10.1016/j.atmosenv.2015.02.059>.
- [25] S. Madala, A.N.V. Satyanarayana, T.N. Rao, Performance evaluation of PBL and cumulus parameterization schemes of WRF ARW model in simulating severe thunderstorm events over Gadanki MST radar facility — case study, *Atmos. Res.* 139 (2014) 1–17.
- [26] P. Gunwani, M. Mohan, Sensitivity of WRF model estimates to various PBL parameterizations in different climatic zones over India, *Atmos. Res.* 194 (2017) 43–65.
- [27] Volta River Authority, *Power Generation: Facts & Figures*, 2016 [cited 196 06–Nov]; Available from: <http://www.vra.com/resources/facts.php>.

- [28] Energy Commission of Ghana, The SWERA Ghana Project. Energy Commission of Ghana.
- [29] National Renewable Energy Laboratory (NREL), Ghana Wind Energy Resource Mapping Activity, 2004.
- [30] reportGhana Statistical Service, 2010 Population And Housing Census: District Analytical Report, Keta Municipality, 2014, Ghana Statistical Service.
- [31] C. McSweeney, M. New, G. Lizcano, UNDP Climate Change Country Profiles: Ghana, 2010, 2016.
- [32] NASA Langley ASDC User Services, NASA Surface Meteorology and Solar Energy - Available Tables [cited 2018 May 25]; Available from: https://eosweb.larc.nasa.gov/cgi-bin/sse/grid.cgi?&num=181096&lat=5.786&submit=Submit&hgt=100&veg=6&sitelev=&email=skip@larc.nasa.gov&p=grid_id&p=T10M&p=DLYRANGE&p=TSKIN_MN&p=wspd50m&p=wnd_dir&p=gipe_wnd&step=2&lon=0.919.
- [33] J. Dudhia, et al., Evaluation of Weather Research and Forecasting (WRF) Model Physics in Simulating West African Monsoon, WAM), 2017.
- [34] Statistical Computation Laboratory, Computing the Pearson correlation coefficient [cited 2018 27/05]; Available from: <http://www.stat.wmich.edu/s216/book/node122.html>.
- [35] P. Berens, CircStat: a MATLAB toolbox for circular statistics, J. Stat. Softw. 31 (10) (2009) 1–21.
- [36] C. Emery, E. Tai, G. Yarwood, Enhanced meteorological modeling and performance evaluation for two Texas ozone episodes, in: Prepared for the Texas Natural Resource Conservation Commission, ENVIRON International Corporation, 2001.
- [37] Cedar Lake Ventures Inc, Average weather in accra, Ghana, year round - weather spark [cited 2018 07/06]; Available from: <https://weatherspark.com/y/42322/Average-Weather-in-Accra-Ghana-Year-Round>, 2018.

Paper III

Article

Impact of Selected Options in the Weather Research and Forecasting Model on Surface Wind Hindcasts in Coastal Ghana

Denis E.K. Dzebre^{1,2,3} and Muyiwa S. Adaramola^{1,*} 

¹ Faculty of Environmental Sciences and Natural Resources, Norwegian University of Life Sciences (NMBU), 1432 Akershus, Norway; dekdzebre.coe@knust.edu.gh

² Department of Mechanical Engineering, Kwame Nkrumah University of Science and Technology (KNUST), Kumasi 00000, Ghana

³ The Brew-Hammond Energy Centre, KNUST, Kumasi 00000, Ghana

* Correspondence: muyiwa.adaramola@nmbu.no

Received: 2 September 2019; Accepted: 21 September 2019; Published: 25 September 2019



Abstract: This paper examines the impacts of five planetary boundary layer (PBL) parameterization schemes paired with several compatible surface layer (SL) parameterization schemes in the Weather Research and Forecasting Model on wind hindcasts for resource assessment purposes in a part of Coastal Ghana. Model predictions of hourly wind speeds at 3×3 km² and 9×9 km² grid boxes were compared with measurements at 40 m, 50 m, and 60 m. It was found that the Mellor-Yamada Nakanishi and Niino Level 3 (MYNN3) PBL scheme generally predicted winds with a relatively better combination of error metrics, irrespective of the SL scheme it was paired with. When paired with the Eta surface layer scheme, it often produced some of the relatively fewest errors in estimated mean wind power density (WPD) and Weibull cumulative density. A change in the simulation grid size did not have a significant impact on the conclusions of the relative performance of the PBL-SL pairs that were tested. The results indicate that the MYNN3 PBL and Eta SL pair is probably best for wind speed and energy assessments for this part of coastal Ghana.

Keywords: wind resource assessment; dynamical downscaling; parameterization schemes; WRF; Ghana

1. Introduction

Over the years, there has been increasing interest in the use of numerical weather prediction (NWP) models, such as the Weather Research and Forecasting (WRF) model [1], for wind resource assessment. By numerically downscaling meteorological datasets, these models are used to generate wind data (wind speeds and directions) at relatively low cost for areas lacking ground measurements of such data for preliminary assessments of wind resources. Owing to diverse model options, identifying optimum model configurations (which are basically combinations of the options available in the models) for an application sometimes requires sensitivity tests, which assess, comparatively, the effects of varying model options on model performance. Predictions of surface winds by NWP models such as WRF are sensitive to model options such as simulation grid size, model physics, initial and boundary data, and parameterization of processes at the subgrid scale [2,3]. This paper focuses on selected parameterization options in the Advanced Research WRF (ARW).

Planetary Boundary and Surface Layer Parameterization

Atmospheric processes play an important role in determining certain fundamental properties of the weather and climate of the earth. Therefore, their correct representation in atmospheric models is

important. In NWP, this is done in part via the model physics, the purpose of which is to resolve and parameterize (approximate) these processes in the models [4]. Where, due to the complexity of the processes or the scales on which they occur or for other reasons, the processes cannot be explicitly represented in or resolved by the models, they are parameterized (or approximated with parameterization schemes) [4]. Parameterization involves relating the effects of such processes to variables that can more easily be determined by the models [4]. The physics parameterization schemes in WRF fall into the microphysics (MP), cumulus, long-wave radiation (Rad-L), short-wave radiation (Rad-S), land surface model (LSM), surface layer (SL), and planetary boundary layer (PBL) categories [1]. Vertical sub-grid scale transport processes in the atmosphere are parameterized by the PBL schemes, which interact directly with the SL and LSM schemes [5].

Transport processes transmit the effect of surface phenomena such as frictional drag, heat transfer, and terrain induced flow modification in the planetary boundary layer to the upper layers of the atmosphere [6]. Turbulence plays a key role in such transport processes and acts as a feedback mechanism in wind circulation [6–8]. PBL schemes compute turbulence flux profiles within the atmosphere, providing atmospheric tendencies of temperature, moisture, and horizontal momentum [5], which are used in predicting variables. A key difference in the PBL schemes in WRF is how they address the turbulence closure problem, which arises in the mathematical representation of turbulence (explained in several texts such as [4,9,10]), due to the difficulty of resolving the smallest turbulent eddies (which are in the order of a few millimeters [6–8]). This is often a challenge in NWP, as they are often run at grid resolutions that do not allow the adequate resolving of such eddies. Depending on how the closure problem is addressed in a PBL scheme, it may be classified according to an order of closure, and as a local or nonlocal closure scheme. Only vertical levels that are directly adjacent to a given point directly influence the estimation of the fluxes at that point in local closure schemes. In nonlocal closure schemes, on the other hand, multiple vertical levels influence the estimation of fluxes at a given point [11]. In addition, in WRF, most nonlocal schemes have diagnostic components for a flux profile, while the local closure schemes use turbulent kinetic energy (TKE) predicted at a point in approximating fluxes [12]. Higher order local closures and nonlocal closures are often more accurate than lower order local closure schemes [4]. Brief descriptions of several PBL schemes as well as their shortcomings have been summarized in the literature [11–14].

Parameterization methods perform differently in different atmospheric stability conditions, which inform their formulation [5,11]. Stability dependent information and other inputs needed by the PBL schemes are provided by SL schemes. The SL schemes also provide exchange coefficients for the calculation of the heat and moisture fluxes by LSM schemes. These fluxes serve as bottom boundary conditions for the PBL schemes [15,16]. Key differences among SL schemes include the approaches and methods used in computing surface exchange coefficients [5]. However, they are mostly based on the similarity theory, which is explained in texts such as [6,9,10]. In WRF, PBL schemes are recommended to be used with specific SL schemes but are generally compatible with most of the LSM schemes in the model.

Given the importance of wind speeds to wind energy extraction, and as wind turbines operate in the lower parts of the PBL, several studies [3,17–23] over the years have examined the impact of PBL schemes in WRF on the wind hindcasts. However, studies in the tropics [17–21] have often not tested the different PBL schemes with different compatible SL schemes. In addition, the impact of the schemes on model performance is influenced by local terrain features and atmospheric conditions, which often vary with geographical location [2,3]. Against this background, in this paper, we investigate the impact of selected PBL schemes, paired with several compatible SL schemes, on wind hindcasts for wind energy assessment purposes in an area in coastal Ghana. The study focuses on five PBL schemes selected from a preliminary study of PBL schemes in coastal Ghana, and other studies in tropical areas [17–21]. These are:

- 1st order hybrid (local/nonlocal) closure Asymmetric Convective Model (ACM2) [24]
- 2nd order TKE closure Mellor-Yamada Nakanishi Niino Level 3 (MYNN3) [25]

- 1.5 order TKE closure University of Washington (UW) [26]
- 1.5 order TKE closure Grenier-Bretherton-McCaa (GBM) [27]
- 1st order nonlocal closure Yonsei University (YSU) [28]

The aim of the study is to offer some insight into the relative impacts of the selected PBL-SL pairs on wind speed and mean wind power density estimates by the model for coastal Ghana. The rest of the paper is organized as follows; Section 2 covers the study area, verification data, model configuration, and experimental design. Section 3 presents and discusses results of analysis, and Section 4 summarizes the study and presents conclusions drawn from the study.

2. Materials and Methods

2.1. Study Area and Data

The study area covers the coastal plains of South East Ghana (shown in Figure 1). The area comprises predominantly low-lying coastal plains with savanna grass vegetation and experiences two main seasons in a year: a harmattan season that is dominated by dry and dusty desert winds from the North-East, starting from around November and lasting until February, and a bimodal rainy season dominated by Monsoon winds that ends around November [29,30]. The Energy Commission of Ghana (EC) has conducted mast measurements at selected sites, mostly along the coast of this region. The observed (measured) data for this study, which comprise hourly measurements of wind speeds (in selected months) in 2013, at heights of 40, 50, and 60 m above ground level, is from one such EC masts, located at 5.7861 °N and 0.9188 °E.

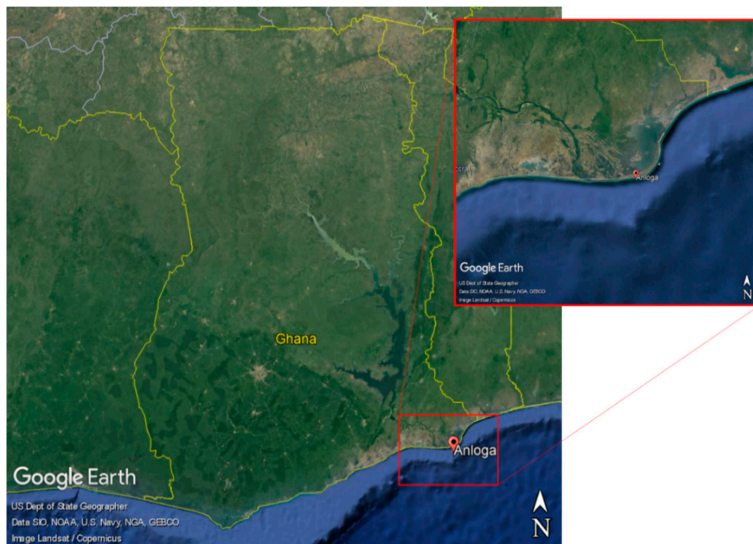


Figure 1. Map of Ghana showing the study area (in yellow and red, respectively).

2.2. Model Configuration

Version 3.8.1 of the Advanced Research WRF (ARW) [1] was used for this study. Key features of the model include a fully compressible, non-hydrostatic Euler equation, a terrain following a vertical coordinate system, and a staggered horizontal grid. Model prognostic variables include three-dimensional wind, turbulent kinetic energy, and potential temperature. Detailed descriptions of the model physics, equations, and dynamics are provided by [1].

The model configuration for the study is summarized in Table 1. Map projections transform atmospheric properties (defined on earth's spherical surface) to a flat model grid [4] to enable the application of grid point methods to solutions of the atmospheric flow equations. Map projections tend to affect model stability as they distort distances at any given point, affecting the maximum stable timestep in the WRF solver. To maintain numerical solution stability, it is recommended to use a projection that keeps the map-scale factor (a measure of distance distortions from the transformation) close to unity over the simulation grid [4]. For low-latitude and tropical regions, the Mercator projection is recommended as it best satisfies this (stability) condition [4,31]. To further ensure model stability, a model timestep of 120 s (less than the maximum 6 times the magnitude of the coarsest horizontal grid distance) was used as suggested by [1]. The domains, shown in Figure 2, have horizontal resolutions of 27 km, 9 km, and 3 km, and a vertical resolution of 40 vertical pressure levels each. The horizontal resolutions were chosen to achieve a nesting ratio of 3, and the final horizontal resolution of 3 km was used because it was found to be optimal for wind simulations in WRF [32,33]. The vertical resolution was chosen following recommendations of [34]. The model top was 50 hPa with the lowest half level at approximately 28 m asl.

Table 1. Model configuration.

Model Version	Advanced Research WRF v3.8.1		
Initial and Boundary Conditions	NCEP Final Analysis (GFS-FNL) [35]: 1° × 1° and 6 h Resolution		
Land Use Data	30-arc-second USGS ¹ with lakes		
Topographical Data	30-arc-second USGS GMTED2010		
Map Projection	Mercator		
Vertical Resolution	40 vertical pressure levels (automatically set)		
Horizontal Resolution (km)	27	9	3
Domain Size (grid points)	91 × 103	82 × 94	64 × 55
Model Timestep (seconds)	120		
FDDA ²	Analysis Nudging (Disabled in the PBL)		
Parameterization Schemes:			
Cloud Microphysics (MP)	Eta microphysics [36]		
Long-Wave Radiation (LW-Rad)	Rapid Radiative Transfer Model [37]		
Short-Wave Radiation (SW-Rad)	Dudhia [38]		
Surface Layer (SL)	i. Mellor-Yamada Nakanishi Niino (MYNN) ii. Pleim-Xiu (PX) [39] iii. Revised MM5 Similarity (R-MM5) [40] iv. Eta Similarity (Eta) [41–43]		
Land Surface Model (LSM)	Unified Noah [44] Pleim-Xiu (PX) [45,46]		
Planetary Boundary Layer (PBL)	i. ACM2 [24] ii. GBM [27] iii. MYNN3 [25] iv. UW [26] v. YSU [28]		
Cumulus	Kain-Fritsch [47] (turned off for domain 3 [1,32])		

¹ United States Geological Survey. ² Four-Dimensional Data Assimilation.

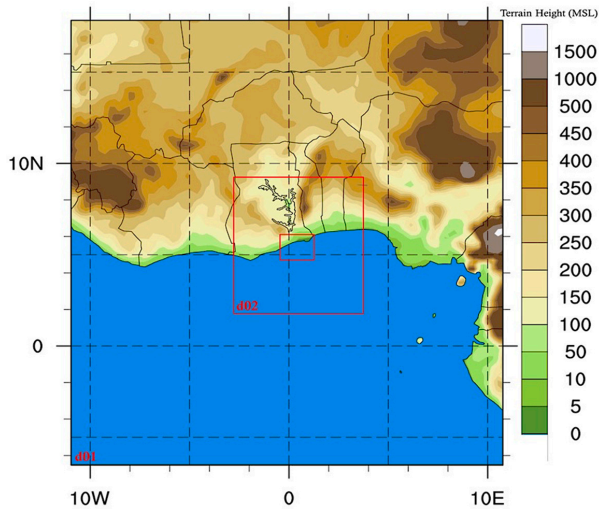


Figure 2. Simulation domains.

The selected PBL parameterization schemes were paired with compatible SL schemes as recommended by [31,48] (except the old MM5 scheme). Other required parameterization schemes were selected based on other wind sensitivity studies in coastal Ghana [49,50], and practices from other wind sensitivity studies (mostly in the tropics) [17–21]. The Eta Microphysics, New Rapid Radiative Transfer Model [37] and Dudhia [38] schemes were used for MP, LW-Rad, and SW-Rad parameterizations, respectively. Cumulus parameterization was not used in domain 3, as the horizontal grid resolution in this domain was considered fine enough for adequate resolving of cumulus processes [1,32]. For domains 1 and 2, however, cumulus processes were parameterized with the updated Kain-Fritsch scheme [47]. The Unified Noah LSM [44], was used for land surface parameterization. In addition, following recommended best practices on the use of the ACM2 PBL scheme and PX SL schemes [51], the PX LSM [45,46] was also tested but with the PX SL scheme only. The resulting PBL-SL-LSM configurations that were tested are presented, with references as obtained from the WRF physics page, in Table 2.

Table 2. Configurations tested.

No.	Designation	PBL Scheme	SL Scheme	LSM Scheme
1	ACM2-P-P	ACM2	PX	PX
2	ACM2-P-N	ACM2	PX	Noah
3	ACM2-R-N	ACM2	R-MM5	Noah
4	GBM-R-N	GBM	R-MM5	Noah
5	MYNN3-M-N	MYNN3	MYNN	Noah
6	MYNN3-R-N	MYNN3	R-MM5	Noah
7	MYNN3-E-N	MYNN3	Eta	Noah
8	UW-R-N	UW	R-MM5	Noah
9	UW-E-N	UW	Eta	Noah
10	YSU-R-N	YSU	R-MM5	Noah

2.3. Experimental Design

A total of 10 configurations were tested. Owing to limited computational resources, each configuration was used to simulate a period comprising four months, January, February, May, and September of 2013, one month at a time. The months were selected for their relatively high or

low monthly average wind speeds in the seasons that pertained in this part of Ghana; January and March represented the harmattan season and May and September, the rainy season. It was hoped that by selecting the periods simulated in this manner (as has been done in other resource assessment sensitivity studies [22,32]), the effect of major seasonal changes on annual winds would be captured by the options being tested. The grid nudging option of the WRF Four-Dimensional Data Assimilation (FDDA) system is a technique that has been used in several studies on wind downscaling for resource assessment purposes [20,52,53]. The technique bridges the gap between the model simulations and time-interpolated values from input data. All three simulation domains were nudged during all the simulations, following practices of previous studies [20,52,53]. Nudging options and simulation lengths were chosen based on recommendations from a previous study in coastal Ghana [49].

2.4. Postprocessing of Data and Evaluation of Options

Post-processing of results generally followed the procedure used in previous studies in the study area [49,50]. However, hourly predictions of winds (at 10 m and other relevant half vertical levels) were bilinearly interpolated to the mast location. Furthermore, winds were interpolated to the heights of analysis (40 m, 50 m, and 60 m), with log-linear interpolation [54]. Scheme performance was assessed in terms of four error metrics, which were calculated with procedures from previous studies [49,50]: mean error (ME), root mean square error (RMSE), standard deviation of the error (STDE), as well as the correlation coefficient (CC) of the predictions. The error metrics were combined into a prediction skill score (SS) (as was done in previous studies [49,50]), which was used to rank the options. In addition, the ME, RMSE, and CC were compared to values that were considered as indicators of good model performance in studies [18,19,55].

As the intended application of the findings of the study is wind energy assessment, the impacts of the options on wind power estimation were evaluated by comparing their Weibull cumulative distributions and mean wind power densities to those from observations for the study period. The Weibull distribution is widely used in many fields of the wind energy industry. The cumulative distribution gives the probability of wind speeds being less than or equal to the speed at which it is evaluated. Its function is given as [56]

$$F(v) = 1 - \exp\left[-\left(\frac{v}{c}\right)^k\right] \quad (1)$$

where v , c , and k are the wind speed, Weibull scale, and shape factors, respectively. The scale and shape parameters were estimated using the empirical (mean and standard deviation) method (with formulas from [56]). This method was chosen after an evaluation of five methods—the empirical, moment, graphical or least squares, the energy pattern factor, and maximum likelihood methods—using an evaluation method from a study by [56]. The empirical method was chosen for its simplicity and often relatively better or on-par relative test rank, which was in terms of total normalized results.

The distributions for observed data and the configurations were compared via the maximum absolute error of the cumulative distribution function (max CDF error), which was determined as the maximum difference between the cumulative distributions of observed and predicted data, (evaluated in 0.5 m/s bins as recommended by [57]) [53]:

$$\text{Max CDF Error} = \max|F(v_i)_{obs} - F(v_i)_{sim}|. \quad (2)$$

The mean wind power densities were expressed as the percent error of the difference between the mean WPD of observed and predicted data for a period of evaluation. The error was then expressed as a percentage of the mean WPD from observations. The mean WPDs were determined from the estimated Weibull parameters as [56,57]

$$\text{WPD} = \left[\frac{1}{2}\rho c^3\Gamma\left(1 + \frac{3}{k}\right)\right] \quad (3)$$

where ρ , the air density, was assumed to be 1.160 kg m^{-3} , as estimated in a previous study [49] in the study area.

3. Results

Results at 60 m for the PBL-SL pair options are presented in Table 3. It can be seen from the error metrics that the impacts of all the tested PBL-SL pairs on model performance were mostly within the acceptable limits: RMSE < 2 m/s, ME < 0.5 m/s. However, the ACM2, GBM, and YSU predictions had CCs that were slightly less than the acceptable limits (CC ≥ 0.7 [18,19,55]). It can also be observed that for the same PBL scheme, the impact (if any at all) was less on the error metrics. Again, for the same PBL scheme, the Eta SL scheme produced higher average wind speeds than the other SL schemes. The YSU PBL scheme predicted higher average wind speeds than the MYNN3 PBL scheme (irrespective of SL scheme). Generally, configurations with the MYNN3 PBL scheme predicted with some of the least RMSEs, the best consistency (least STDEs), and highest correlations, and therefore, gave the best skill scores, although as has been mentioned, the error metrics for all the other configurations (except for the CCs of the ACM2, GBM, and YSU PBL schemes) were within acceptable limits for good model performance. In contrast to the average wind speed predictions, the configurations had more significant impacts on WPD estimates. However, some of the trends observed in the speed predictions were also observed in the WPD estimates; the configurations with the Eta SL scheme gave relatively smaller absolute WPD errors than the R-MM5 SL scheme. The MYNN3-E-N and ACM2-R-N configurations gave the best average WPD estimates for the entire study period. However, as can be seen from the table, the MYNN3-E-N configuration had a better maximum error of CDF. In addition, it can be observed from the CDF plots presented in Figure 3 that the probability plot of the MYNN3-E-N configuration was closest to the plot of observed data for speeds below 7 m/s; the other options gave relatively lower probabilities. For higher speeds, the MYNN3-E-N together with the UW-E-N configurations gave the closest probability plots.

Table 3. Error metrics and skill scores at 60 m for study period.

	Average Wind Speeds (m/s)	ME (m/s)	RMSE (m/s)	STDE (m/s)	CC	Skill Score	Weibull <i>k</i>	Weibull <i>c</i>	Mean WPD (Wm^{-2})	WPD Error (%)	Max CDF Error
Observation	5.87						2.93	6.58	167		
ACM2-P-P	5.83	−0.04	1.65	1.65	0.67	0.3	3.78	6.59	145	−13.1	0.0645
ACM2-P-N	5.95	0.08	1.66	1.66	0.67	0.2	3.78	6.59	154	−7.6	0.0693
ACM2-R-N	6.08	0.21	1.65	1.64	0.67	1.0	3.86	6.72	163	−2.2	0.0888
GBM-R-N	6.06	0.19	1.60	1.59	0.69	2.0	4.04	6.68	158	−5.1	0.0964
MYNN3-M-N	5.68	−0.19	1.55	1.54	0.71	3.3	3.56	6.31	137	−17.6	0.0731
MYNN3-R-N	5.71	−0.16	1.55	1.54	0.72	3.5	3.34	6.36	143	−14.2	0.0545
MYNN3-E-N	5.96	0.09	1.58	1.57	0.72	2.6	3.33	6.64	163	−2.2	0.0399
UW-R-N	5.86	−0.01	1.57	1.57	0.70	2.1	3.67	6.49	149	−10.9	0.0530
UW-E-N	6.19	0.32	1.63	1.60	0.70	2.2	3.70	6.85	174	4.6	0.0932
YSU-R-N	6.01	0.14	1.60	1.59	0.69	1.9	3.85	6.64	157	−5.7	0.0802

Similar trends were often observed when the analysis was restricted to the seasons in the area; a change in SL scheme did not often produce a significant change in metrics. The Eta SL scheme produced higher average wind speed estimates than the R-MM5. The YSU scheme simulated higher wind speeds than the MYNN3 scheme. Configurations with the MYNN3 PBL scheme still ranked best in the rainy season and all the options satisfied all the criteria for good performance (except the ACM2 configurations, which had CCs < 0.7 in the rainy season). Notable exceptions to these trends are the ACM2 PBL scheme with the Noah LSM (with either SL schemes) ranking relatively better for speed prediction during the harmattan season. In addition to the MYNN3-E-N configuration, the UW-R-N

configuration gave a relatively good WPD error with a better max CDF error in the harmattan season. Results on the seasonal analyses at 60 m are available in Table A2 in the Appendix A.

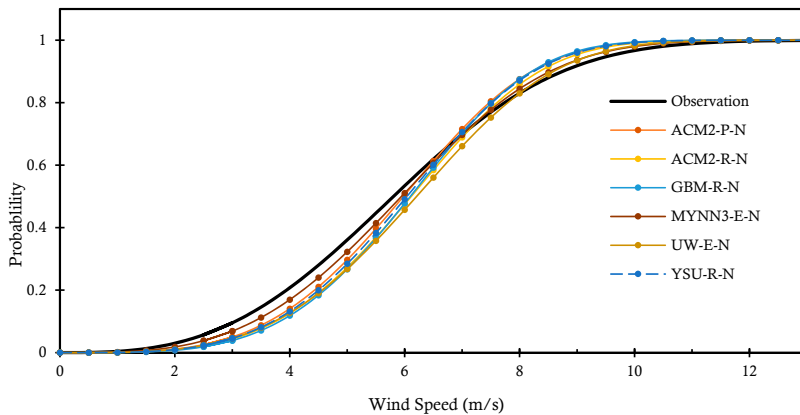


Figure 3. Cumulative probability plots of data for selected options.

Changes in heights of analysis and the simulation grid box sizes did not have significant impacts on most of the above trends either. At the lower heights, the relative performances of the configurations for speed predictions at the lower heights were also largely the same. However, the UW-E-N and GBM-R-N configurations tended to give relatively better mean WPD errors, although the max CDF error of the MYNN3-E-N configuration was still relatively better. In the seasonal analyses, the MYNN3-E-N still tended to give some of the relatively best (if not the best) mean WPD and max CDF error. Data from the 9×9 km² grid produced generally lower average wind speeds and general increase in absolute ME with little impact on the scheme rankings presented earlier. Max CDF errors were also higher when compared to those estimated with data from the 3×3 km² grid. The MYNN3-E-N and UW-E-N configurations still tended to give relatively lower mean WPD errors with the max CDF error of the former better as compared to the other options. Selected results on these analyses are available in Tables A1 and A3 in the Appendix A.

4. Discussion

The performance of PBL and SL schemes differ in different atmospheric stability conditions, which inform the methods used by the schemes [58]. Due to inadequate data, we were not able to assess stability conditions in the study area, and so are unable to assess the performance of the schemes against some of these conditions. However, we find that our observations are consistent with results from several studies. For instance, the YSU scheme was observed to generally predict higher wind speeds than the MYNN3 scheme due to the relatively shallower mixed layer that it simulates [2,3,21]. PBL schemes were found to have more significant impacts on error metrics of surface wind speed hindcasts than other parameterization schemes in studies in similarly coastal terrains [2,22]. Furthermore, the often relatively better ranking of the MYNN3 PBL scheme (over the other local closure schemes) is possible due to it being of a higher order closure. Higher order local (and nonlocal) closure schemes generally yield more accurate results than schemes that employ lower order local closures [4].

The diurnal profiles of average wind speeds for the seasons in the area (shown in Figure 4) are also consistent with what has been reported from other sensitivity studies of PBL schemes in WRF to wind hindcasts in tropical and coastal areas [3,19,21]. Similar peak winds and a relatively high overestimation of winds around and after sunset have been reported for a tropical area. In addition, winds peaking between noon and sunset were also reported in a relatively cooler season in the same area [19]. It was explained that the overestimation of winds after sunset can be attributed to the

inability of the PBL schemes to decouple air near the surface and aloft at night, as a result of differences in vertical mixing strength and entrainment of air above the PBL [3,21].

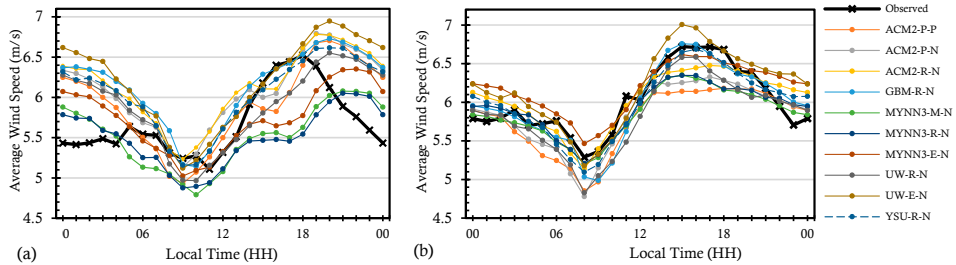


Figure 4. Diurnal variation of average wind speeds for the (a) harmattan season and the (b) rainy season.

The profiles also suggest local winds to be from land-sea circulations. Land and sea breezes result from a convective cycle where warm air over land rises to be replaced by cool sea breezes during the day. The cycle reverses at night as land cools more rapidly than the sea. The Land-sea temperature difference plays a key role in the strength of this cycle, often producing stronger sea breezes (Figure 4), as it is higher during the day [59]. The profiles and reports on the relative predictions of temperature by the Eta and R-MM5 SL scheme also offer possible explanations as to why winds produced by configurations with the Eta scheme are higher than those with the R-MM5. Higher land temperatures during the day should result in higher land-sea temperature differences (as the sea temperature rises at a relatively lower rate) and thus stronger winds [59]. The Eta SL scheme was reported to produce relatively higher temperatures (due to its higher heat fluxes and exchange coefficients) than the R-MM5 [60] (citing [61,62]). The diurnal plots of the average temperature at 2 m (T_2) shown in Figure 5, which are consistent with those reported by [19] and [60] (citing [62–65]), suggests this to be the case in the area. In addition, we see from the profiles for both seasons that the MYNN3-M-N configuration, which often predicted some of the lowest average wind speeds (in both seasons), also recorded some of the lowest T_2 s diurnally. However, despite the relatively higher temperatures in the harmattan season, relatively lower average wind speeds were observed during this season. This is possibly due to a weakening of the breezes by the northeast winds that blow during the harmattan.

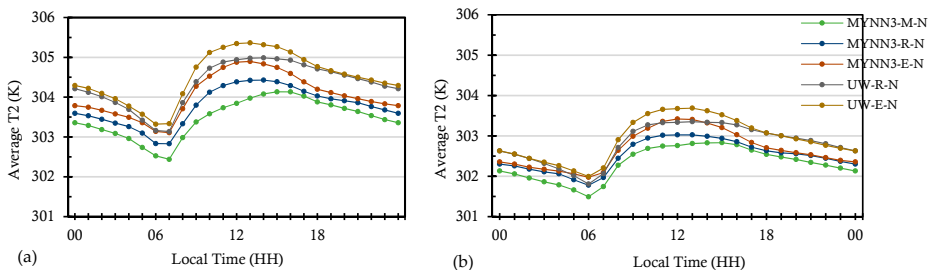


Figure 5. Diurnal variation of selected configurations in (a) harmattan season and (b) rainy season.

5. Summary and Conclusions

Though the Mesoscale Atmospheric Simulation System (MASS) NWP model from the AWS Truewind MesoMap system has been used to assess Ghana's wind resources in the past, it is a proprietary model. In addition, there was a lack of adequate mast measurements at the time limited verifications and adjustments of the model for optimum performance over coastal Ghana [66]. The open source nature and increasing popularity of WRF for similar purposes makes it an attractive alternative for

future assessments. Predictions of surface winds by WRF are sensitive to model options such as physics, simulation grid size, and parameterization of processes at the subgrid scale. In this paper, we tested the sensitivity of wind in coastal Ghana to five planetary boundary layer (PBL) parameterization schemes (selected based on a preliminary study and other studies [17–21,50,67]), paired with different compatible surface layer (SL) schemes [31,48]).

It was found that hindcasts from all 10 PBL-SL pairs generally had speed prediction error metrics within or close to acceptable limits for good performance, as established from other sensitivity studies (RMSE < 2 m/s, ME < 0.5, CC > 0.7 [18,19,55]). However, they differed in their prediction of the mean wind power densities (WPD) and cumulative distribution functions for the period, in consistency and accuracy. Hindcasts with the MYNN3 PBL scheme generally had a relatively better combination of error metrics, and when combined with the Eta SL scheme, it often gave the best or some of the best WPD and maximum errors of CDF. Relative to the other SL schemes, the Eta SL scheme tended to predict relatively higher wind speeds for the same PBL scheme. At lower heights, the UW and GBM PBL schemes (with the Eta and R-MM5 SL schemes, respectively) tended to give better mean WPD errors, but the MYNN3 with the Eta SL scheme still gave better skill scores and max CDF errors. The above trends were also largely observed in the two seasons that pertain along the coast of Ghana with few exceptions. A change in grid resolution was not found to significantly affect the trends in the relative performance of the options.

Though we were not able to assess the performance of the schemes against different atmospheric conditions, several of the trends from our results were found to be consistent with what has been reported by other studies in the literature, based on which we believe our other observations and conclusions are largely credible. Some of such results from other studies include the following: a change in SL scheme did not have significant impacts on most of the error metrics [2,22]; the YSU PBL scheme simulated higher winds than the MYNN3 PBL scheme [2,3,21]; average wind speeds between sunset and sunrise were overpredicted [3,21]; the Eta SL scheme predicted higher T2s than the R-MM5 scheme [60,63]; and no one option was always superior to the others [2,11].

The MYNN3-E-N configuration (as tested in this study with the GFS FNL) is most consistent in predicting with relatively better combined wind speed error metrics and errors of CDF, as well as relatively good mean WPD errors with changing factors (i.e., height, simulation grid box size, and seasons in coastal Ghana). In addition, when predictions from this configuration (MYNN3-E-N) for the study period were compared with monthly average wind speeds for four other locations along the coast of Ghana estimated from [68], results were largely reasonable; average mean error was within 0.5 m/s for the locations (see Table A4 in the Appendix A). Based on this we conclude that the MYNN3-E-N configuration could be considered suitable for wind hindcasts for resource assessments in coastal Ghana.

Author Contributions: Both authors conceived and designed the simulations. D.E.K.D. performed the simulations and analyzed the data. Both authors wrote and revised the manuscript.

Funding: This research was funded by the ENERGY and PETROLEUM (EnPe) Project of the Norwegian Agency for Development Cooperation (Norad).

Acknowledgments: D.E.K.D. acknowledges the PhD scholarship support by the UPERCRET Program in KNUST. The authors also appreciate the constructive criticisms of the three anonymous reviewers, whose comments were of immense help in improving the manuscript.

Conflicts of Interest: The authors declare no conflict of interest.

Table A3. Error metrics skill scores and WPD for PBL-SL pairs for entire study period at 60 m (9 × 9 km² grid).

Observation	Average Wind Speeds (m/s)	ME (m/s)	RMSE (m/s)	STDE (m/s)	CC	Skill Score	k	c	Mean WPD (Wm ⁻²)	WPD Error (%)	Max CDF Error
5.87							2.93	6.58	167		
ACM2-P-P	5.62	-0.25	1.68	1.66	0.66	0.6	3.63	6.38	132	-20.8	0.4392
ACM2-P-N	5.75	-0.12	1.66	1.66	0.66	0.6	3.69	6.38	141	-15.4	0.1537
ACM2-R-N	5.89	0.02	1.64	1.64	0.67	0.9	3.75	6.53	151	-9.7	0.1374
GBM-R-N	5.87	0.00	1.59	1.59	0.69	1.9	3.96	6.49	146	-12.5	0.1027
MYNN3-M-N	5.45	-0.42	1.61	1.56	0.71	3.3	3.47	6.07	123	-26.2	0.7957
MYNN3-R-N	5.50	-0.37	1.58	1.54	0.72	3.8	3.27	6.14	130	-22.2	0.7249
MYNN3-E-N	5.77	-0.10	1.58	1.57	0.72	2.9	3.22	6.45	151	-9.3	0.1606
UW-R-N	5.69	-0.17	1.59	1.58	0.70	2.5	3.61	6.33	138	-17.3	0.2823
UW-E-N	6.05	0.18	1.61	1.60	0.69	2.1	3.66	6.72	165	-1.2	0.4565
YSU-R-N	5.81	-0.06	1.61	1.61	0.68	1.7	3.82	6.43	143	-14.2	0.0372

Table A4. Comparison of monthly average wind speeds at 60 m for other locations in coastal Ghana (observations were estimated from [68]).

	January	February	May	September	Average
SEGE (5.872 °N, 0.345 °E)					
WRF	4.91	5.76	4.86	6.49	5.55
Observations	4.6	5.7	4.1	6.6	5.25
Error	0.31	0.06	0.76	-0.11	0.25
DZITA (5.774 °N, 0.714 °E)					
WRF	4.93	6.05	4.84	6.88	5.68
Observations	5	6.1	4.5	7.3	5.73
Error	-0.07	-0.05	0.34	-0.42	-0.05
MANKOAZE (5.317 °N, 0.70 °W)					
WRF	4.56	5.11	4.24	6.20	5.03
Observations	4.5	5.3	4.5	5.4	4.93
Error	0.06	-0.19	-0.26	0.8	0.1
DENU (6.112 °N, 1.141 °E)					
WRF	5.00	6.01	4.89	6.27	5.54
Observations	4.5	5.5	4	6.2	5.05
Error	0.50	0.51	0.89	0.07	0.49

* WRF speeds are from the MYNN3-E-N hindcasts (on the 9 × 9 km² grid box).

References

1. Skamarock, W.C.; Klemp, J.B.; Dudhia, J.; Gill, D.O.; Barker, D.M.; Wang, W.; Powers, J.G. A Description of the Advanced Research WRF Version 3. *Ncar Tech. Note Ncar/Tn-475+Str* **2008**, 1–113. [[CrossRef](#)]
2. Fernández-González, S.; Martín, M.L.; García-Ortega, E.; Merino, A.; Lorenzana, J.; Sánchez, J.L.; Valero, F.; Sanz Rodrigo, J. Sensitivity Analysis of the WRF Model: Wind-Resource Assessment for Complex Terrain. *J. Appl. Meteorol. Climatol.* **2017**. [[CrossRef](#)]
3. Draxl, C.; Hahmann, A.N.; Peña, A.; Giebel, G. Evaluating winds and vertical wind shear from Weather Research and Forecasting model forecasts using seven planetary boundary layer schemes. *Wind Energy* **2014**, *17*, 39–55. [[CrossRef](#)]
4. Warner, T.T. *Numerical Weather and Climate Prediction*; Cambridge University Press: Cambridge, UK, 2011.
5. Giannaros, C. Sensitivity analysis and optimization of a mesoscale atmospheric model. Ph.D. Thesis, Aristotle University of Thessaloniki, Thessaloniki, Greece, 2018.
6. Stull, R.B. *An Introduction to Boundary Layer Meteorology*; Kluwer Academic Publishers: Dordrecht, The Netherlands, 1988; Volume 13.
7. Wallace, J.M.; Hobbs, P.V. *Atmospheric Science: An introductory Survey*; Elsevier: Amsterdam, The Netherlands, 2006; Volume 92.
8. Boadh, R.; Satyanarayana, A.N.V.; Rama Krishna, T.V.B.P.S.; Madala, S. Sensitivity of PBL schemes of the WRF-ARW model in simulating the boundary layer flow parameters for its application to air pollution dispersion modeling over a tropical station. *Atmósfera* **2016**, *29*, 61–81. [[CrossRef](#)]
9. Jacobson, M.Z. *Fundamentals of Atmospheric Modeling*; Cambridge university press: Cambridge, UK, 2005.
10. Holton, J.R. An Introduction to Dynamic Meteorology. *Am. J. Phys.* **1973**, *41*, 752–754. [[CrossRef](#)]
11. Cohen, A.E.; Cavallo, S.M.; Coniglio, M.C.; Brooks, H.E. A review of planetary boundary layer parameterization schemes and their sensitivity in simulating southeastern US cold season severe weather environments. *Weather Forecast.* **2015**, *30*, 591–612. [[CrossRef](#)]
12. Banks, R.F.; Tiana-Alsina, J.; Baldasano, J.M.; Rocadenbosch, F.; Papayannis, A.; Solomos, S.; Tzanis, C.G. Sensitivity of boundary-layer variables to PBL schemes in the WRF model based on surface meteorological observations, lidar, and radiosondes during the HygrA-CD campaign. *Atmos. Res.* **2016**, *176–177*, 185–201. [[CrossRef](#)]
13. Salby, M.L. *Fundamentals of Atmospheric Physics*; Elsevier Science: London, UK, 1996; Volume 61.
14. Mohammadpour Penchah, M.; Malakooti, H.; Satkin, M. Evaluation of planetary boundary layer simulations for wind resource study in east of Iran. *Renew. Energy* **2017**, *111*, 1–10. [[CrossRef](#)]
15. Bianco, L. Land Surface Processes and their Modeling in WRF. Available online: http://cires1.colorado.edu/science/groups/pielke/classes/at7500/Bianco_SFC.pdf (accessed on 15 June 2019).
16. Jiménez-Esteve, B. *Land Use Influence in WRF Model. A High Resolution Mesoscale Modeling Over Oriental Pyrenees*; Universitat de Barcelona: Barcelona, Spain, 2015.
17. Madala, S.; Satyanarayana, A.N.V.; Srinivas, C.V.; Kumar, M. Mesoscale atmospheric flow-field simulations for air quality modeling over complex terrain region of Ranchi in eastern India using WRF. *Atmos. Environ.* **2015**, *107*, 315–328. [[CrossRef](#)]
18. Mughal, M.O.; Lynch, M.; Yu, F.; McGann, B.; Jeanneret, F.; Sutton, J. Wind modelling, validation and sensitivity study using Weather Research and Forecasting model in complex terrain. *Environ. Model. Softw.* **2017**, *90*, 107–125. [[CrossRef](#)]
19. Gunwani, P.; Mohan, M. Sensitivity of WRF model estimates to various PBL parameterizations in different climatic zones over India. *Atmos. Res.* **2017**, *194*, 43–65. [[CrossRef](#)]
20. Surussavadee, C. Evaluation of WRF near-surface wind simulations in tropics employing different planetary boundary layer schemes. In Proceedings of the 2017 8th International Renewable Energy Congress (IREC), Amman, Jordan, 21–23 March 2017. [[CrossRef](#)]
21. Chadee, X.; Seegobin, N.; Clarke, R. Optimizing the Weather Research and Forecasting (WRF) Model for Mapping the Near-Surface Wind Resources over the Southernmost Caribbean Islands of Trinidad and Tobago. *Energies* **2017**, *10*, 931. [[CrossRef](#)]
22. Santos-Alamillos, F.J.; Pozo-Vázquez, D.; Ruiz-Arias, J.A.; Lara-Fanego, V.; Tovar-Pescador, J. Analysis of WRF Model Wind Estimate Sensitivity to Physics Parameterization Choice and Terrain Representation in Andalusia (Southern Spain). *J. Appl. Meteorol. Climatol.* **2013**, *52*, 1592–1609. [[CrossRef](#)]

23. García-Díez, M.; Fernández, J.; Fita, L.; Yagüe, C. Seasonal dependence of WRF model biases and sensitivity to PBL schemes over Europe. *Q. J. R. Meteorol. Soc.* **2013**, *139*, 501–514. [[CrossRef](#)]
24. Pleim, J.E. A Combined Local and Nonlocal Closure Model for the Atmospheric Boundary Layer. Part I: Model Description and Testing. *J. Appl. Meteorol. Climatol.* **2007**, *46*, 1383–1395. [[CrossRef](#)]
25. Nakanishi, M.; Niino, H. An Improved Mellor–Yamada Level-3 Model with Condensation Physics: Its Design and Verification. *Bound.-Layer Meteorol.* **2004**, *112*, 1–31. [[CrossRef](#)]
26. Park, S.; Bretherton, C.S. The University of Washington Shallow Convection and Moist Turbulence Schemes and Their Impact on Climate Simulations with the Community Atmosphere Model. *J. Clim.* **2009**, *22*, 3449–3469. [[CrossRef](#)]
27. Grenier, H.; Bretherton, C.S. A Moist PBL Parameterization for Large-Scale Models and Its Application to Subtropical Cloud-Topped Marine Boundary Layers. *Mon. Weather Rev.* **2001**, *129*, 357–377. [[CrossRef](#)]
28. Hong, S.-Y.; Noh, Y.; Dudhia, J. A New Vertical Diffusion Package with an Explicit Treatment of Entrainment Processes. *Mon. Weather Rev.* **2006**, *134*, 2318–2341. [[CrossRef](#)]
29. McSweeney, C.; New, M.; Lizcano, G. UNDP Climate Change Country Profiles: Ghana. 2010. Available online: <http://country-profiles.geog.ox.ac.uk/> (accessed on 23 September 2019).
30. Armah, F.A.; Odoi, J.O.; Yengoh, G.T.; Obiri, S.; Yawson, D.O.; Afrifa, E.K. Food security and climate change in drought-sensitive savanna zones of Ghana. *Mitig. Adapt. Strateg. Glob. Chang.* **2011**, *16*, 291–306. [[CrossRef](#)]
31. Wei Wang, C.B.; Duda, M.; Dudhia, J.; Gill, D.; Kavulich, M.; Keene, K.; Chen, M.; Lin, H.; Michalakes, J.; Rizvi, S.; et al. *ARW Version 3 Modeling System User's Guide*; NCAR: Boulder, CO, USA, 2016.
32. Carvalho, D.; Rocha, A.; Gómez-Gesteira, M.; Santos, C. A sensitivity study of the WRF model in wind simulation for an area of high wind energy. *Environ. Model. Softw.* **2012**, *33*, 23–34. [[CrossRef](#)]
33. Giannakopoulou, E.-M.; Nhili, R. WRF Model Methodology for Offshore Wind Energy Applications. *Adv. Meteorol.* **2014**, *2014*, 319819. [[CrossRef](#)]
34. namelist.input: Best Practices. Available online: http://www2.mmm.ucar.edu/wrf/users/namelist_best_prac_wrf.html (accessed on 10 January 2019).
35. National Centers for Environmental Prediction; National Weather Service, NOAA; U.S. Department of Commerce. *NCEP FNL Operational Model Global Tropospheric Analyses, Continuing from July 1999*; Computational and Information Systems Laboratory: Boulder, CO, USA, 19 July 2000; Volume 99. [[CrossRef](#)]
36. Rogers, E.; Black, T.; Ferrier, B.; Lin, Y.; Parrish, D.; DiMego, G. Changes to the NCEP Meso Eta Analysis and Forecast System: Increase in resolution, new cloud microphysics, modified precipitation assimilation, modified 3DVAR analysis. *Nws Tech. Proced. Bull.* **2001**, *488*, 15.
37. Iacono, M.J.; Mlawer, E.J.; Clough, S.A.; Morcrette, J.J. Impact of an improved longwave radiation model, RRTM, on the energy budget and thermodynamic properties of the NCAR community climate model, CCM3. *J. Geophys. Res. Atmos.* **2000**, *105*, 14873–14890. [[CrossRef](#)]
38. Dudhia, J. Numerical study of convection observed during the winter monsoon experiment using a mesoscale two-dimensional model. *J. Atmos. Sci.* **1989**, *46*, 3077–3107. [[CrossRef](#)]
39. Pleim, J.E. A Simple, Efficient Solution of Flux–Profile Relationships in the Atmospheric Surface Layer. *J. Appl. Meteorol. Climatol.* **2006**, *45*, 341–347. [[CrossRef](#)]
40. Jiménez, P.A.; Dudhia, J.; González-Rouco, J.F.; Navarro, J.; Montávez, J.P.; García-Bustamante, E. A revised scheme for the WRF surface layer formulation. *Mon. Weather Rev.* **2012**, *140*, 898–918. [[CrossRef](#)]
41. Janjić, Z.I. *Nonsingular Implementation of the Mellor–Yamada Level 2.5 Scheme in the NCEP Meso Model*; NOAA: Silver Spring, MD, USA, 2002.
42. Janjić, Z. *The Surface Layer in the NCEP Eta Model, Paper Presented at 11th Conference on Numerical Weather Prediction*; American Meteorological Society: Norfolk, VA, USA, 1996.
43. Janjić, Z.I. The Step-Mountain Eta Coordinate Model: Further Developments of the Convection, Viscous Sublayer, and Turbulence Closure Schemes. *Mon. Weather Rev.* **1994**, *122*, 927–945. [[CrossRef](#)]
44. Mukul Tewari, N.; Tewari, M.; Chen, F.; Wang, W.; Dudhia, J.; LeMone, M.; Mitchell, K.; Ek, M.; Gayno, G.; Wegiel, J. Implementation and verification of the unified NOAA land surface model in the WRF model (Formerly Paper Number 17.5). In *Proceedings of the 20th Conference on Weather Analysis and Forecasting/16th Conference on Numerical Weather Prediction*, Seattle, WA, USA, 14 January 2004; pp. 11–15.
45. Xiu, A.; Pleim, J.E. Development of a land surface model. Part I: Application in a mesoscale meteorological model. *J. Appl. Meteorol.* **2001**, *40*, 192–209. [[CrossRef](#)]

46. Pleim, J.E.; Xiu, A. Development and testing of a surface flux and planetary boundary layer model for application in mesoscale models. *J. Appl. Meteorol.* **1995**, *34*, 16–32. [[CrossRef](#)]
47. Kain, J.S. The Kain–Fritsch convective parameterization: An update. *J. Appl. Meteorol.* **2004**, *43*, 170–181. [[CrossRef](#)]
48. Dudhia, J. Overview of WRF Physics. Available online: <https://www.climate-science.org.au/sites/default/files/physics-3.9-new-pt1.pdf> (accessed on 23 May 2019).
49. Dzebre, D.E.K.; Acheampong, A.A.; Ampofo, J.; Adaramola, M.S. A sensitivity study of Surface Wind simulations over Coastal Ghana to selected Time Control and Nudging options in the Weather Research and Forecasting Model. *Heliyon* **2019**, *5*, e01385. [[CrossRef](#)] [[PubMed](#)]
50. Dzebre, D.E.K.; Adaramola, M.S. A preliminary sensitivity study of Planetary Boundary Layer parameterisation schemes in the weather research and forecasting model to surface winds in coastal Ghana. *Renew. Energy* **2020**, *146*, 66–86. [[CrossRef](#)]
51. Pleim, J.; Gilliam, R. Description and Procedures for using the Pleim–Xiu LSM, ACM2 PBL and Pleim Surface Layer Scheme in WRF. Available online: <http://www2.mmm.ucar.edu/wrf/users/docs/PX-ACM.pdf> (accessed on 2 March 2018).
52. Ohsawa, T.; Kato, M.; Uede, H.; Shimada, S.; Takeyama, Y.; Ishihara, T. Investigation of WRF configuration for offshore wind resource maps in Japan. In Proceedings of the Wind Europe Summit, Hamburg Messe, Hamburg, Germany, 27–29 September 2016; pp. 26–30.
53. Misaki, T.; Ohsawa, T.; Konagaya, M.; Shimada, S.; Takeyama, Y.; Nakamura, S. Accuracy Comparison of Coastal Wind Speeds between WRF Simulations Using Different Input Datasets in Japan. *Energies* **2019**, *12*, 2754. [[CrossRef](#)]
54. Deserno, M. Linear and Logarithmic Interpolation. Available online: https://www.cmu.edu/biolphys/deserno/pdf/log_interpol.pdf (accessed on 20 November 2018).
55. Emery, C.; Tai, E.; Yarwood, G. *Enhanced Meteorological Modeling and Performance Evaluation for Two Texas Ozone Episodes*; ENVIRON: Washington, DC, USA, 2001.
56. Kang, D.; Ko, K.; Huh, J. Comparative Study of Different Methods for Estimating Weibull Parameters: A Case Study on Jeju Island, South Korea. *Energies* **2018**, *11*, 356. [[CrossRef](#)]
57. Carrillo, C.; Cidrás, J.; Díaz-Dorado, E.; Obando-Montaño, A. An approach to determine the Weibull parameters for wind energy analysis: The case of Galicia (Spain). *Energies* **2014**, *7*, 2676–2700. [[CrossRef](#)]
58. Burlando, M.; Georgieva, E.; Ratto, C.F. Parameterisation of the Planetary Boundary Layer for Diagnostic Wind Models. *Bound.-Layer Meteorol.* **2007**, *125*, 389–397. [[CrossRef](#)]
59. Pokhrel, R.; Lee, H. Estimation of the effective zone of sea/land breeze in a coastal area. *Atmos. Pollut. Res.* **2011**, *2*, 106–115. [[CrossRef](#)]
60. Giannaros, C.; Melas, D.; Giannaros, T.M. On the short-term simulation of heat waves in the Southeast Mediterranean: Sensitivity of the WRF model to various physics schemes. *Atmos. Res.* **2019**, *218*, 99–116. [[CrossRef](#)]
61. Shin, H.H.; Hong, S.-Y. Intercomparison of Planetary Boundary-Layer Parametrizations in the WRF Model for a Single Day from CASES-99. *Bound.-Layer Meteorol.* **2011**, *139*, 261–281. [[CrossRef](#)]
62. Xie, B.; Fung, J.C.H.; Chan, A.; Lau, A. Evaluation of nonlocal and local planetary boundary layer schemes in the WRF model. *J. Geophys. Res. Atmos.* **2012**, *117*. [[CrossRef](#)]
63. Hari Prasad, K.B.R.R.; Srinivas, C.V.; Singh, A.B.; Vijaya Bhaskara Rao, S.; Baskaran, R.; Venkatraman, B. Numerical simulation and intercomparison of boundary layer structure with different PBL schemes in WRF using experimental observations at a tropical site. *Atmos. Res.* **2014**, *145–146*, 27–44. [[CrossRef](#)]
64. Hari Prasad, K.B.R.R.; Venkata Srinivas, C.; Venkateswara Naidu, C.; Baskaran, R.; Venkatraman, B. Assessment of surface layer parameterizations in ARW using micro-meteorological observations from a tropical station. *Meteorol. Appl.* **2016**, *23*, 191–208. [[CrossRef](#)]
65. Sathyanadh, A.; Prabha, T.V.; Balaji, B.; Resmi, E.A.; Karipot, A. Evaluation of WRF PBL parameterization schemes against direct observations during a dry event over the Ganges valley. *Atmos. Res.* **2017**, *193*, 125–141. [[CrossRef](#)]
66. National Renewable Energy Laboratory (NREL). *Ghana Wind Energy Resource Mapping Activity*; NREL: Golden, CO, USA, 2004.

67. Surussavadee, C.; Wu, W. Evaluation of WRF planetary boundary layer schemes for high-resolution wind simulations in Northeastern Thailand. In Proceedings of the 2015 IEEE International Geoscience and Remote Sensing Symposium (IGARSS), Milan, Italy, 26–31 July 2015; pp. 3949–3952. [[CrossRef](#)]
68. Energy Commission of Ghana. Summary Results Of Wind Energy Resource Assessment At 8 Locations Along The Coast Of Ghana Conducted By The Energy Commission Under GEDAP/MoEP. Available online: <http://bit.do/e3WA4> (accessed on 5 August 2019).



© 2019 by the authors. Licensee MDPI, Basel, Switzerland. This article is an open access article distributed under the terms and conditions of the Creative Commons Attribution (CC BY) license (<http://creativecommons.org/licenses/by/4.0/>).

Paper IV

Impacts of selected Meteorological and Land Cover Datasets on dynamically Downscaled wind speeds for a coastal area using the Weather Research and Forecasting Model

Denis E. K. Dzebre^{a,b,c}, and Muiyiwa S. Adaramola^a

^a Faculty of Environmental Sciences and Natural Resources, Norwegian University of Life Sciences, Ås, Norway.

^b Department of Mechanical Engineering, Kwame Nkrumah University of Science and Technology, Kumasi, Ghana.

^c The Brew-Hammond Energy Centre, Kwame Nkrumah University of Science and Technology, Kumasi, Ghana.

Abstract

Analysis, reanalysis and Land Use and Land Cover (LULC) datasets serve as sources of initial and boundary conditions, as well as surface properties data required for simulations in the Weather Research and Forecasting model (WRF). The accuracy of these datasets is among factors that significantly impact the prediction of surface winds in WRF. In this study, we examine sensitivity of surface wind and wind energy potential estimates in an area in coastal Ghana to five analysis and reanalysis datasets, as well as the two global LUCL datasets currently found in the static datasets of WRF. In contrast to the LULCs tested, model estimates were significantly impacted by the different analysis or reanalysis datasets. For the same type of reanalysis datasets, those prepared with higher resolution forecasts combined with more advanced data assimilation techniques produced better estimates, and vice versa. The Atmosphere–Ocean–Sea Ice–Land NCEP CFSv2 Reanalysis generally gave higher predictions of wind speeds and the best predictions of wind energy. However, the JMA JRA-55 Reanalysis data, and the NCEP GFS Analysis data, also had good impacts on model performance and are recommended as alternatives or complements to the NCEP CFSv2 for wind simulations in the study area.

Keywords:

Weather research and forecasting model (WRF), Wind resource assessment, Analysis and reanalysis, Land use and land cover

1 Introduction

Assessments of the wind resources, key to commercial development of wind power, have traditionally been done with data from mast mounted instruments, and in recent times, remote sensors such as Light Detection and Ranging (LIDAR) and Sound Detection and Ranging (SODAR). However, owing to the time consuming and the expensive nature of measuring campaigns with these instruments, Numerical Weather Prediction (NWP) models, such as the Weather Research and Forecasting model (WRF) model, are now being used to downscale meteorological datasets for the preliminary assessments. In a process referred to as dynamical downscaling, these models modify initial conditions (from the meteorological datasets) to predict time varying atmospheric data at each point on a simulation grid, to generate data at desired spatial and temporal resolutions [1, 2]. The process takes into account the land cover and topographical properties of the area for which the data is desired, in addition to other things [3, 4]. The land cover and topographical properties serve as inputs in the calculation of heat and energy fluxes which affect turbulence in the atmosphere [3]. Turbulence acts as a feedback mechanism in wind circulation [5]. Therefore, in addition to other factors (such as the parameterisation of the processes occurring on the sub-grid scale and model resolution), the accuracy of the surface properties, and the meteorological (initialisation) datasets for downscaling, significantly impact the quality of the generated data [5-11]. This paper focuses on the impact selected meteorological and land cover datasets on the accuracy of wind that is downscaled (wind hindcasts) using the WRF model.

For wind hindcasts in the WRF model, Analysis and Reanalysis datasets often serve as sources of initial and boundary conditions. They are produced via data assimilation, a process that uses observations and model-based forecasts to estimate atmospheric conditions and produce a gridded set of model dependent variables that are consistent with both the model dynamics and the information from the observations. The process involves the provision of a forecast of the atmosphere, which is updated in light of observations [2, 12]. Reanalysis datasets are produced with a frozen system (forecast models and data assimilation methods) that remains unchanged over the temporal coverage (or range) of the dataset. The systems for producing Analysis datasets on the other hand benefit from model updates and upgrades over time [2, 4, 13-16]. In addition, unlike Analysis datasets, Reanalysis datasets comprise data from a Retrospective Analysis; the process of assimilating data for past periods, using a current model and all available data for those periods, to produce a long-term, model-consistent dataset [12].

Due to differences in the (capabilities of the) forecast models and data assimilation techniques, as well as the amount and quality of the raw observational data that are used in their production, analysis and reanalysis datasets tend to vary in quality (accuracy when compared to observations). For instance, based on the incremental advancement of reanalysis techniques, datasets can be classified as first, second and third generation datasets; each new generation employing data assimilation techniques that offer improvements over the previous generation's techniques [13]. In addition to the data assimilation techniques, the forecast models, can also have an impact on quality of the datasets. The forecast models, which in the case of global datasets are often spectral Atmospheric General Circulation Models (AGCMs), are basically NWP models that are formulated with the spectral method, as opposed to finite difference method used in finite-grid

AGCMs. A key advantage of the spectral method (which might explain its wide use in global forecast models) is that, it is comparatively less computationally expensive [17]. Differences in the methods and how they impact model formulation and performance are explained in texts such as [17]. The resolution of spectral models is governed by a wavenumber of truncation [17]. Higher wavenumbers mean higher resolutions (and often better datasets as model resolution significantly impact forecasts from NWP models), but at increased computational cost. In addition, parameterisation techniques (for approximating atmospheric processes occurring at sub-grid scale or are not fully understood) in these models affects their performance, and often varies among models. Lastly, the quality of the datasets might also be affected by the raw observational data that are used in their production. Sources of the observational data include radiosonde, satellite, buoy, aircraft among others. Changes in observation locations and observation platforms, as well as periodic data voids, sometimes throughout entire nations or regions for varying reasons, results in an inherent lack of uniformity in the quality of the raw data available [2, 13, 14]. These factors introduce unavoidable differences in the quality of initialisation datasets and their impacts on the results of the downscaling process [2, 13, 17].

In producing wind hindcasts, Planetary Boundary Layer (PBL) parameterisation schemes in the WRF model need moisture and heat fluxes at the lower levels of the atmosphere. These fluxes are essential for better simulations of surface winds by NWPs [5]. Surface terrain parameters, such as surface roughness length, albedo, moisture, and emissivity, among others, serve as inputs in the estimation of these fluxes. They are calculated by the surface layer parameterization schemes in the WRF model, based on tabulated values associated with different Land Use And Land Cover (LULC) category datasets [6]. LULC datasets are prepared by classifying raw satellite data into categories based on the satellite imagery [18] and serve as sources of surface properties in WRF simulations.

Owing to the different levels of impact on WRF predictions of surface winds for different areas, as has been realised from several studies on in open literature [4, 6, 8-10, 19-21], and also that analysis and reanalysis datasets are sometimes “tuned” for different objectives, making their performance dependent on their intended use [16], a sensitivity analysis of available datasets might be necessary to determine the best dataset(s) to use for simulations for an application in an area.

Against this background, in this paper, we assess the impact of selected initialisation and LULC datasets to surface wind speed and energy predictions by WRF, for an area in coastal Ghana. We aim to identify that might correlate well with accuracy of the hindcasts (when compared to observations) in order to suggest guidelines for their selection for generating wind hindcasts in the area (and probably the west African sub-region). In addition, we aim to recommend dataset(s) for generating wind hindcasts with the WRF model for resource assessments in coastal Ghana. The rest of the paper is organised as follows; Section 2 covers the study area, verification data, selected details of the datasets tested and the experimental design. Section 3 is on the results and discussions and section 4, the conclusions drawn from the results.

2 Data and Methods

2.1 Study Area and Measured Data

The study area covers the coastal plains of south east Ghana. The measured wind data for this study was measured on a mast (location: 5.786 °N, 0.918 °E) used in a wind measurement campaign by the Energy Commission of Ghana. The data comprises wind speeds measured at heights of 40, 50, and 60 m above ground level. The area experiences two main seasons in a year; a Harmattan season that is dominated by dry and dusty desert winds from the North-East, lasting till around February, and a bimodal Rainy season dominated by Monsoon winds ends around November [22].

2.2 Model Configuration

The Advanced Research WRF (ARW) 3.8.1 is used for this study. Key features of the model include a Eulerian mass solver, a terrain following vertical coordinate and staggered horizontal grid system. A detailed description of the model physics, equations and dynamics is available [23]. The model configuration, summarized in Table 1 is the same as that used in an earlier study in the area [24].

Table 1: Model Configuration

Model Version	Advanced Research WRF v3.8.1			
Initial and boundary conditions	a) NCEP GFS-FNL b) NCEP CFSv2 c) ECWMF ERA-Interim d) JMA JRA-55 e) NCEP/DOE R2			
Topographical data	USGS GMTED2010			
Land Use data	a) USGS with lakes b) MODIS with lakes			
Vertical Resolution	40 vertical levels (automatically set)			
Domains	d01	d02	d03	d04
Horizontal resolution (km)	81	27	9	3
Domain size (grid points)	74 x 77	100 x 103	103 x 103	55 x 55
Parameterisation Schemes:	Same as was used by [24]			

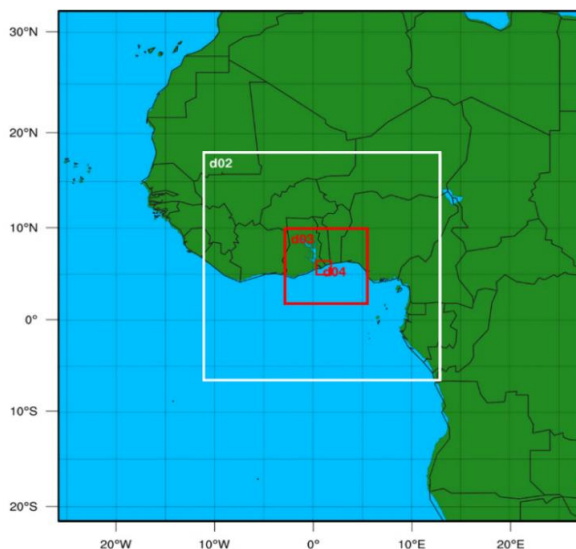


Figure 1: Simulation domains.

The two global LULC datasets available in the WRF Static data [25] were tested. These are the United States Geological Survey (USGS), and the IGBP-Modified Moderate Resolution Imaging

Spectroradiometer (MODIS) LULC datasets. The USGS dataset takes its primary inputs from composite images from the Advanced Very High-Resolution Radiometer (AVHRR) satellite, sourced from April 1992 to March 1993 [7]. It has 24 land cover categories, classified according to the Normalised Difference Vegetation Index (NDVI) [7]. The MODIS LULC on the other hand is derived from data from the Terra/Aqua Earth Observation System satellites, and has 20 land cover classes, as defined by the International Geosphere Biosphere Program (IGBP) [7]. Both LULC datasets were tested in combination with the special land cover dataset in the WRF model that distinguishes between oceans and inland water bodies (lakes) [26, 27]. Plots of both LULC categories from both datasets (for simulation domain 2) are shown in Figure 2. The MODIS LULC plot has been reclassified to USGS according to [7] for easy comparison.

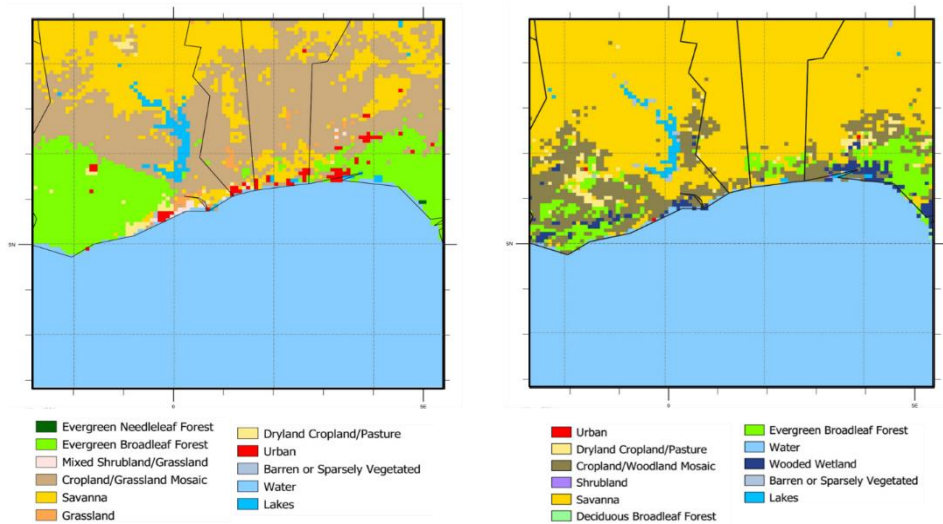


Figure 2: Plot of the MODIS (left) and USGS (right) LULC in the Second Domain.

Five Gridded Binary (GRIB) meteorological datasets from the Research Data Archive (RDA) of the National Centre of Atmospheric Research (NCAR) [28] were tested. These are;

- i. The 1 degree NCEP Final Analysis (NCEP GFS-FNL) [29].
- ii. The NCEP Climate Forecast System Version 2 (NCEP-CFSv2) [30].
- iii. The ECMWF ERA Interim [31].
- iv. The Japan Meteorological Agency JRA-55 Reanalysis (JMA JRA-55) [32].
- v. The NCEP/DOE R2 [33].

Selected characteristics of the meteorological datasets (as tested) are summarised in Table 2. Other datasets were not tested because they did not cover the period for which we had observational data for verification (2013) or have been improved upon by one of the five tested. The latter was the case with the NCEP/NCAR R1.

Table 2: Selected specifications of initialisation datasets tested [15, 29-38].

Dataset	Data Type	AGCM Model Resolution	Data Assimilation Technique	Resolution tested (lon. x lat. x pressure levels)
NCEP GFS-FNL	Analysis	T574/T190, L64	Hybrid 3DVAR *	1 x 1 x 26
NCEP CFSv2	Reanalysis	T126, L64 0.266 hPa top	3DVAR	0.5 x 0.5 x 37
ECMWF ERA-I	Reanalysis	T255, L60 0.1 hPa top	4DVAR	0.703 x ~0.702 x 37
JMA JRA-55	Reanalysis	T319, L60 0.1 hPa top	4DVAR	1.25 x 1.25 x 37
NCEP/DOE R2	Reanalysis	T62, L28 3 hPa top	3DVAR	2.5 x 2.5 x 18

* as at 2012 [35]

Experimental Design

Ten experiments, each involving two simulations; one each, for the months of February and September 2013, were conducted. These months were chosen because of their relatively high monthly average wind speeds in the seasons in the study area. It was hoped that by selecting these months, seasonal variations of winds could be accounted for in the study. A similar approach has been used in past sensitivity studies [39, 40]. Possible interactions between LULC and initialisation datasets were explored by using a different combination of LULC and initialisation dataset in each experiment. Details of the dataset combinations are presented in Table 3. Initial runs with the JMA JRA-55 dataset were not successful (as a result of unsuccessful pre-processing of soil data that is needed by the Noah LSM, which was used in the configuration for this study). Therefore, the JRA-55 dataset was complemented with soil data from the GFS-FNL dataset for both JRA-55 experiments. Following practices of past studies in the area [24, 41, 42], a spin-up time of 12 hours was used for each simulation. To save on computational power, the nudging technique in the WRF model's Four Dimensional Data Assimilation (FDDA) System was applied in each simulation with a simulation run time of 30 days as recommended in a previous study in the area [24]. All the experiments except for the R2 experiments were run with the three inner domains (d02, d03, and d04). Due to the larger spatial resolution the R2 dataset, domain d01 was used in addition to the inner 3 in the R2 experiments.

Table 3: Experimental Design

No.	Experiment Name	Initialisation Data	LULC Data	Domains Used
1	USGS_CFSv2	NCEP CFSv2	USGS	d02, d03, d04
2	MODIS_CFSv2	NCEP CFSv2	MODIS	d02, d03, d04
3	USGS_FNL	NCEP GFS FNL	USGS	d02, d03, d04
4	MODIS_FNL	NCEP GFS FNL	MODIS	d02, d03, d04
5	USGS_ERA-I	ECWMF ERA-Interim	USGS	d02, d03, d04
6	MODIS_ERA-I	ECWMF ERA-Interim	MODIS	d02, d03, d04
7	USGS_JRA-55	JMA JRA-55	USGS	d02, d03, d04
8	MODIS_JRA-55	JMA JRA-55	MODIS	d02, d03, d04
9	USGS_R2	NCEP/DOE R2	USGS	d01, d02, d03, d04
10	MODIS_R2	NCEP/DOE R2	MODIS	d01, d02, d03, d04

2.5 Evaluation

Evaluation of predictions followed the same procedures as has been used in previous studies in the area [41]. Predictions were assessed with the Root Mean Square Error (RMSE), Mean Error (ME), Standard Deviation of the Error (STDE) and a Correlation Coefficient (CC) which were combined into a Skill Score as was done in previous studies [24]. Calculation of each metric followed the procedures used in previous

studies in the study area [24]. The error metrics were also compared to performance benchmarks as had been used in a previous study in the study area.

The Weibull cumulative distributions and mean wind power densities estimated with data from the experiments and observations were also compared as has been done in previous studies. Weibull parameters, and other metrics of comparison (Maximum absolute Cumulative Density Function Error, and Mean Wind Power Density Error as explained in [41]) were calculated with the same formulations from [41]. However, in this study, the Empirical, and the Power Density methods were used since they compared closely in an evaluation with observational covering the study period. Formulations for the two methods were from [43].

3. Results and Discussion

Averages of observed and downscaled wind speeds, and evaluation metrics at 60 m for the study period are presented in Table 4. It can be seen from the Table that, even though the MODIS LULC often gave better metrics, its values did not differ greatly from those of the USGS LULC, irrespective of meteorological dataset it was paired with. However, average wind speeds and error metrics differed significantly for the different meteorological datasets. Most of the meteorological datasets met most of the RMSE and CC benchmarks for performance (i.e. $RMSE < m/s$, $CC \geq 0.7$). However, the CC of the CFSv2 was less than the benchmark, and all the metrics of the NCEP/DOE R2 did not meet any of the benchmarks. None of the datasets met the benchmark for ME. However, the JMA JRA-55 had the relatively least absolute ME. While the CC of NCEP GFS FNL was best. JMA JRA-55 had the best combination of metrics followed by the NCEP GFS FNL, then the ECWMF ERA-I. The NCEP/DOE R2 had the relatively worst combination of metrics.

Table 4: Average predictions and Statistical Metrics at 60 m for the entire study period.

Experiment	Average Wind Speeds (m/s)	RMSE (m/s)	STDE (m/s)	CC	ME (m/s)	Speed Prediction Skill Score
Observation	6.89					
USGS_FNL	5.94	1.52	1.19	0.8	-0.9	3.4
MODIS_FNL	6.00	1.49	1.20	0.8	-0.9	3.5
USGS_CFSv2	6.10	1.65	1.45	0.6	-0.8	2.5
MODIS_CFSv2	6.11	1.64	1.45	0.6	-0.8	2.5
USGS_ERA-I	5.74	1.77	1.34	0.7	-1.2	2.3
MODIS_ERA-I	5.82	1.68	1.29	0.7	-1.1	2.7
USGS_JRA-55	6.22	1.46	1.30	0.7	-0.7	3.5
MODIS_JRA-55	6.26	1.43	1.28	0.7	-0.6	3.7
USGS_R2	5.54	2.18	1.71	0.5	-1.4	0.1
MODIS_R2	5.65	2.15	1.76	0.5	-1.2	0.2

Similar trends were observed on the Mean WPD, as well as the Mean WPD and Max CDF Errors as well, as can be seen in Table 5. Though the MODIS LULC generally had lower errors, it was often not more than 2 points better than the USGS LULC. The JMA JRA-55 again had the relatively best predictions of Mean WPD, Max CDF Error while the NCEP/DOE R2 had the relatively worst. However, these estimates for the CFSv2 were better than those for the NCEP-GFS FNL and ERA-I datasets. These trends were not affected by the methods we used in computing the Weibull parameters. However, errors were slightly smaller

when the Power Density Method was used. Significant differences were not observed in the above trends in similar analyses at 50 m and 40 m (see Tables in appendix). A repeat of the analysis with data from the 9 km resolution domain did not change trends observed in the earlier analysis. Error margins in the two LUCL datasets were greater. But the MODIS LULC still had better impacts than the USGS LULC.

Table 5: Weibull parameters, Mean WPD Error, and Max CDF Error calculated with Empirical and Power Density Methods.

	Empirical Method					Power Density Method				
	c	k	Mean WPD	Mean WPD Error (%)	Max CDF Error	c	k	Mean WPD	Mean WPD Error (%)	Max CDF Error
Observation	7.6	4.2	230			7.6	4.1	233		
USGS_FNL	6.5	4.7	143	-38.1	0.25	6.5	4.2	148	-36.5	0.22
MODIS_FNL	6.6	4.8	147	-36.3	0.23	6.6	4.2	152	-34.6	0.21
USGS_CFSv2	6.7	4.7	154	-33.1	0.21	6.7	4.2	160	-31.3	0.18
MODIS_CFSv2	6.7	4.9	153	-33.4	0.22	6.7	4.2	160	-31.2	0.18
USGS_ERA-I	6.3	4.2	133	-42.3	0.28	6.3	4.1	134	-42.3	0.27
MODIS_ERA-I	6.4	4.3	138	-40.1	0.26	6.4	4.1	140	-40.0	0.25
USGS_JRA-55	6.9	4.1	171	-25.9	0.15	6.9	4.0	172	-26.2	0.15
MODIS_JRA-55	6.9	4.2	173	-24.9	0.15	6.9	4.0	175	-25.1	0.14
USGS_R2	6.2	3.5	128	-44.5	0.29	6.1	3.9	123	-47.2	0.30
MODIS_R2	6.3	3.5	136	-41.0	0.27	6.2	3.9	131	-44.0	0.28

4. Discussion

The quality downscaled data depends on a combination of several factors such as the quality of the input datasets (which are in turn affected by factors discussed earlier), the capabilities of the downscaling model itself which also depends on several other factors. It will be difficult to satisfactorily explain trends in our results without considering all these factors and how they interact with each other to affect the final downscaled data. Nonetheless, some of the trends in the comparisons of the initialisation datasets can be explained to some extent.

The meteorological datasets can be classified according to some key characteristics, which include; the type of dataset (whether analysis or reanalysis), the data assimilation technique that was used in the (analysis/reanalysis) process, the type of AGCM and the resolution at which it produced the forecasts for the (analysis/reanalysis) process, and the final resolution of the datasets from this process. These characteristics are summarised for each meteorological dataset tested, in Table 2. In terms of data assimilation techniques, the ECMWF ERA-I and JMA JRA-55 can be classified as third-generation Reanalyses, with the NCEP R2, a first generation Reanalysis, as explained by [13]. The NCEP GFS-FNL is an analysis dataset, and the NCEP CFSv2 differs from all the other datasets tested here, in that it is a Coupled Reanalysis, as it utilises forecasts from a Coupled Forecast Model (a coupled atmosphere–ocean–sea ice–land model to better account for ocean interactions) in its forecasts [13, 44].

The mathematical concepts and basis for various approaches to data assimilation (which have evolved over the years), are described in texts such as [2, 45]. A major improvement to the data assimilation process was achieved with the variational 3DVAR method which enabled the use of worldwide observations [2, 46]. However, limitations of 3DVAR data assimilation include its inability to use asynoptic data (data measured at times either than the synoptic hours of 00, 06, 12 and 18 UTC) and account for the time-evolution of the errors associated with data [45, 47, 48]. The 4DVAR method accounts for this to some extent with a

linear forecast model to account for the evolution of perturbations in the atmospheric state, representing and calculating the time-evolution of errors from the forecast and observational data, albeit at extra computational cost [45, 48, 49]. The Hybrid (Variational–Ensemble) data assimilation technique combines the variational data assimilation with another technique; the Ensemble Kalman Filter (EnKF) technique. The Ensemble Kalman Filter (EnKF) technique (like the 4DVAR,) accounts for time-evolution errors by deriving error estimates from nonlinear short-range forecasts from an ensemble prediction system (EPS) [48, 49]. The Hybrid data assimilation technique has been found to sometimes offer comparatively better performance over the pure variational and pure ensemble techniques in both 3DVAR and 4DVAR modes [49, 50].

Generally, better data assimilation techniques (used for the latter generation datasets) and higher resolutions of the forecasts by the AGCM models, should produce better analysis/reanalysis products (datasets) [13, 17]. Our results suggest that, the relative performances are probably significantly impacted by the forecast resolutions and data assimilation techniques employed in their production.

This will explain the relative worse quality of the of the R2 Reanalysis as compared to all the other datasets, as they both use AGCM forecasts of relatively better resolution and relatively better data assimilation techniques in their reanalysis process (See Table 2). The NCEP GFS-FNL’s forecast model (the Global Forecast System (GFS)) and data assimilation systems (the Global Data Assimilation System (GDAS)) have, and continue to benefit from updates since its introduction [35], hence it is an analysis dataset. In May 2012, the GDAS started employing the Hybrid 3D-VAR technique and the GFS resolution was T574/T190L64 (depending on forecast time) [35]. As has been noted by [49, 50], the Hybrid 3DVAR technique sometimes produces better results than more sophisticated assimilation techniques. This, with its higher resolution model forecasts, is probably responsible to some extent, for its relatively better prediction metrics. Atmospheric forecast models use somewhat simplified physics representations compared with the physics representations of Coupled Forecast Models[2]. Giving that the study area is near the coast with possible ocean influences on local winds (land and sea breezes), the possible influence of the coupled model forecasts (even though are of a relatively coarse resolution) cannot be ruled out on the quality of the CFSv2 dataset.

The results did not suggest a trend in the impact of the spatial resolution of the produced datasets (as downloaded) on the quality of the data downscaled from them, as the JMA-55 is of a relatively lower (worse) resolution than the CFSv2, ERA-I and GFS-FNL datasets, yet it seems to outperform them.

4 Summary and Conclusion

Land Use and Land Cover (LULC) and meteorological datasets have been reported to have varying impacts on the quality of dynamically downscaled wind data by the WRF model worldwide [4, 6, 8-10, 19-21]. Against this background, this study sought to recommend LULC and GriB formatted meteorological datasets data from the options available at [25] and [28] respectively on wind speeds downscaled with the WRF model for a coastal area in Ghana. The study also sought to identify characteristics of the meteorological datasets that often correlated well with good hindcasts to inform choices in future

downscaling exercises or studies Two LULC datasets and five meteorological datasets were tested in 10 dynamical downscaling experiments.

Results confirm that, the accuracy of the downscaled data depends on the meteorological datasets that are downscaled [5, 9, 11]. In addition, results also confirm that when newer generation reanalysis meteorological datasets are downscaled, the end products are better (in terms of all the evaluation criteria considered in this study) than older generation ones [13, 21]. Among the meteorological datasets tested, the JMA JRA-55 gave the best combination of error metrics, Mean Wind Power Density and Cumulative Density Function error. Though the CFSv2 gave the next best WPD and Cumulative Density Errors, its combination of wind speed error metrics was not as good as that of the GFS FNL dataset. In addition, the GFS FNL had the relatively best CC of all the datasets tested. The first generation NCEP R2 reanalysis was the worst of the meteorological datasets tested. On the LULC datasets, results indicate the MODIS LULC gave the relatively better combination of error metrics as well as Mean WPD and CDF Errors when compared to the USGS LULC, though the difference between the metrics of the two were not so different. Trends were not significantly affected by a change in the grid size or the method of estimating the Weibull parameters for Power Density estimations.

From our results we conclude that tests of different meteorological datasets are necessary to determine the best one to downscale for wind data for different areas and periods. For areas in coastal Ghana (and perhaps the west African sub region), where the meteorological datasets are of the same type, the resolution of the global model forecasts and the data assimilation techniques used in their preparation can be used as criteria select candidate options for testing. Based on the current results, we conclude that the JMA JRA-55 probably gives the best downscaled wind data for this area in coastal Ghana. However, all the other meteorological datasets except the NCEP R2 are worth considering in future tests and downscaling activities.

Annex

Average predictions, error metrics at 40 m and 50 m. Weibull parameters are calculated with the Empirical method

	40 m										
	50 m					40 m					
	Average Wind Speeds (m/s)	ME (m/s)	RMSE (m/s)	STDE (m/s)	CC	Skill Score	c	k	Mean WPD (Wm ⁻²)	WPD Error (%)	Max CDF Error
Observation	6.79								220	0	0
USGS_FNL	5.87	1.49	1.17	0.8	-0.92	3.4	7.5	4.2	137	-37.9	0.25
MODIS_FNL	5.93	1.47	1.19	0.8	-0.86	3.5	6.4	4.8	141	-35.9	0.24
USGS_CFSv2	5.97	1.68	1.46	0.6	-0.83	2.2	6.5	4.7	144	-34.5	0.22
MODIS_CFSv2	5.97	1.68	1.46	0.6	-0.82	2.1	6.5	4.9	143	-35.1	0.23
USGS_ERA-I	5.69	1.73	1.32	0.7	-1.11	2.3	6.3	4.2	129	-41.5	0.27
MODIS_ERA-I	5.77	1.64	1.28	0.7	-1.02	2.7	6.3	4.3	134	-39.0	0.25
USGS_JRA-55	6.18	1.43	1.29	0.7	-0.62	3.6	6.8	4.2	166	-24.6	0.15
MODIS_JRA-55	6.21	1.39	1.26	0.7	-0.58	3.7	6.8	4.2	169	-23.4	0.14
USGS_R2	5.46	2.15	1.68	0.5	-1.34	0.1	6.1	3.6	121	-44.9	0.30
MODIS_R2	5.57	2.11	1.72	0.5	-1.22	0.2	6.2	3.6	130	-41.1	0.27

Average predictions, error metrics at 60 m with data from 9 km domain. Weibull parameters are calculated with the Empirical method

	60 m										
	9 km domain					60 m					
	Average Wind Speeds (m/s)	ME (m/s)	RMSE (m/s)	STDE (m/s)	CC	Skill Score	c	k	Mean WPD (Wm ⁻²)	WPD Error (%)	Max CDF Error
Observation	6.89								230	0	0
USGS_FNL	5.68	1.74	1.25	0.74	-1.21	2.97	7.6	4.2	122	-46.8	0.33
MODIS_FNL	6.07	1.41	1.15	0.78	-0.82	3.93	6.6	5.0	151	-34.6	0.23
USGS_CFSv2	5.72	1.87	1.46	0.61	-1.17	2.09	6.2	5.0	126	-45.4	0.32
MODIS_CFSv2	6.14	1.59	1.41	0.65	-0.75	2.96	6.7	5.0	155	-32.5	0.21
USGS_ERA-I	5.62	1.80	1.28	0.72	-1.27	2.75	6.2	4.5	122	-47.0	0.32
MODIS_ERA-I	6.00	1.51	1.23	0.75	-0.89	3.54	6.6	4.4	149	-35.1	0.22
USGS_JRA-55	5.69	1.83	1.38	0.68	-1.20	2.47	6.3	4.2	129	-43.9	0.29
MODIS_JRA-55	6.03	1.61	1.36	0.70	-0.86	3.09	6.6	4.2	155	-32.8	0.20
USGS_R2	5.04	2.54	1.74	0.50	-1.85	0.02	5.6	3.5	97	-57.9	0.41
MODIS_R2	5.45	2.27	1.75	0.52	-1.44	0.69	6.1	3.5	122	-46.8	0.31

References

1. Tang, J., et al., *Statistical downscaling and dynamical downscaling of regional climate in China: Present climate evaluations and future climate projections*. Journal of Geophysical Research: Atmospheres, 2016. **121**(5): p. 2110-2129.
2. Warner, T.T., *Numerical weather and climate prediction*. Cambridge University Press. Cambridge CB2 8RU, UK. 2011
3. Jiménez-Esteve, B., et al. *Land Use and Topography Influence in a Complex Terrain Area: A High Resolution Mesoscale Modelling Study over the Eastern Pyrenees using the WRF Model*. 2017. **Volume 202**, 49-62 DOI: 10.1016/j.atmosres.2017.11.012.
4. Chadee, X., N. Seegobin, and R. Clarke *Optimizing the Weather Research and Forecasting (WRF) Model for Mapping the Near-Surface Wind Resources over the Southernmost Caribbean Islands of Trinidad and Tobago*. Energies, 2017. **10**, 931 DOI: 10.3390/en10070931.
5. Boadh, R., et al. *Sensitivity of PBL schemes of the WRF-ARW model in simulating the boundary layer flow parameters for its application to air pollution dispersion modeling over a tropical station*. Atmósfera, 2016. **29**, 61-81 DOI: 10.20937/ATM.2016.29.01.05.
6. Santos-Alamillos, F.J., et al., *Influence of land-use misrepresentation on the accuracy of WRF wind estimates: Evaluation of GLCC and CORINE land-use maps in southern Spain*. Atmospheric Research, 2015. **157**: p. 17-28.
7. Schicker, I., D. Arnold Arias, and P. Seibert, *Influences of updated land-use datasets on WRF simulations for two Austrian regions*. Meteorology and Atmospheric Physics, 2016. **128**(3): p. 279-301.
8. Zhao, D.-M. and J. Wu, *Evaluating the impacts of land use and land cover changes on surface air temperature using the WRF-mosaic approach*. Atmospheric and Oceanic Science Letters, 2018. **11**(3): p. 262-269.
9. Yang, J. and K. Duan, *Effects of Initial Drivers and Land Use on WRF Modeling for Near-Surface Fields and Atmospheric Boundary Layer over the Northeastern Tibetan Plateau*. Advances in Meteorology, 2016. **2016**: p. 16.
10. De Meij, A. and J.F. Vinuesa, *Impact of SRTM and Corine Land Cover data on meteorological parameters using WRF*. Atmospheric Research, 2014. **143**: p. 351-370.
11. Fernández-González, S., et al. *Sensitivity Analysis of the WRF Model: Wind-Resource Assessment for Complex Terrain*. Journal of Applied Meteorology and Climatology, 2017. DOI: 10.1175/JAMC-D-17-0121.1.
12. Parker, W.S., *Reanalyses and Observations: What's the Difference?* Bulletin of the American Meteorological Society, 2016. **97**(9): p. 1565-1572.
13. Dee, D., Fasullo, John, Shea, Dennis, Walsh, John & National Center for Atmospheric Research Staff (Eds). *The Climate Data Guide: Atmospheric Reanalysis: Overview & Comparison Tables*. Available from: <https://climatedataguide.ucar.edu/climate-data/atmospheric-reanalysis-overview-comparison-tables> [Accessed on March 26 2019]
14. National Center for Atmospheric Research Staff (Eds). *The Climate Data Guide: Simplistic Overview of Reanalysis Data Assimilation Methods*. Available from: <https://climatedataguide.ucar.edu/climate-data/simplistic-overview-reanalysis-data-assimilation-methods> [Accessed on March 26 2019]
15. Dee, D.P., et al. *The ERA-Interim reanalysis: Configuration and performance of the data assimilation system*. Quarterly Journal of the royal meteorological society, 2011. **137**, 553-597.
16. Peng, G., *Analysis, Reanalysis, Forecast - What's the Difference*. 2014.
17. McGuffie, K. and A. Henderson-Sellers, *A climate modelling primer*. John Wiley & Sons. 2005
18. NCSU Libraries. *Land Use/Land Cover Data*. Available from: <https://www.lib.ncsu.edu/gis/lulc> [Accessed on May 1 2019]
19. Ghati, S. and M. Mohan, *The Impact of Land Use/Land Cover on WRF Performance in a Sub-Tropical Urban Environment*. 2015, Presentation.
20. Mughal, M.O., et al. *Wind modelling, validation and sensitivity study using Weather Research and Forecasting model in complex terrain*. Environmental Modelling & Software, 2017. **90**, 107-125 DOI: 10.1016/j.envsoft.2017.01.009.
21. Carvalho, D., et al. *WRF wind simulation and wind energy production estimates forced by different reanalyses: Comparison with observed data for Portugal*. Applied Energy, 2014. **117**, 116-126 DOI: 10.1016/j.apenergy.2013.12.001.
22. Armah, F.A., et al., *Food security and climate change in drought-sensitive savanna zones of Ghana*. 2011. **16**(3): p. 291-306.
23. Skamarock, W.C., J. B. Klemp, J. Dudhia, D. O. Gill, D. M. Barker, M. G Duda, X.-Y. Huang, W. Wang, and J. G. Powers *A Description of the Advanced Research WRF Version 3*. NCAR Tech. Note NCAR/TN-475+STR, 2008. DOI: doi:10.5065/D68S4MVH
24. Dzebre, D.E.K., et al. *A sensitivity study of Surface Wind simulations over Coastal Ghana to selected Time Control and Nudging options in the Weather Research and Forecasting Model*. Heliyon, 2019. **5**, e01385 DOI: 10.1016/j.heliyon.2019.e01385.
25. *WRF V3 Geographical Static Data Downloads Page Page*. Available from: http://www2.mmm.ucar.edu/wrf/users/download/get_sources_wps_geog_V3.html [Accessed on 30 Sep 2019]

26. Wei Wang, C.B., Michael Duda, Jimy Dudhia, Dave Gill, Michael Kavulich, Kelly Keene, Ming Chen, Hui-Chuan Lin, John Michalakes, Syed Rizvi, Xin Zhang, Judith Berner, Soyoun Ha and Kate Fossell, *ARW Version 3 Modeling System User's Guide*. 2016, NCAR: Colorado, USA.
27. Duda, M. *Running the WRF Preprocessing System*. The WRF Users' Basic Tutorial Available from: <https://pdfs.semanticscholar.org/presentation/bdd9/87db4d0661c5e8d5fd3157a14d106da56887.pdf> [Accessed on Dec 2018]
28. Available GRIB Datasets from NCAR. Available from: http://www2.mmm.ucar.edu/wrf/users/download/free_data.html [Accessed on 30/09 2018]
29. NCEP FNL Operational Model Global Tropospheric Analyses, continuing from July 1999. 2000, Research Data Archive at the National Center for Atmospheric Research, Computational and Information Systems Laboratory: Boulder, CO.
30. Saha, S., et al., *NCEP Climate Forecast System Version 2 (CFV2) 6-hourly Products*. 2011, Research Data Archive at the National Center for Atmospheric Research, Computational and Information Systems Laboratory: Boulder, CO.
31. *ERA-Interim Project*. 2009, Research Data Archive at the National Center for Atmospheric Research, Computational and Information Systems Laboratory: Boulder, CO.
32. *JRA-55: Japanese 55-year Reanalysis, Daily 3-Hourly and 6-Hourly Data*. 2013, Research Data Archive at the National Center for Atmospheric Research, Computational and Information Systems Laboratory: Boulder, CO.
33. *NCEP/DOE Reanalysis 2 (R2)*. 2000, Research Data Archive at the National Center for Atmospheric Research, Computational and Information Systems Laboratory: Boulder, CO.
34. Neh Patel. *Create Global Reanalyses*. Available from: https://esgf.nccs.nasa.gov/projects/create-ip/CREATE_global_reanalyses [Accessed on March 29 2019]
35. *GFS/GDAS CHANGES SINCE 1991*. Available from: https://www.emc.ncep.noaa.gov/gmb/STATS/html/model_changes.html [Accessed on March 29 2019]
36. Kanamitsu, M., et al. *NCEP-DOE AMIP-II Reanalysis (R-2)*. *Bulletin of the American Meteorological Society*, 2002. **83**, 1631-1644 DOI: 10.1175/bams-83-11-1631.
37. Harada, Y., et al. *The JRA-55 Reanalysis: Representation of Atmospheric Circulation and Climate Variability*. *Journal of the Meteorological Society of Japan*. Ser. II, 2016. **94**, 269-302 DOI: 10.2151/jmsj.2016-015.
38. Kleist, D. and Y. Trémolet, *Data Assimilation Plans at NOAA/NWS/NCEP*. 2018, Presentation.
39. Carvalho, D., et al. *A sensitivity study of the WRF model in wind simulation for an area of high wind energy*. *Environmental Modelling & Software*, 2012. **33**, 23-34 DOI: 10.1016/j.envsoft.2012.01.019.
40. Santos-Alamillos, F.J., et al. *Analysis of WRF Model Wind Estimate Sensitivity to Physics Parameterization Choice and Terrain Representation in Andalusia (Southern Spain)*. *Journal of Applied Meteorology and Climatology*, 2013. **52**, 1592-1609 DOI: 10.1175/jamc-d-12-0204.1.
41. Dzebre, D.E.K. and M.S. Adaramola, *Impact of Selected Options in the Weather Research and Forecasting Model on Surface Wind Hindcasts in Coastal Ghana*. *Energies*, 2019. **12**(19): p. 3670.
42. Dzebre, D.E.K. and M.S. Adaramola, *A preliminary sensitivity study of Planetary Boundary Layer parameterisation schemes in the weather research and forecasting model to surface winds in coastal Ghana*. *Renewable Energy*, 2020. **146**: p. 66-86.
43. Kang, D., K. Ko, and J. Huh *Comparative Study of Different Methods for Estimating Weibull Parameters: A Case Study on Jeju Island, South Korea*. *Energies*, 2018. **11**, 356 DOI: 10.3390/en11020356.
44. Saha, S., et al. *The NCEP Climate Forecast System Version 2*. *Journal of Climate*, 2014. **27**, 2185-2208 DOI: 10.1175/jcli-d-12-00823.1.
45. Rabier, F. and Z. Liu, *Variational data assimilation: theory and overview* In Conference Proceedings. ECMWF Seminar on Recent developments in data assimilation for atmosphere and ocean, 2003
46. Stull, R., *Practical meteorology: An Algebra-based Survey of Atmospheric Science*. BC Campus. 2016
47. Huang, X.-Y., et al. *Four-Dimensional Variational Data Assimilation for WRF: Formulation and Preliminary Results*. *Monthly Weather Review*, 2009. **137**, 299-314 DOI: 10.1175/2008mwr2577.1.
48. Lorenc, A., *Relative Merits of 4D-Var and Ensemble Kalman Filter*.
49. Barker, D., et al. *The weather research and forecasting model's community variational/ensemble data assimilation system: WRFDA*. *Bulletin of the American Meteorological Society*, 2012. **93**, 831-843.
50. KALNAY, E., et al., *4-D-Var or ensemble Kalman filter?* *Tellus A*, 2007. **59**(5): p. 758-773.

Errata



Norwegian University
of Life Sciences

FORM 4.7 Errata

Application for permission to correct formal errors in the thesis

Errata is a list of corrections made in a thesis after it has been approved, but before it is printed.

The PhD candidate may apply for permission to correct formal errors in the thesis (cf. the PhD regulations, section 15.3-2). The application must include a complete list of the errors that the PhD candidate wishes to correct. The application must be e-mailed to the faculty PhD contact person at the latest 4 weeks before the planned disputation date.

An errata application can be made only once. The errata list must be inserted as the last page of the printed version of the thesis.

It is allowed to correct the following formal errors:

- spelling and language mistakes that make the text linguistically incorrect
- punctuation and reference errors
- page layout, text format etc.

It is not allowed to:

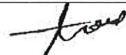

- specify or change the meaning of the text
- make changes in tables
- change version or change status in manuscripts/ articles in your PhD thesis. For example, an article with the status "in press" cannot be exchanged with a journal's printed version, and change status to "published" prior to printing.

Corrections to the cover, in preface and acknowledgements, can be made without applying for permission.


Name of PhD candidate:	Denis Edem Kwame Dzebre
Thesis title:	Sensitivity Analyses Of The Weather Research And Forecasting Model For Wind Resource Assessment In Coastal Ghana.

The application is to be signed by the PhD candidate and the main supervisor and sent to the faculty for approval.

Signatures and dates:

PhD candidate:		Date:	18/11/2019
Main supervisor:		Date:	18/11/2019

Errata approved by the faculty: Yes No

For the faculty:		Date:	18.11.2019
------------------	---	-------	------------

Errata list

PhD candidate: Denis Edem Kwame Dzebre

Thesis: Sensitivity Analyses Of The Weather Research And Forecasting Model For Wind Resource Assessment In Coastal Ghana.

Date:18/11/2019

Page	Line	Original text	Corrected text
1	9	greenhouse emmissions	greenhouse gases emmissions
	18	As at	As of
2	17	several texts	several textbooks
3	6	explained in texts	explained in textbooks
	8	shown below	shown in Figure 2
4	12	validation process of NWP	validation process of NWP models
5	2	energy sources of energy including variable renewable	energy sources including renewable
	5	towards development	towards the exploitation
	6	sector is still faced with several	is still facing several
	7	limited or unavailability of	limited or non availability of
	19	over the few years	over the past years
	20	reliable easily accessible	reliable and easily accessible
	22	owing to diversse model options, sensitivity studies of the model, several model-validation studies towards	owing to diverse physics and dynamics options, several model-validation studies towards
24	reported in open literature	reported in the literature	
	26-30		Limited scope of past studies added as requested by opponent 2
6	10	insights, either than	insights, other than
	22	thesis presents the research data and verification criteria.	thesis presents the verification data and criteria.
	22-26		Rearranged to reflect changes in the structure of chapter 2
7-14			Restructured as directed by opponent 2. Figure numbers and Section numbers revised accordingly.
9	2-3	where p is the pressure at level in the atmosphere, p_s , is the pressure below p , and p_t is the pressure at the top of the atmosphere above p .	where p is the pressure at a particular level in the atmosphere, p_s , is the surface pressure, and p_t is the pressure at the top of the atmosphere.
	12	recommended that it's value (in seconds) is a maximum six times	recommended that its value (in seconds) is maximum six times
	15	which offers resolves gravity waves more accurately	which allows for resolving gravity waves more accurately
10	21	Literature	papers and textbooks
11	11	done with aim of	followed with the aim of
11	11	in WRF, once can choose to apply nudging variables	in WRF, one can choose to apply nudging to variables
13	2	as well as	and

	17	for evaluations was from mast	for evaluations were derived from mast
	19	addition to this data	addition to these data
13	25	data was measured	data were measured
15	18	studies in open literature	studies in the literature
	28	in Figure 10	in Figure 9
16	27-28	This preliminary assessment was aimed reducing the number of PBL schemes to fully examine	This preliminary assessment aimed at reducing the number of PBL schemes to be examined
	30	illustrated Figure 11	illustrated Figure 10
17	1	(in terms of a several error metrics) in assessing	(in terms of several error metrics) of assessing
18	6	were not so different	were not so large
	9	in terms of verification techniques	in terms of verification
	10	downscaling for wind data	downscaling wind data
	18-19	configuration from the tests could predict annual wind speeds winds	configuration from the tests could predict annual wind speeds winds
	20	exhibited more bias	exhibited larger bias
19-20			Restructured as directed by opponent 2
19		for the dynamically downscaling of	for dynamical downscaling of
		Wind data was downscaled	Wind data were downscaled
20		Surface Sea Temperature	Sea Surface Temperature

ISBN: 978-82-575-1676-5

ISSN: 1894-6402



The Norwegian Programme for Capacity Development in Higher Education and Research for Development within the Fields of Energy and Petroleum (EnPe)
Norwegian Agency for Development Cooperation (Norad)
Pb. 1303 Vika, NO-0112 Oslo, Norway
<https://norad.no/>



The Brew-Hammond Energy Center
Kwame Nkrumah University of Science and Technology (KNUST)
PMB
Kumasi, Ghana.
<https://energycentre.knust.edu.gh>



Norwegian University
of Life Sciences

Postboks 5003
NO-1432 Ås, Norway
+47 67 23 00 00
www.nmbu.no